DIFFUSION OF SODIUM IN MIXED GLASS FORMER OXIDE GLASSES

A Dissertation

Presented to the Faculty of the Graduate School

of Cornell University

in Partial Fulfillment of the Requirements for the Degree of

Doctor of Philosophy

by

Xinwei Wu

August 2012

DIFFUSION OF SODIUM IN MIXED GLASS FORMER OXIDE GLASSES

Xinwei Wu, Ph.D.

Cornell University 2012

The mixed glass former effect (MGFE) is a non-linear variation of transport properties as a function of the glass former composition when one glass network former is replaced by another one. In order to better understand the MGFE, the effect of the variation of the glass former composition on the transport of a selected ion was studied. The composition and temperature dependencies of sodium tracer diffusion coefficients, D^*_{Na}, were determined for different mixed glass former oxide glasses, which are two types of sodium borosilicate glasses, sodium boroaluminosilicate glasses and a commercial, ion-exchangeable alkali aluminosilicate glass.

In the case of sodium borosilicate glasses of the type $(Na_2O)_{0.2}[(BO_{1.5})_x(SiO_2)_{1-x}]_{0.8}$, the tracer diffusion coefficient of sodium as a function of the glass composition at constant temperatures between 208 and 503 °C shows a shallow minimum at values of the composition parameter x of around 0.7. Values determined for the Haven-ratio, H_R, are all smaller than one and show as a function of x a shallow minimum at $x \approx 0.7$. Some structural information was obtained by analyzing ^{11}B magic-angle-spinning (MAS) nuclear magnetic resonance (NMR) spectra of this series of glass samples indicated above. For another type of sodium borosilicate glasses, $(Na_2O)_{0.2}(B_2O_3)_y(SiO_2)_{0.8-y}$, the tracer diffusion coefficient of sodium decreases with an increase of the value of the

composition parameter y at constant temperatures between 208 and 346 °C. At temperatures below about 2/3 of the glass transition temperature, the temperature dependencies of the measured tracer diffusion coefficients are of Arrhenius-type; at higher temperatures a slight increase in the temperature dependence with increasing temperature was observed.

For both iron-free and iron-containing sodium boroaluminosilicate glasses of the types $[(Na_2O)_{0.71}(B_2O_3)_{0.24}(Fe_2O_3)_{0.05}]_{0.2}[(SiO_2)_x(Al_2O_3)_{1-x}]_{0.8}$ and $[(Na_2O)_{0.743}(B_2O_3)_{0.253}(As_2O_3)_{0.004}]_{0.18}[(SiO_2)_x(Al_2O_3)_{1-x}]_{0.82}$ with x varying from 0.8 to 1 at constant temperatures between 198 and 350 °C, the sodium tracer diffusion coefficients were found to decrease with a decrease of the concentration of alumina. The composition dependence of the sodium tracer diffusion coefficients is related to structural changes which are found to occur by analyzing ^{27}Al and ^{11}B MAS NMR spectra of the glass samples studied.

A commercial, ion-exchangeable alkali aluminosilicate glass (Corning Code 2317) developed for being used to produce chemically strengthened glass by ion exchange was also studied for the temperature dependence of the sodium tracer diffusion in it.

Whether different glass samples take up water during annealing in moist atmospheres and whether water taken up can influence the diffusion of sodium was also investigated.

BIOGRAPHICAL SKETCH

Xinwei Wu was born on September 28, 1984 in Zhuji, Zhejiang, P.R. China, a town with a lot of historic sites as well as beautiful landscapes. She is the only child in her family. Her interest in science was nurtured by her parents who were both high school teachers in science at that time. She finished her bachelor's degree in Materials Science and Engineering at Shanghai Jiao Tong University. In August 2007, she joined the Ph.D. program with Professor Rüdiger Dieckmann in the Department of Materials Science and Engineering at Cornell University at Ithaca, New York.

TO MY PARENTS

ACKNOWLEDGMENTS

I want to express my deepest gratitude to my advisor, Professor Rüdiger Dieckmann, for his excellent guidance, constant mentoring and enormous support over the last five years. I will remain inspired by his dedication to perfection. My gratitude also extends to Professor Richard G. Hennig and Professor David A. Muller for serving in my thesis committee as minor advisors.

Special thanks go to Professor Arun K. Varshneya and Professor Steve Martin for fruitful collaborations and Dr. Adam J. Ellison for providing glass samples for this study as well as giving me the opportunity to work with many experts in glass research at Corning as an intern last summer. I thank several staff members, Paul Bishop, John Hunt and Jonathan Shu for their technical support and the undergraduate researchers, Jun Tong, Changhao Yu, Murli Gupta, Christine Lee, Jeremy Moskowitz, Ashwin Shahani and Maggie Tse for their help in data collection.

Last but not the least, I want to thank my family for their love and support.

TABLE OF CONTENTS

LIST OF FIGURES

LIST OF TABLES

LIST OF SYMBOLS

A_g	absorbance of glass
A(x)	residual radioactivity after removal of material with the thickness x
a_i	elementary jump length of a diffusing species i
$\overline{a}_i$	average jump distance for the species i
c_{H_2O}	concentration of water
Δc_{H_2O}	change of the concentration of water
c_i	concentration of the species i
$\tilde{D}$	interdiffusion coefficient
D_{H_2O}	chemical diffusion coefficient of water molecules
D_i	self-diffusion coefficient of a species i
D_i^*	tracer diffusion coefficient of a species i
$D_{i,glass}$	diffusion coefficient of a species i diffusing in a glass
$D_{i,\sigma}$	conductivity diffusion coefficient of a species i
D_{K^+}	component diffusion coefficient of K^+
D_{Na^+}	component diffusion coefficient of Na^+
D_{Na}^o	pre-exponential factor of a sodium tracer diffusion coefficient
D_{Na}^*	diffusion coefficient of the tracer Na-22
D_{OH}	chemical diffusion coefficient of OH groups
$\tilde{D}_{eff,OH}$	effective chemical diffusion coefficient of OH groups
$\tilde{D}_{eff,water}$	effective chemical diffusion coefficient of water
D_σ	conductivity diffusion coefficient
d	thickness
d_g	thickness of a glass sample
ΔE_a	activation enthalpy
F	Faraday constant
f_i	correlation factor of a species i
f_{NBO}	value for the fraction of non-bridging oxygen
H_R	Haven-ratio
I	intensity of a transmitted IR signal
I_0	intensity of an initial IR signal
j_i	flux of a diffusing species i per unit area and unit time
K	$= n_{SiO_2}/n_{B_2O_3}$
K_{eq}	equilibrium constant
M_0	initial total water content

M_∞	saturation water content at an infinite annealing time
M_{H_2O}	molar mass of water
M_t	total water content after diffusion-annealing for the time t
m	molar fraction
m_{pw}	mass of the pycnometer filled with water
m_{pws}	mass of the pycnometer with glass sample(s) in it filled with water
m_s	mass of the glass sample in air
N_4	value for the fraction of boron in a fourfold coordination
N_A	Avogadro constant
$n_{B_2O_3}$	number of moles of B_2O_3
n_{Na_2O}	number of moles of Na_2O
n_{SiO_2}	number of moles of SiO_2
P_{H_2O}	water vapor pressure
Q_i	initial concentration of a tracer i per unit area
R	gas constant, = $n_{Na_2O}/n_{B_2O_3}$
$\overline{R}_n$	mean square displacement after n jumps
r	jump distance
$r_{B^{3+}}$	radius of B^{3+}
r_{Na^+}	radius of Na^+
$r_{Si^{4+}}$	radius of Si^{4+}
T	temperature
T_g	glass transition temperature
t	time
t_{pa}	pre-annealing time
V_f	free volume
V_m	molar volume
x	composition parameter, direction
y	composition parameter
z	composition parameter
z_i	ionic charge number of a diffusing species i
Γ	jump frequency
$\Gamma_{i,eff}$	effective jump frequency of a species i
$\overline{\Gamma}_{i,eff}$	average effective jump frequency of a species i
ε_{H_2O}	molar absorption coefficient of water
ε_{OH}	molar absorption coefficient of OH groups, $\varepsilon_{OH} \approx ½\ \varepsilon_{H_2O}$
μ	mass absorption coefficient for γ-radiation

ξ	distance
ρ	density
ρ_g	density of a glass
ρ_{glass}	density of a glass
ρ_w	density of water
σ_i	electrical conductivity of a species i

CHAPTER ONE

INTRODUCTION

According to a definition provided by Varshneya [1] glass is “an inorganic product of fusion which has been cooled to a rigid condition without crystallization”. Due to rapid cooling, the atoms of a liquid do not have sufficient time to completely rearrange to the equilibrium positions. Therefore this liquid becomes an amorphous solid lacking long range order of the structure. Besides being formed by cooling a melt, glasses can also be made by sol-gel processing of solutions, vapor deposition, neutron irradiation of crystalline materials, etc. In addition to the traditional inorganic, non-metallic glasses, organic glasses and metallic glasses become widely used nowadays [2]. All these amorphous solids without long range order and periodic atomic structures are called glasses. This study focuses on traditionally made inorganic oxide glasses, including sodium borosilicate glasses, sodium aluminosilicate glasses and sodium aluminoborosilicate glasses. General information related to glass formation, glass structure and transport properties of glasses will be introduced first. Then two well known effects in glasses, the mixed alkali effect and the mixed glass former effect, will be discussed briefly. Water as one type of impurity in glasses which plays a critical role will be discussed at the end of this chapter.

1.1 Glass Formation

Early research was focused on finding which melts can allow for easy glass formation and which ones prevent glass formation. It is now widely believed that virtually any material can be formed as a glass, provided that proper cooling conditions are used. In this section, traditional theories of glass formation based

on structural properties will be briefly summarized and then more recent kinetic theories will be surveyed.

1.1.1 Structural Theories of Glass Formation

Zachariasen [3] first pointed out that after melting and cooling oxides like SiO_2 and B_2O_3 form glasses instead of crystallizing have special structures. These structures are formed by tetrahedra, like SiO_4 or BO_4, connected at four corners, forming a continuous network structure. Unlike in crystals, these structures do not exhibit translational symmetry. Furthermore, these structures are homogeneous on average along all directions, making the properties of glasses to be isotropic. Based on this idea, Zachariasen investigated the structural organizations that can lead to such networks, which became the foundation for the glass structure model termed as the continuous random network (CRN) model which will be introduced in detail later in Section 1.2.1.

There are also several other theories of glass formation based upon the properties of chemical bonds. Smekal and Klemm [4] proposed that only melts of components whose chemical bonds are intermediate in character between purely covalent and purely ionic bonds like Si can form glasses. Bond strength has also been viewed as an important factor to predict the possibility of glass formation. For example, Sun [5] pointed out that strong bonds facilitate glass formation by preventing the melt structure to transform into a crystalline structure during cooling. Further refinements of this idea continued. For instance, Rawson [6] argued that Sun did not consider the role of temperature in his theory. The ratio of the bond strength to the energy available at the melting point, which is proportional to the melting temperature, indicates the ability for structural rearrangements to occur during crystallization. The higher the value of this ratio

is, the smaller is the probability for chemical bonds to break at the melting temperature and the higher is the tendency to form glass. Therefore, a material with strong chemical bonds and a relatively low melting temperature has a good chance to be an effective glass former.

1.1.2 Kinetic Theories of Glass Formation

It is accepted now that, when a cooling process is fast enough to prevent detectable crystallization, virtually any material can form a glass [2]. Hence, unlike in the structural theories, here the question is not which material can form a glass, but at which cooling rates.

Crystallization requires two conditions: the formation of a sufficient number of critical nuclei and a sufficient crystal growth rate. Therefore, lacking either or both of the conditions can prevent crystallization. Glasses can be obtained when the cooling rate is higher than the critical cooling rate which is the minimum cooling rate required to form a sample containing less than an arbitrary volume fraction of crystals usually taken as 10^{-6} [2]. When comparing different melts of identical size, the melt with the smallest critical cooling rate has the best glass forming ability. The ease of forming glasses from different melts obtained from results of kinetic studies generally agree well with the results predicted by applying the earlier structural theories of glass formation.

1.2 Oxide Glass Structure

1.2.1 Sodium Silicate Glasses

The structure of a glass differs from that of crystals by the fact that it lacks symmetry and periodicity. Zachariasen's CRN model [3] proposed in 1932 is the

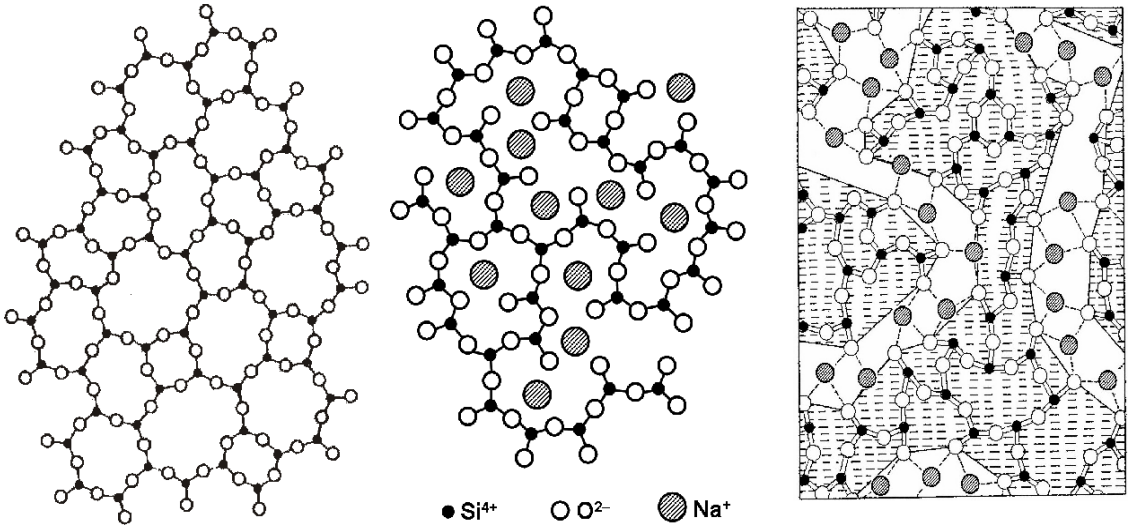

(a) (b) (c)

Figure 1.1: Two-dimensional representations of random network models: (a) continuous random network model (CRN) for the structure of SiO_2 glass [7], (b) continuous random network model (CRN) for the structure of $Na_2O{\cdot}SiO_2$ glass [7], and (c) modified random network (MRN) model for the structure of $Na_2O{\cdot}SiO_2$ glass [8]. In (c), bridging oxygen atoms are located within the network regions and non-bridging oxygen atoms in channels formed by glass network modifiers [8].

most significant glass structure model and became the basis for the development of other glass structure models. In Zachariasen's CRN model, the basic units in vitreous silica, which are SiO_4 tetrahedra, are linked together at their corners with bonds of various lengths and angles forming a three-dimensional continuous random network, as shown in Fig. 1.1(a) [7]. The oxygen atoms present in silica glass are practically all bridging oxygen atoms, i.e., all four oxygen atoms in SiO_4 tetrahedra are shared. When a highly ionic oxide like Na_2O ($2\,Na^+ + O^{2-}$) is added to silica, a reaction takes place which can be described by Eq. (1.1).

$$2\,[SiO_{4/2}]^0 + Na_2O \rightleftharpoons 2\,[SiO_{3/2}O]^- + 2\,Na^+ \qquad (1.1)$$

The effect of adding Na_2O is to "break" the Si-O-Si linkage and to create $Si\text{-}O^-$ terminations. Oxygen in the Si-O-Si linkage, which links the network forming polyhedra, is known as bridging oxygen (BO) and oxygen in $Si\text{-}O^-$, which does not link network polyhedra, is called non-bridging oxygen (NBO).

Cations in glass within network forming oxygen polyhedra, which constitute the network, are glass network formers (e.g., Si^{4+}, B^{3+} and P^{5+}). Cations between network building oxygen polyhedra, which break the network, are called glass network modifiers (e.g., Na^+, K^+, Ca^{2+} and Ba^{2+}). Besides, there are some cations called glass network intermediates (e.g., Al^{3+}, Mg^{2+}, Zn^{2+} and Fe^{3+}), which can behave either like network formers or like network modifiers, depending on the glass composition.

According to Zachariasen's continuous random network (CRN) model, in sodium silicate glass, the glass network modifiers (Na^+ ions) are randomly located in interstices close to $Si\text{-}O^-$ terminations as shown in Fig. 1.1(b). However, this picture is too simple to describe the real structure of glasses. Results from Nuclear Magnetic Resonance (NMR) and X-ray Absorption Fine Structure (XAFS)

measurements [8] have indicated the existence of a non-uniform distribution of network modifiers. Therefore, Greaves proposed a modified random network (MRN) model that is based on attributing different regions to network-forming and network-modifying cations. XAFS measurements [8] further showed that network and modifier components are microsegregated and that modifier ions form channels within a depolymerized network structure as illustrated in Fig. 1.1(c). In the case of silica-based glasses, the SiO_2-rich and SiO_2-poor regions are interwoven with each other. Network-regions are primarily made up by network formers and inter-network regions have an increased concentration of network modifiers.

1.2.2 Sodium Borosilicate Glasses

The basic structural units in B_2O_3 glass are BO_3 triangles. When a glass network modifier like sodium oxide is added to boric oxide glass, the introduction of an extra oxygen atom by the addition of sodium oxide can either covert a 3-coordinated boron to a 4-coordinated boron or lead to the formation of a nonbridging oxygen. In sodium borosilicate glasses, sodium ions added can associate with boron or with silicon depending on the glass composition [1]. When the molar ratio of Na_2O to B_2O_3 is smaller than 0.5, oxygen atoms introduced with sodium oxide prefer to converting 3-coordinated boron to 4-coordinated boron. When this molar ratio is larger than 0.5, the sodium oxide will be partitioned between boron and silicon [9]. There are different structural models of sodium borosilicate glasses proposed by Yun and Bray [10], Yun et al. [11] and by Dell et al. [12] to predict the fraction of 4-coordinated boron, which will be discussed and used in Chapters Two and Three when considering $(Na_2O)_{0.2}[(BO_{1.5})_x(SiO_2)_{1-x}]_{0.8}$ and $(Na_2O)_{0.2}(B_2O_3)_y(SiO_2)_{0.8-y}$ glasses.

1.2.3 Sodium Aluminosilicate Glasses

Aluminum is a glass network intermediate, which can act either as a glass network former in tetrahedral coordination when the molar concentration of Al_2O_3 is not larger than that of Na_2O or some of the Al behaves like a glass network modifier having an octahedral coordination when the molar concentration of Al_2O_3 is larger than that of Na_2O [1]. According to this theory, when the molar concentration of Al_2O_3 is equal to the molar concentration of Na_2O, there is no NBO present in the sodium aluminosilicate glass structure. However, Stebbbins and Xu [13] found about 5 mol% NBO existing in an aluminosilicate glass which has the same molar concentration of Na_2O and of Al_2O_3. The presence of NBO can be explained by the existence of a small fraction of Al^{3+} remaining in triclusters, where one oxygen atom is shared by three tetrahedra of which two can be SiO_4 and one AlO_4 or two AlO_4 and one SiO_4. The first type, two SiO_4 and one AlO_4 tricluster, is electrically neutral and does not need a cation for charge compensation. This explanation was supported by the results a ^{17}O NMR study of calcium aluminosilicate glass structure [14]. One complex type of sodium aluminosilicate glass and one type of sodium boroaluminosilicate glass will be considered in Chapters Four and Five, respectively.

1.3 Transport Properties of Glasses

Many properties of glasses, like the electrical conductivity, the ionic conductivity etc., of glasses are controlled by the transport of ions. The transport of alkali ions in glass under an external electric field determines the electrical conductivity of the alkali glasses. In principle, glasses with high ionic conductivities can be used as electrolytes in solid state batteries. A strengthened surface under compression can be generated by an ion exchange between two kinds of alkali ions when glasses

are immersed in a molten salt bath containing alkali ions with larger radius comparing to that of the alkali ions in the glasses. Ion exchange can also be used to produce optical devices with a graded refractive index near the surface of the glass. Studying the transport of cations in glasses is very important for improving ion exchange processes, e.g., for increasing the ion exchange speed.

1.3.1 Diffusion Equations

Fick's first law is the basic equation used to describe the diffusion of atoms at a steady state in glasses as well as in other substances. At one dimension, if the x axis is taken parallel to the concentration gradient of component i, the flux of component i (j_i) can be described by the equation

$$j_i = -D_i \cdot \frac{\partial c_i}{\partial x} \tag{1.2}$$

where j_i is the flux of a diffusing species i per unit area and unit time, D_i is the relevant diffusion coefficient of the diffusing species i and $\partial c_i/\partial x$ is the concentration gradient of the diffusing species i in the direction x. Assuming D_i does not change with c_i, if local changes of the concentration of species i, c_i, occur with time, i.e., at a non-steady state, Fick's second law applies:

$$\frac{\partial c_i}{\partial t} = D_i \cdot \frac{\partial^2 c_i}{\partial x^2} \tag{1.3}$$

where t is the diffusion time.

The thin film solution of the Fick's second law is of great interest for measuring ion diffusion coefficients in homogenous glass samples. For measuring a diffusion coefficient of a solute i in a solid, a thin film with a solute concentration per unit area, Q_i, is applied to a solute-free homogeneous sample with infinite thickness compared to the thickness of the film. After the sample has been annealed for a

time t, the solute concentration $c_i(\xi,t)$ at a distance ξ from the surface where the solute was applied can be expressed as [15]

$$c_i(\xi,t) = \frac{Q_i}{\sqrt{\pi \cdot D_i \cdot t}} \cdot \exp\left(- \frac{\xi^2}{4 D_i \cdot t} \right) \tag{1.4}$$

The radioactive isotope Na-22, with a half-life of 2.6 year and the γ-radiation energies associated with the decay at 0.51 and 1.28 MeV [16], was used to study the diffusion of sodium in different types of glass samples in this study. After the tracer Na-22 in a chloride solution was applied as a thin film on a plane-parallel glass sample, followed by diffusion-annealing for a certain time t, residual radioactivities, A(x,t), were measured by using a high resolution, high-purity Ge detector (EG&G Ortec) as a function of the distance x from the initial sample surface where the tracer was applied. Departing from Eq. (1.4), a new equation describing the normalized residual radioactivity, A(x,t)/A(x=0,t), can be derived; the result is Eq. (1.5).

$$\frac{A(x,t)}{A(x=0,t)} = \frac{\int_x^\infty c_i(\xi,t) \cdot d\xi}{\int_0^\infty c_i(\xi,t) \cdot d\xi} = 1 - \mathrm{erf}\left(\frac{x}{2\sqrt{D_i^* \cdot t}} \right) \tag{1.5}$$

where D_i^* is the tracer diffusion coefficient of the species I, in this work Na-22.

1.3.2 Atomistic Theory of Diffusion

Due to thermal excitation atoms can jump from original positions to some nearby sites over potential barriers, which is a random walk process when there is no preferred jump direction. The mean square displacement of an atom described in Eq. (1.6) [17] is introduced to describe the net displacement of an atom after a given time t, assuming that all jumps are of the same length r

$$\overline{R}_n^2 = t \cdot \Gamma \cdot r^2 \tag{1.6}$$

Γ is a jump frequency.

When only one out of all possible six directions is of interest, the mean square displacement in three dimensions needs to be normalized to one direction and the self-diffusion coefficient of a species i can be derived. The result is Eq. (1.7).

$$D_i = \lim_{t \to \infty} \frac{\overline{R}_n^2}{6t} = \frac{1}{6} \cdot a_i^2 \cdot \Gamma_{i,eff} \tag{1.7}$$

where a_i is an elementary jump length, which is related to the lattice constant of the crystal considered, and $\Gamma_{i,eff}$ is an effective jump frequency.

For tracer diffusion by a vacancy mechanism, although the direction of the first step of tracer-vacancy exchange direction is random, the direction of the second step is not random. The probability for the tracer to jump into the neighboring vacancy which was created by the first jump, i.e., jumping back, is higher than jumping to any other direction. This reduces the number of effective jumps for tracer transport, due to the tracer and non-tracer atoms being distinct. The correlation factor of the diffusion of a species i, f_i (≤ 1 for tracer diffusion), is introduced to relate the tracer diffusion coefficient of a species i, D_i^*, to its component-diffusion coefficient, D_i:

$$D_i^* = D_i \cdot f_i \tag{1.8}$$

The conductivity diffusion coefficient $D_{i,\sigma}$ can be derived from the ionic conductivity σ_i by the Nernst-Einstein relation. The result is

$$D_{i,\sigma} = \frac{R \cdot T \cdot \sigma_i}{z_i^2 \cdot F^2 \cdot c_i} \tag{1.9}$$

where R is the gas constant, T is the temperature in Kelvin, z_i is the ionic charge

number of the diffusing species i, F is the Faraday constant and c_i is the concentration of the species i.

The Haven-ratio, H_R, [18] is the ratio of the tracer diffusion coefficient, D_i^*, to the conductivity diffusion coefficient $D_{i,\sigma}$:

$$H_R = \frac{D_i^*}{D_{i,\sigma}} \tag{1.10}$$

H_R equals the correlation factor of diffusion f_i if the diffusion of an ion follows a vacancy mechanism, i.e., an ion exchanges with a vacancy in one single jump. When the ion diffusion involves more than one jump, H_R will differ from the value of f_i.

Due to the lack of periodic structure in glasses, the diffusion of cations in glasses is much more complicated than in crystalline materials. Since the parameters important for diffusion like jump lengths, jump frequencies and barrier heights can vary due to structural variations in a given glass, average quantities need to be introduced when considering diffusion in glasses, i.e., an average jump distance $\bar{a}_i$ for the species i and an average effective jump frequency $\overline{\Gamma}_{i,eff}$. Therefore, departing from Eq. (1.7), the diffusion coefficient of a species i diffusing in a glass can be described by Eq. (1.11).

$$D_{i,glass} = \frac{1}{6} \cdot \bar{a}_i^2 \cdot \overline{\Gamma}_{i,eff} \tag{1.11}$$

The values of the Haven-ratio in glasses are found to be smaller than those obtained for the diffusion of ions by vacancy mechanisms in crystals [19]. Indirect interstitialcy mechanisms may also be involved in the diffusion process [20]. In Chapters Two and Three, values for Haven-ratios for Na-22 diffusion in two types of sodium borosilicate glasses will be discussed which were obtained by comparing sodium tracer diffusion coefficients and conductivity diffusion coefficients.

1.4 Mixed Alkali Effect

When an alkali atom is substituted by another one, e.g., Na by K, in glasses, strong deviations from an additive behavior in certain properties are observed. This phenomenon is known as Mixed Alkali Effect (MAE). Properties depending on the ionic mobility are affected the most, such as the ionic conductivity, the diffusivity, the dielectric loss, the internal friction, the chemical durability and the viscosity [21].

Voss et al. [22] studied the tracer diffusion of sodium and of rubidium and the electrical conduction in glasses of the type $(Na_2O)_{1-x}(Rb_2O)_x(B_2O_3)_4$ with x increasing from 0 to 1 in steps of 0.2 and proposed that what caused the MAE is an increase of the activation energy of the mobility of one type of mobile cation when it is replaced by another type of mobile cation. The significance of the MAE depends on the total concentration of the alkali as well as the temperature of observation.

Although no single theory for the MAE has been universally accepted so far, two recent models for this effects will be discussed below. The dynamic structure model proposed by Bunde et al. [23,24] emphasizes the indirect interaction between cations in mixed alkali glasses assuming that there is a structural relaxation in the glass. According to this model, each alkali prefers to maintain its own distinct characteristic environment in a mixed alkali glass, which leads to mismatches between cations and sites occupied by different cations and this site memory effect introduces vacancies of different sizes according to the sizes of different kinds of mobile ions. A mismatch energy needs to be overcome when one type of cation jumps into a vacancy left behind by a cation of another type in a mixed alkali glass. For simplicity, this model neglects direct interactions between mobile species, the existence of mobile interstitial pairs and long-range Coulomb interactions. However,

the direct Coulomb interaction between alkali cations and non-bridging oxygen anions, the broad distribution of cation site energies and the network packing density do affect the ion mobility. These parameters, which are not included in the dynamic structural model discussed before, are the major considerations in a model proposed by Kirchheim [25-28] and by Kirchheim and Paulmann [29] called site energy distribution model. In this model, the interplay of network modifications and a distribution of site energies affect the diffusion in mixed alkali glasses. The diffusivity of larger alkali ions is reduced because the mesh size is reduced by the presence of smaller cations. The mobility of smaller cations also decreases because their activation energies for diffusion should be larger on the average since smaller cations allow a closer approach of anions and therefore are located at sites of lower energy. The main limitation of this model is that the mesh size of the network is supposed to be additively determined by the two alkali ions and that only one single site energy value is used.

Both models, the dynamic structural model and the site distribution energy model, can explain some features of the MAE. However, they are both based on several simplifying assumptions, which lead to some discrepancies between experimental and simulation results. Therefore, the long-standing problem of the MAE in glasses still poses a fascinating challenge in transport theory and a fully satisfactory explanation covering all aspects of the effect has not been established so far.

1.5 Mixed Glass Former Effect

In 1983, Magistris et al. [30] observed a maximum in the electrical conductivity, which is practically identical with the ionic conductivity, occurring at a $P_2O_5/(B_2O_3+P_2O_5)$-ratio of about 0.8 in a study of the electrical conductivity of AgI-

doped and undoped Ag_2O-B_2O_3-P_2O_5 glasses. The authors named this non-linear variation of the ionic conductivity “mixed anion effect”.

A high ionic conductivity is required for any glassy solid electrolytes in batteries and/or fuel cells. One way to improve the ionic conductivity is to increase content of mobile cations, i.e., the glass network modifier content, which is limited due to the poor chemical and mechanical stability of glasses with very high glass network modifier content. Therefore, it attracts a lot of interest to find out whether mixing glass network formers can also lead to high ionic conductivities. Currently, the relationships between composition, structure and properties in mixed glass former glasses are not well understood. The non-additive variation of transport properties as a function of the glass former composition when one network former is replaced by another one is in this study called “mixed glass former effect” (MGFE) [31].

For lithium borosilicate glasses, Tatsumisago et al. [32,33] found an ionic conductivity maximum at a concentration of Li_3BO_3 between 50 and 60 mol% when investigating the ionic conductivity of Li_4SiO_4-Li_3BO_3 glasses at 300, 400 and 500 K. The glass samples investigated were prepared by a twin-roller quenching technique. However, Maia and Rodriguez [34] observed a shallow minimum of the ionic conductivity at x-values of about 0.3 when studying glasses of the type $(Li_2O)_{0.4}[(B_2O_3)_x(Si_2O_4)_{1-x}]_{0.6}$ with $0 \leq x \leq 1$ at 373, 423 and 473 K. The differences between these results and those obtained by earlier Tatsumisago’s group [33] may be attributed to different thermal histories of the different types of glasses investigated. Maia and Rodriguez used annealed glass samples in their study.

Different composition dependencies of transport properties have been observed when replacing one glass network former by another one. For some glass compositions, parameters used for describing transport properties, like the

electrical conductivity, the diffusivity, etc., show a maximum value as a function of glass former composition. Such a behavior is called a positive MGFE. For example, for borophospate glasses, Tsuchiya and Moriya [35] reported in 1980 maxima in the electrical conductivity of $40Li_2O\text{-}xB_2O_3\text{-}(60-x)P_2O_5$ glasses as a function of x at 30, 60 and 90 °C. In contrast, minima of electrical conductivities and sodium tracer diffusivities were observed in sodium aluminosilicate glasses of the types $13Na_2O\text{-}xAl_2O_3\text{-}(87-x)SiO_2$ and $20Na_2O\text{-}xAl_2O_3\text{-}(80-x)SiO_2$ glasses with x varying from 0 to 13 and from 0 to 20, respectively [36]. Such a behavior is denoted as a negative MGFE.

In order to further study the MGFE, different glass compositions with more than one type of glass former and experimental data, which are related to the transport of ions of interest as a function of the network former composition, need to be investigated. In this study, the sodium tracer diffusion in three major different types of glasses is considered. These glasses are sodium borosilicate glasses (see Chapters Two and Three), sodium aluminosilicate glasses (see Chapter Four) and sodium aluminoborosilicate glasses (see Chapter Five). For sodium borosilicate glasses, which are widely used for producing laboratory glassware, optical components, sealing materials, etc., three different types of glasses, $(Na_2O)_{0.2}[(BO_{1.5})_x(SiO_2)_{1-x}]_{0.8}$, $(Na_2O)_{0.2}(B_2O_3)_x(SiO_2)_{0.8-x}$ and $(Na_2O)_{0.17}(B_2O_3)_x(SiO_2)_{0.8-x}$, are investigated.

1.6 Water in Oxide Glasses

Water can be introduced into oxide glasses by moist raw materials used to make glasses or from water vapor being present in the atmosphere inside the furnace(s) used for melting and annealing. Water exists in all kinds of oxide glasses either as hydroxyl groups bonded to glass network formers and/or as molecular

water residing in interstices between the building blocks of a glass network [2] and can influence various oxide glass properties. For instance, an increase of the water content reduces the viscosity of silica and soda-lime glasses [37], the glass transition temperature and the chemical durability of sodium silicate glasses [38], and increases the electrical resistivity of sodium silicate glasses [39] and the rates of structural relaxation and recrystallization of vitreous silica [40].

At elevated temperatures oxide glasses can take up water from the atmosphere. After water molecules have been incorporated into glasses, they can either diffuse further into glass samples or react with the glass network to form hydroxyl groups. A model for the diffusion of water in silica glass has been proposed by Doremus [41] in which molecular water moves through the glass and reacts with the glass network forming relatively immobile hydroxyl groups, see Eq. (1.12).

$$\mathrm{Si{-}O{-}Si + H_2O\ (glass) \rightleftharpoons Si{-}OH + HO{-}Si} \tag{1.12}$$

The equilibrium constant of the glass-molecular water reaction, K_{eq}, is

$$K_{eq}' \approx \frac{[OH]^2}{[Si{-}O{-}Si]\cdot[H_2O]} \propto \frac{[OH]^2}{[H_2O]} = K_{eq} \tag{1.13}$$

If local equilibrium is reached, the concentration of hydroxyl groups is proportional to the square root of the concentration of dissolved molecular water. Applying the solution of Fick's 2nd law coupled with the chemical reaction (Eq. (1.12)), the equation describing the diffusion of molecular water can be written as [15]

$$\frac{\partial [H_2O]}{\partial t} = D_{H_2O} \cdot \frac{\partial^2 [H_2O]}{\partial x^2} - \frac{1}{2} \cdot \frac{\partial [OH]}{\partial t} \tag{1.14}$$

Since

$$\frac{\partial [H_2O]}{\partial x} = \frac{2\,[OH]}{K_{eq}} \cdot \frac{\partial [OH]}{\partial x} \tag{1.15}$$

and the change of the concentration of molecular water with time is much smaller than that of the hydroxyl groups in silica glasses at equilibrium at relatively low water pressures, Eq. (1.14) becomes

$$\frac{\partial [OH]}{\partial t} = \frac{\partial}{\partial x}\left(\frac{4 [OH] D_{H_2O}}{K_{eq}} \cdot \frac{\partial [OH]}{\partial x} \right) \tag{1.16}$$

Eq. (1.16) has the form of the Fick's 2nd Law with a concentration-dependent diffusion coefficient. Therefore the effective chemical diffusion coefficient of hydroxyl groups, $\tilde{D}_{eff,\,OH}$, can be written as

$$\tilde{D}_{eff,OH} = 4 \frac{[OH]}{K_{eq}} D_{H_2O} \tag{1.17}$$

This effective chemical diffusion coefficient of hydroxyl groups increases with the concentration of the hydroxyl groups, which is in agreement with experimental observations for the diffusion of water into vitreous silica at relatively low water pressures at high temperatures (above 900 °C or from 700 to 900 °C when there are quenched-in defects or strains in silica glasses) [41-44]. However, in glasses with high water contents, the effective chemical diffusion coefficient of water increases almost exponentially with the increase of the hydroxyl content [45,46]. At low temperature, the diffusion depth of water increases linearly instead of proportionally to the square root of the diffusion time in glasses [47,48]. Tomozawa [49] proposed that structural relaxation, additional stress and swelling induced by water incorporation are at least partially responsible for these diffusion behaviors being different from that described by the Doremus model [41]. He modified the Doremus model by assuming that water also diffuses in the silica glass by the motion of OH groups in addition to diffusion of molecular water [50]. In this way, the total water concentration, [water], can be expressed as the sum of the

concentrations of water molecules, $[H_2O]$, and of hydroxyl groups, [OH], i.e., [water] = $[H_2O]$ + ½ [OH]. Zhang et al. [51] and Dieckmann [52] both derived diffusion equations for the diffusion of water in the form of water molecules and hydroxyl groups in silicates glasses and in crystalline and amorphous oxides, respectively.

$$\frac{\partial\left([H_2O] + \frac{1}{2}[OH] \right)}{\partial t} = \frac{\partial}{\partial x}\left(D_{H_2O} \frac{\partial [H_2O]}{\partial x} + \frac{1}{2} D_{OH} \frac{\partial [OH]}{\partial x} \right) \tag{1.18}$$

Since the Fick's 2nd Law for the diffusion of water with a concentration-dependent diffusion coefficient can be written as

$$\frac{\partial [water]}{\partial t} = \frac{\partial}{\partial x}\left(\tilde{D}_{eff,water} \frac{\partial [water]}{\partial x} \right) \tag{1.19}$$

$\tilde{D}_{eff,\ water}$ can be described in terms of the chemical diffusion coefficients of water D_{H_2O} and of hydroxyl groups D_{OH}:

$$\tilde{D}_{eff,water} = D_{H_2O} \frac{\partial [H_2O]}{\partial [water]} + \frac{1}{2} D_{OH} \frac{\partial [OH]}{\partial [water]} \tag{1.20}$$

When the total water content is smaller than 0.2 wt%, almost all water in silicate glasses is in the form of hydroxyl groups [53], i.e., [water] ≈ [OH]/2. Eq. (1.15) can be rewritten as:

$$\frac{\partial [H_2O]}{\partial x} = \frac{4[OH]}{K_{eq}} \cdot \frac{\partial [water]}{\partial x} \tag{1.21}$$

$$\frac{\partial [H_2O]}{\partial [water]} = \frac{4[OH]}{K_{eq}} \tag{1.22}$$

$\tilde{D}_{eff,\ water}$ or $\tilde{D}_{eff,OH}$ in this case can be written as:

$$\tilde{D}_{eff,OH} = D_{OH} + 4\frac{[OH]}{K_{eq}} D_{H_2O} \tag{1.23}$$

When $D_{H_2O} \gg D_{OH}$, Eq. (1.23) is identical with Eq. (1.17).

Doremus [54] in 1995 used the same concepts as discussed when introducing Eqs. (1.12) and (1.13) and applied it to the diffusion of water in silica glass under different conditions including at non-equilibrium conditions, i.e., when the surface concentration and the diffusion coefficient of hydroxyl groups are both time-dependent. At temperatures above 900 °C, equilibrium of the reaction shown in Eq. (1.12) can be reached quickly. The almost immobile hydroxyl groups can at this high temperature move far enough into the glass to meet other OH groups to form water molecules. At temperatures between 700 and 900 °C, when there are quenched-in defects or strains in the silica glass, the mechanism proposed by Doremus in Ref. [41] still applies. However, when these defects or strains have been annealed out of the silica glass, the OH groups cannot diffuse far enough into the glass to reach other OH groups, especially at temperatures below 500 °C. In this case, equilibrium cannot be reached within a short time and the surface reaction becomes the controlling step, i.e., before a constant water concentration is reached, the concentration of reacted hydroxyl groups near the surface increases with time.

Since water can diffuse into glasses in addition to the original water existing in glass samples and can influence glass properties, the presence of water should not be ignored in any glass characterization. Therefore the initial water content in all glass samples considered in this study was measured using Fourier Transform Infrared Spectroscopy (FTIR) and whether these glasses take up water at the temperature range of the tracer diffusion annealing was determined. Comparing to the water contents found in glasses studied by Tomozawa [49], which are above 1 wt%, the water concentrations in the oxide glasses studied in this work are at a

much lower (ppm) level. With such small water contents, almost all of the water in glass samples exists as OH groups [49]. Lu [55] studied the diffusion of water in calcium aluminosilicate glasses of the type $(CaO{\cdot}Al_2O_3)_x(2SiO_2)_{1-x}$ with x varying from 0.2 to 0.9. Data for the spatial distribution of OH groups obtained by using FTIR and analyzing cross-sections of glass samples annealed in wet air were found to be very well modeled by using one single effective chemical diffusion coefficient of water. This water diffusion coefficient was assumed to be independent of the OH content. One single water diffusion coefficient not varying with the OH concentration was also used in this work when analyzing the uptake of water by sodium boroaluminosilicate glasses. Details on this topic will be considered in Chapter Four.

REFERENCES

[1] A.K. Varshneya, Fundamentals of Inorganic Glasses, [1994], Academic Press, Inc., San Diego, CA, U.S.A.

[2] J.E. Shelby, Introduction to Glass Science and Technology, 2nd Ed., [2005], The Royal Society of Chemistry, Cambridge, U.K.

[3] W.H. Zachariasen, “The Atomic Arrangement in Glass,” Journal of the American Chemical Society, **54** [1932] 3841-3851.

[4] A. Smekal and W. Klemm, “Mechanical Measurement of Chemical Bond Strength,” Monatshefte für Chemie, **82** [1951] 411-421.

[5] K.H. Sun, "Fundamental Condition of Glass Formation," Journal of the American Ceramic Society, **30** (9) [1947] 277-281.

[6] H. Rawson, Inorganic Glass-Forming Systems, [1967] Academic Press, London, U.K.

[7] W.D. Kingery, H.K. Brown and D.R. Uhlmann, Introduction to Ceramics, 2nd Ed., [1976], John Wiley & Sons Inc., New York, U.S.A.

[8] G.N. Greaves, "EXAFS and the Structure of Glass," Journal of Non-Crystalline Solids, **71** (1-3) [1985] 203-217.

[9] M.E. Milberg, J.G. O’Keefe, R.A. Verhelst and H.O. Hooper, “Boron Coordination in Sodium Borosilicate Glasses,” Physics and Chemistry of Glasses, **13** (3) [1972] 79-84.

[10] Y.H. Yun and P.J. Bray, “Nuclear Magnetic Resonance Studies of Glasses in the System Na_2O-B_2O_3-SiO_2,” Journal of Non-Crystalline Solids, **27** (3) [1978] 363-380.

[11] Y.H. Yun, S.A. Feller and P.J. Bray, “Correction and Addendum to 'Nuclear Magnetic Resonance Studies of Glasses in the System Na_2O-B_2O_3-SiO_2',” Journal of Non-Crystalline Solids, **33** (2) [1979] 273-277.

[12] W.J. Dell, P.J. Bray and S.Z. Xiao, “^{11}B NMR Studies and Structural Modeling of Na_2O-B_2O_3-SiO_2 Glasses of High Soda Content,” Journal of Non-Crystalline Solids, **58** (1) [1983] 1-16.

[13] J.F. Stebbins and Z. Xu, “NMR Evidence for Excess Non-Bridging Oxygen in an Aluminosilicate Glass,” Nature, **390** (6655) [1997] 60-62.

[14] J.F. Stebbins, J.V. Oglesby and S. Kroeker, “Oxygen Triclusters in Crystalline $CaAl_4O_7$ (Grossite) and in Calcium Aluminosilicate Glasses: ^{17}O NMR,” American Mineralogist, **86** (10) [2001] 1307-1311.

[15] J. Crank, The Mathematics of Diffusion, 2nd Ed., [1975], Clarendon Press, Oxford, U.K.

[16] B.J. Wilson, The Radiochemical Manual, 2nd Ed., [1966], The Radiochemical Centre, Amersham, U.K.

[17] P. Shewmon, Diffusion in Solids, 2nd Ed., [1989] The Minerals, Metals and Materials Society, Warrendale, PA, U.S.A.

[18] A.D. Le Claire, “Correlation Effects in Diffusion in Solids,” Physical Chemistry - an Advanced Treatise, Ed.H. Eyring, D. Henderson and W. Jost, **Vol. X** (Chap. 5) [1970] 261-330, Academic Press, New York, U.S.A.

[19] J.O. Isard, “The Haven Ratio in Glasses,” Journal of Non-Crystalline Solids, **246** (1-2) [1999] 16-26.

[20] Y. Haven and B. Verkerk, “Diffusion and Electrical Conductivity of Sodium Ions in Sodium Silicate Glasses,” Physics and Chemistry of Glasses, **6** (2) [1965] 38-45.

[21] H.L. Downing, N.L. Peterson and H. Jain, "Mixed Isotope Electrical Conductivity in Lithium Borate Glasses," Journal of Non-Crystalline Solids, **50** (2) [1982] 203-213.

[22] S. Voss, A.W. Imre and H. Mehrer, “Mixed-alkali Effect in Na-Rb Borate Glasses: a Tracer Diffusion and Electrical Conductivity Study,” Physical Chemistry Chemical Physics, **6** (13) [2004] 3669-3675.

[23] A. Bunde, M.D. Ingram, P. Maass and K.L. Ngai, “Diffusion with Memory - a Model for Mixed Alkali Effects in Vitreous Ionic Conductors,” Journal of Phyics A - Mathematical and General, **24** (15) [1991] L881-L886.

[24] A. Bunde, M.D. Ingram and P. Maass, "The Dynamic Structure Model for Ion Transport in Glasses," Journal of Non-Crystalline Solids, **172-174** (Pt.2) [1994] 1222-1236.

[25] R. Kirchheim, “Hydrogen Solubility and Diffusivity in Defective and Amorphous Metals,” Progress in Materials Science, **32** (4) [1988] 261-325.

[26] R. Kirchheim, “Interstitial Diffusion in Glasses and the Mixed Alkali Effect,” Diffusion in Amorphous Materials, [1994] The Minerals, Metals and Materials Society, Warrendale, PA, U.S.A.

[27] R. Kirchheim, “Diffusion of Hydrogen and Other Interstitials in Disordered and Amorphous Materials,” Defect and Diffusion Forum, **143-147** (Pt.2) [1997] 911-925.

[28] R. Kirchheim, “The Mixed Alkali Effect as a Consequence of Network Density and Site Energy Distribution,” Journal of Non-Crystalline Solids, **272** (2-3) [2000] 85-102.

[29] R. Kirchheim and D. Paulmann, “The Relevance of Site Energy Distribution for the Mixed Alkali Effect,” Journal of Non-Crystalline Solids, **286** (3) [2001] 210-223.

[30] A. Magistris, G. Chiodelli and M. Duclot, “Silver Borophosphate Glasses: Ion Transport, Thermal Stability and Electrochemical Behavior,” Solid State Ionics, **9/10** (Pt.1) [1983] 611-615.

[31] V.K. Deshpande, A. Pradel and M. Ribes, “The Mixed Glass Former Effect in The Li_2S : SiS_2 : GeS_2 System,” Materials Research Bulletin, **23** (3) [1988] 379-384.

[32] M. Tatsumisago, T. Minami and M. Tanaka, “Properties of Highly Ionic Conducting Li_4SiO_4-Li_3BO_3 Glasses Prepared by Rapid Quenching,” Glastechnische Berichte, **56** (Pt.2) [1983] 945-950.

[33] M. Tatsumisago, N. Machida and T. Minami, “Mixed Anion Effect in Conductivity of Rapidly Quenched Li_4SiO_4-Li_3BO_3 Glasses” (in Japanese), Yogyo Kyokaishi, **95** (2) [1987] 197-201.

[34] L.F. Maia and A.C.M. Rodriguez, “Electrical Conductivity and Relaxation Frequency of Lithium Borosilicate Glasses,” Solid State Ionics, **168** (1-2) [2004] 87-92.

[35] T. Tsuchiya and T. Moriya, “Anomalous Behavior of Physical and Electrical Properties in Borophosphate Glasses Containing R_2O and Vanadium(V) Oxide,” Journal of Non-Crystalline Solids, **38-39** (1) [1980] 323-328.

[36] V.A. Tsekhomskii, O.V. Mazurin and K.K. Evstrop'ev, “The Nature of Conductivity of Aluminosilicate Glasses,” Soviet Physics, Solid State, **5** (2) [1963] 586-589.

[37] H. Scholze, “Gases and Water in Glass,” Glass Industry, **47** (10) [1966] 546-551.

[38] M. Tomozawa, C.Y. Erwin, M. Takata and E.B. Watson, “Effect of Water Content on the Chemical Durability of $Na_2O{\cdot}3SiO_2$ Glass,” Journal of the American Ceramic Society, **65** (4) [1982] 182-183.

[39] M. Takata, J. Acocella, M. Tomozawa and E.B. Watson, “Effect of Water Content on the Electrical Conductivity of Alkali Silicate ($Na_2O{\cdot}3SiO_2$) Glass,” Journal of the American Ceramic Society, **64** (12) [1981] 719-724.

[40] F.E. Wagstaff, S.D. Brown and I.B. Cutler, “The Effect of H_2O and O_2 Atmospheres on the Crystallization of Vitreous Silica,” Physics and Chemistry of Glasses, **5** (3) [1964] 76-81.

[41] R.H. Doremus, “The Diffusion of Water in Fused Silica,” in “Reactivity of Solids,” edited by J.N. Mitchell, R.C. Devris, R.W. Roberts and P. Cannon, John Wiley, New York, U.S.A. [1969] 667-673.

[42] R. Pfeffer and M. Ohring, “Network Oxygen Exchange During Water Diffusion in Silicon Dioxide,” Journal of Applied Physics, **52** (2) [1981] 777-784.

[43] M. Tomozawa, “Concentration Dependence of the Diffusion Coefficient of Water in Silica Glass,” Journal of the American Ceramic Society, **68** (9) [1985] C251-C252.

[44] M. Helmich and F. Rauch, “The Mechanism of Diffusion of Water in Silica Glass,” Glastechnische Berichte, **66** (8) [1993] 195-200.

[45] R.F. Bartholomew and H.L. Hoover, “Infrared Technique for Measuring Water Profiles in Hydrosilicate Glass,” Glastechnische Berichte, **56** (13) [1983] 671-676.

[46] M. Nogami and M. Tomozawa, “Diffusion of Water in High Silica Glasses at Low Temperature,” Physics and Chemistry of Glasses, **25** (3) [1984] 82-85.

[47] Y. Moriya and M. Nogami, “Hydration of Silicate Glass in Steam Atmosphere,” Journal of Non-Crystalline Solids, **38-39** (2) [1980] 667-672.

[48] M. Tomozawa, S. Ito and J. Molinelli, “Hygroscopicity of Glasses with High Water Content,” Journal of Non-Crystalline Solids, **64** (1-2) [1984] 269-278.

[49] M. Tomozawa, “Water in Glass,” Journal of Non-Crystalline Solids, **73** (1-3) [1985] 197-204.

[50] M. Tomozawa, “Concentration Dependence of The Diffusion Coefficient of Water in SiO_2 Glass,” Journal of the American Ceramic Society, **18** (9) [1985] C251-C252.

[51] Y.X. Zhang, E.M. Stolper and G.J. Wasserburg, “Diffusion of a Multi-Species Component and Its Role in Oxygen and Water Transport in Silicates,” Earth and Planetary Science Letters, **103** (1-4) [1991] 228-240.

[52] R. Dieckmann, “Solution and Transport of Water in Oxides,” Materials at High Temperatures, **22** (1-2) [2005] 93-103.

[53] K.M. Davis and M. Tomozawa, “An Infrared Spectroscopic Study of Water-Related Species in Silica Glasses,” Journal of Non-Crystalline Solids, **201** (3) [1996] 177-198.

[54] R.H. Doremus, “Diffusion of Water in Silica Glass,” Journal of Materials Research, **10** (9) [1995] 2379-2389.

[55] H. Lu, “Diffusion of Sodium in Calcium Aluminosilicate Glasses with a 1:1 Molar Calcia-to-Alumina Ratio and the Influence of Water Taken Up from the Environment,” Ph.D. Thesis, Cornell University [2006].

CHAPTER TWO

SODIUM TRACER DIFFUSION IN GLASSES OF THE TYPE $(Na_2O)_{0.2}[(BO_{1.5})_x(SiO_2)_{1-x}]_{0.8}$

Section I*

2.1 Abstract

Sodium tracer diffusion coefficients, D^*_{Na}, have been measured in sodium borosilicate glasses of the type $(Na_2O)_{0.2}[(BO_{1.5})_x(SiO_2)_{1-x}]_{0.8}$ as a function of temperature and the composition parameter x. In these glasses, which can alternatively also be described by using the formula $Na_2O{\cdot}(2B_2O_3)_x{\cdot}(4SiO_2)_{1-x}$, one network former unit, SiO_2, is replaced by another one, $BO_{1.5}$, while keeping the sodium concentration constant. At constant temperature, the tracer diffusion coefficient of sodium as a function of x has a shallow minimum at about x = 0.7. At temperatures below about 310 °C the temperature dependences of the measured tracer diffusion coefficients are of Arrhenius-type; at higher temperatures one observes an increase in the temperature dependence with increasing temperature. The activation energy derived from sodium tracer diffusion data for temperatures up to about 310 °C increases about linearly with increasing x from about 70 to 80 kJ/mol. The pre-exponential factor as a function of x varies by about one order of magnitude and has a minimum at about x = 0.4. Values derived for the Haven-ratio are smaller than one and show a shallow minimum as a function of x at around x = 0.75. Furthermore, it was investigated whether there is a significant, directly measurable uptake of water during annealing in moist atmospheres and whether water taken up from moist atmospheres can influence the diffusion of sodium.

2.2 Introduction

Sodium borosilicate glasses are of great importance both technologically and

---

* Reprinted with permission from Xinwei Wu and Rüdiger Dieckmann, Journal of Non-Crystalline Solids, 357 (15) [2011] 2846-2856.

scientifically. Glasses of this type are widely used in many applications, ranging from chemically resistant laboratory glassware, host materials for encapsulation of radioactive waste to optical components and sealing materials [1]. These glasses also present a challenge for structural studies. Since they contain two network formers, B and Si, a larger variety of basic structural units than binary borate or silicate glasses may occur in addition to changes in the boron coordination when sodium oxide is added.

The so-called “mixed glass former effect” (MGFE) is a non-additive variation of transport properties as a function of the glass former composition resulting when one network former is replaced by another one. In order to study the effect of the variation of the glass former composition on the transport of ions, experimental data are needed which are related to the transport of ions of interest as a function of the network former composition.

In 1983, Magistris et al. [2] studied the electrical conductivity of AgI-doped and undoped Ag_2O-B_2O_3-P_2O_5 glasses and observed that a maximum in the electrical conductivity occurred at a $P_2O_5/(B_2O_3+P_2O_5)$-ratio of about 0.8. In these and all other glasses considered in the present article the electrical conduction is almost completely due to the movement of ions, i.e., the electrical conductivity is practically identical with the ionic conductivity. The authors called the non-linear variation of the ionic conductivity mentioned above “mixed anion effect”. Also in 1983, Tatsumisago et al. [3] investigated the ionic conductivity of Li_4SiO_4-Li_3BO_3 glasses, which were prepared by a twin-roller quenching technique, and found at 500 K an ionic conductivity maximum at a composition near to $40Li_4SiO_4$-$60Li_3BO_3$ with a very similar concentration of Li^+ in the whole range of glass formation. In a follow-up paper published in 1987, Tatsumisago et al. [4] used glass flakes instead of the previously used pelletized samples obtained by pulverizing and pressing glassy flakes of the same compositions as studied earlier [3] and measured ionic conductivities at temperatures of 300, 400 and 500 K. At a concentration of Li_3BO_3 between 50 and 60 mol%, an ionic conductivity maximum was observed at all temperatures investigated [4].

Maia and Rodriguez [5] published data for the ionic conductivity of glasses of the type $(Li_2O)_{0.4}[(B_2O_3)_x(Si_2O_4)_{1-x}]_{0.6}$ with $0 \leq x \leq 1$. Instead of a maximum, they observed a shallow minimum of the ionic conductivity at x-values of about 0.3 at 100, 150 and 200 °C. The authors proposed that this difference in comparison with the results from Tatsumisago's group [4] was related to different thermal histories of the different types of glasses investigated. In Maia and Rodriguez's study, the glasses were annealed, while Tatsumisago's group used rapidly quenched, unannealed glasses.

In 1985, Wakabayashi and Terai [6] published ionic conductivity data measured over a large temperature range from the solid to the liquid state and sodium tracer diffusion data measured at 600 °C for glasses of the type $2Na_2O \cdot yB_2O_3 \cdot (8-y)SiO_2$. The values of the Haven-ratio, obtained by combining sodium tracer diffusion coefficients with sodium diffusion coefficients calculated from ionic conductivity data, varied between 0.5 and 0.3 with a minimum at a Na_2O/B_2O_3 molar ratio of one. The ionic conductivity and the sodium tracer diffusion coefficient both decrease with increasing y until a Na_2O/B_2O_3 molar ratio of one is reached and remain almost unchanged when the B_2O_3 content is increased further. A follow-up paper by Wakabayashi and Terai [7] in the same year reports ionic conductivity data for the same type of glasses at 800 °C, which showed the same trend as the conductivity data measured at 600 °C in Ref. [6]. In the following year, Kaps et al. [8] measured ionic conductivities and sodium tracer diffusion coefficients in sodium borosilicate glasses. They studied compositions starting from $Na_2O \cdot 2SiO_2$ and then stepwise replaced Na_2O with B_2O_3 or replaced $Na_2O \cdot 2SiO_2$ by units of $0.5(B_2O_3) \cdot 2.5(SiO_2)$. The ionic conductivities and sodium tracer diffusion coefficients both decreased with an increase of the B_2O_3 concentration at constant Na_2O concentration. The values of the Haven-ratio varied between about 0.25 and 0.7. Sufficient data allowing any conclusions with regard to non-linearities of transport properties as a function of the network former composition in glasses with more than one network former are so far not available.

The composition dependence of the transport properties in alkali ion conducting glasses is related to structural changes. The structure of sodium borosilicate glasses has been studied by several groups. Based on low field, wide line ^{11}B data from Nuclear Magnetic Resonance (NMR) studies and on ideas provided by Krogh-Moe [9], Bray and co-workers proposed a detailed model for the atomic structure of sodium borosilicate glasses [10-13]. Added sodium may associate either with silicon, generating non-bridging oxygen atoms (NBO), i.e., SiO^-Na^+, or with boron, presumably converting trigonal BO_3 units to tetrahedral BO_4 units, the latter not generating any NBO [14]. In this model, when the molar ratio R (= $n_{Na_2O}/n_{B_2O_3}$; n = number of moles) is smaller than 0.5, all oxygen atoms introduced into glass with the addition of Na_2O are proposed to be consumed by converting trigonal BO_3 units to tetrahedral BO_4 units. In this case, the fraction of boron atoms in fourfold coordination, N_4, is equal to R. The sodium ions neutralize the net negative charge of the tetrahedral BO_4 units. There are no or nearly no non-bridging oxygen atoms present in this case [11]. Milberg et al. [15] found that in this range, $R < 0.5$, boron- and silicon-based networks do not mix with each other. Therefore, the glass can be treated as a binary sodium borate glass diluted by silica. However, when the molar concentration ratio R is larger than 0.5, the situation becomes more complicated. At $R > 0.5$, sodium is distributed between boron and silicon and the concentration of NBO depends on the molar ratio K (= $n_{SiO_2}/n_{B_2O_3}$). That such a partitioning of sodium occurs was confirmed by Soules et al. [16] based on the results of molecular dynamics (MD) calculations. The fraction of NBO increases with an increasing content of Na_2O at a fixed content of SiO_2 and with an increasing content of silica at a fixed content of Na_2O [15]. The existing knowledge on the structure does not allow any detailed conclusions with regard to diffusion paths and/or the height of barriers involved in the motion of sodium ions and therefore is insufficient for predicting the behavior of ion mobilities as a function of the glass composition.

Very important factors influencing properties of glasses are structure and chemical composition. In addition, the types and concentrations of impurities can

also play a critical role. On an atom-for-atom basis, the effect of oxide impurities is most pronounced when the impurity species is water, usually present in the form of hydroxyl (OH) [17]. All oxide glasses contain chemically bound water, which may occur in the form of hydroxyl bonded to the basic building blocks of the network structure and as molecular water dispersed in interstices of the network. Hydroxyl can be introduced into glasses in many ways, for example, by raw materials used to make glasses. Water has a much larger effect on some properties of oxide glasses per unit of concentration than any other oxide component. It can change the glass transition temperature, the viscosity, the density, the refractive index and the dielectric constant of glasses [17].

In addition, glasses can take up water from the environment, especially at elevated temperatures. Doremus [18] proposed that molecular water is the mobile diffusing species and that molecular water moves through the glass until it encounters an energetically favorable oxygen bridge site to form relatively immobile hydroxyl groups by the following reactions:

$$H_2O\,(gas) \rightleftharpoons H_2O\,(glass) \tag{2.1}$$

and

$$R\text{–}O\text{–}R' + H_2O\,(glass) \rightleftharpoons R\text{–}O\text{–}H + H\text{–}O\text{–}R' \tag{2.2}$$

where R and R' denote parts of the glass network. Since the hydroxyl groups are relatively immobile and practically do not contribute to the transport of water within the glass matrix, water molecules must diffuse in and out of the glass network to form or remove hydroxyl groups. Since water can significantly influence some properties of glasses, including the diffusivity of ions, the presence of water must not be ignored in any glass characterization and structure discussion.

One goal of this study is to experimentally determine the composition and temperature dependences of sodium tracer diffusion coefficients for sodium borosilicate glasses of the type $(Na_2O)_{0.2}[(BO_{1.5})_x(SiO_2)_{1-x}]_{0.8}$. An alternative formula for such glasses is $Na_2O{\cdot}(2B_2O_3)_x{\cdot}(4SiO_2)_{1-x}$. The characteristic feature of the

selected composition join is the replacement of one type of network unit, SiO_2, by a second one, $BO_{1.5}$, while keeping the sodium oxide content constant. Another goal is to examine the composition dependence of parameters such as the activation enthalpy of the sodium tracer diffusion and the pre-exponential factor of the sodium tracer diffusion coefficient. A third goal is to determine the variation of the Haven-ratio with the glass composition and to relate it to the glass structure. Finally, whether or not water taken up from moist atmospheres during diffusion-annealing influences the sodium tracer diffusion is also a topic of interest.

2.3 Experiments

The following sections are concerned with details of the glass samples used in this study, their characterization with regard to water being present in them and their density, and of the sodium tracer diffusion experiments performed, including the derivation of values for sodium tracer diffusion coefficients from their results. Errors related to the results obtained for water contents, densities and tracer diffusivities are addressed in Section 3 where the results of this study are reported.

2.3.1 Glass Samples

Samples of glasses along the compositional join $(Na_2O)_{0.2}[(BO_{1.5})_x(SiO_2)_{1-x}]_{0.8}$ with x varying from 0 to 1 in steps of 0.1 were prepared and provided by Corning Inc. Fig. 2.1a shows a composition triangle for the system Na_2O-$BO_{1.5}$-SiO_2 and Fig. 2.1b shows such a triangle for the system Na_2O-B_2O_3-SiO_2 using the more traditional endmember B_2O_3 instead of $BO_{1.5}$; in these figures circles indicate the location of the specific compositions considered in this study. The nominal and the actual compositions of the sodium borosilicate glasses used in this study, the latter determined by chemical analyses at Corning Inc., are reported in Table 2.1. To make these glass samples, batches of glasses with different compositions were prepared from reagent grade chemicals which were turbula-mixed and calcined. The powder mixtures were melted at 1450 °C in platinum crucibles and held for 6 hours. After that, each melt was poured hot and rolled into thin sheet, which was later ground into small cullets. These cullets were remelted at different melting

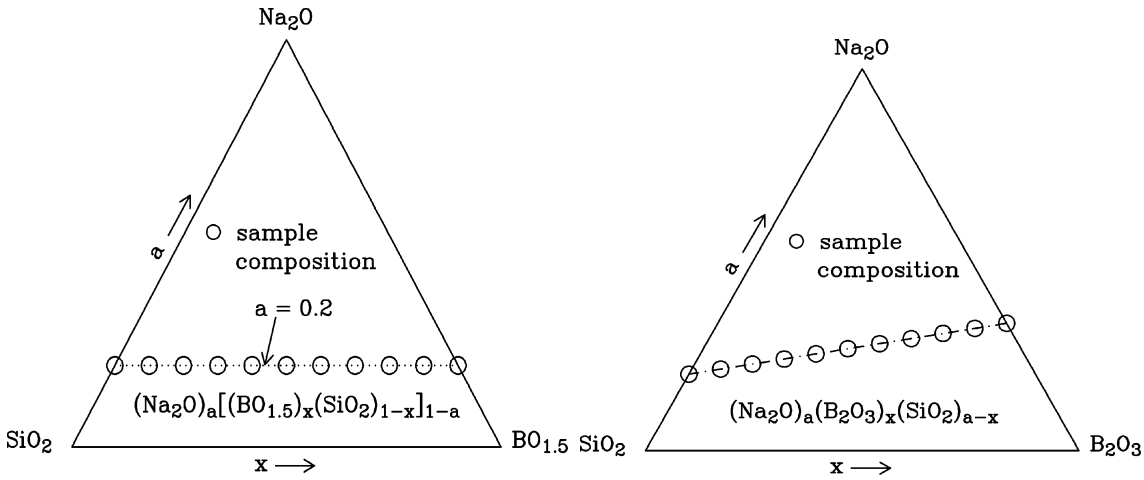

Fig. 2.1: Composition triangles for the systems (a) Na_2O-$BO_{1.5}$-SiO_2 and (b) Na_2O-B_2O_3-SiO_2. The circles in the diagrams denote the compositions of the sodium borosilicate glasses of the type $(Na_2O)_{0.2}[(BO_{1.5})_x(SiO_2)_{1-x}]_{0.8}$ considered in this article.

Table 2.1: Nominal and actual compositions, R- and K-ratios ($R = n_{Na_2O}/n_{B_2O_3}$ and $K = n_{SiO_2}/n_{B_2O_3}$ determined based on the actual compositions), glass transition temperature and density values of the sodium borosilicate glasses of the type $(Na_2O)_{0.2}[(BO_{1.5})_x(SiO_2)_{1-x}]_{0.8}$ considered in this study. The actual compositions were obtained by chemical analyses performed by Corning Inc. The errors reported below for the density are the standard deviations obtained from the results of three density measurements for each glass composition. The true errors including systematic errors of the reported density values are estimated not to exceed ± 1 %.

x	nominal mol%			actual mol%			R	K	T_g (°C)	density (g/cm^3)	
	Na_2O	$BO_{1.5}$	SiO_2	Na_2O	$BO_{1.5}$	SiO_2					± error ($\times 10^{-3}$)
0	20	0	80	20.1	0.20	79.7			500	2.39	3.70
0.1	20	8	72	19.7	8.61	71.7	4.57	16.6	520	2.44	2.44
0.2	20	16	64	19.4	16.7	63.9	2.32	7.66	540	2.48	3.05
0.3	20	24	56	19.3	25.6	55.1	1.50	4.30	555	2.52	7.54
0.4	20	32	48	18.8	33.3	47.8	1.13	2.87	555	2.53	6.82
0.5	20	40	40	18.8	41.3	39.9	0.91	1.93	540	2.53	2.28
0.6	20	48	32	20.0	47.8	32.2	0.84	1.35	530	2.52	7.66
0.7	20	56	24	20.0	55.9	24.1	0.71	0.86	520	2.50	3.26
0.8	20	64	16	19.8	64.0	16.1	0.62	0.50	510	2.48	21.7
0.9	20	72	8	19.4	72.4	8.13	0.54	0.22	480	2.42	3.07
1	20	80	0	19.3	80.3	0.42	0.48	0.01	470	2.36	1.73

temperatures, ranging between 1200 and 1550 °C, depending on the glass composition, poured and formed into bars, and thereafter annealed for stress removal at 550 °C for 1 hour. This relatively short annealing, for several compositions above T_g, did not lead to any visible crystallization and/or densification. Finally, by cutting, grinding and polishing, suitable glass pieces were obtained.

As received, the samples were square sheets with dimensions of 10×10×1 mm with both large, plane-parallel surfaces having been polished. Very often, such glass samples were cut into quarters to have a larger number of samples available for tracer diffusion experiments. To avoid any contamination by alkali and alkaline-earth compounds, which may be introduced by fingerprints, all glass samples were cleaned ultrasonically in de-ionized water, acetone and ethanol. Tweezers were used thereafter to handle the glass samples for tracer diffusion and/or water-related experiments.

2.3.2 Water Content Measurements

A Bruker Optics Equinox 55 Fourier Transform Infrared (FTIR) Spectrometer was used to determine the initial water content of all glass samples by measuring the IR absorbance related to the presence of OH groups. The glass samples were first ultrasonically washed with de-ionized water, acetone, ethanol and finally, to minimize the adsorption of water on glass surfaces, the samples were dipped in HPLC grade acetone and then were dried in an oven at 130 °C for about ten minutes right before their water content was determined. After a continuous purge of the FTIR instrument by dry air, 64 accumulated scans were performed over a wavelength range between 400 and 4000 cm^{-1} using a KBr beam splitter and a deuterated triglycine sulfate (DTGS) detector to measure infrared spectra. The signal-to-noise ratio usually increases with an increasing number of scans. Since it was found that the results for the spectra did not significantly improve when more than 64 scans were performed, the number of scans was limited to 64.

Almost all water in silicate glasses is accommodated in the form of hydroxyl

groups at relatively small concentrations of water [17]. An IR band related to the stretching of Si-OH groups occurs at wavelengths between 3500 and 3700 cm^{-1}, depending on the glass composition. After drying in an oven, a sample to be investigated was rapidly inserted into the IR sample chamber which was continuously purged with dry air. Data collection started about 30 minutes after the sample was inserted. This reduced the water concentration in the optics bench of the spectrometer and therefore helped to avoid the contamination of the glass surface with water. More than 10 spectra were collected for each sample, each with 64 scans. The averaged interferogram from the 64 scans for each spectrum was Fourier-transformed into an IR spectrum by the software OPUS-NT (Version 3) associated with the instrument. The three spectra with the lowest noise levels for each sample were selected for further data analysis.

Based on the Beer-Lambert law, the average of the overall water concentration in the area of a glass plate through which the IR beam travels is

$$c_{H_2O} = \frac{1}{2} \cdot \frac{A_g}{\varepsilon_{OH} \cdot d_g} \cdot \frac{M_{H_2O}}{\rho_g} = \frac{A_g}{\varepsilon_{H_2O} \cdot d_g} \cdot \frac{M_{H_2O}}{\rho_g} \qquad (2.3)$$

with

$$A_g = -\log_{10}\left(\frac{I}{I_0}\right), \qquad (2.4)$$

where d_g (in cm) is the thickness of the glass sample, ε_{OH} is the molar absorption coefficient related to the overall concentration of Si-OH groups present in the glass (in $\ell/(mol_{OH} \cdot cm)$), c_{H_2O} is the mass fraction of H_2O in the glass, M_{H_2O} is the molar mass of H_2O (= 18.02 g/mol), ρ_g is the density of the glass (in g/cm^3), A_g is the measured absorbance of the glass and I/I_0 is the ratio between the transmitted and initial IR signals. The molar absorption coefficient of Si-OH groups is in good approximation one half of that related to the overall water present in the glass, i.e., $2\ \varepsilon_{OH} \approx \varepsilon_{H_2O}$; both of these coefficients refer to the stretching of Si-OH groups.

The molar absorption coefficients denoted in Eq. (2.3) and associated with the stretching of Si-OH groups are based on the assumption that practically all water

incorporated into the glass is accommodated in the form of OH groups. An absorption peak near 1600 cm^{-1} which would indicate the presence of molecular water was not observed. The value of the molar absorption coefficient may vary to some extent with the composition of the glass. Reliable data for the molar absorption coefficient for the sodium borosilicate glasses considered in this study are not available. However, all molar absorption coefficients for silicate glasses are of the same order of magnitude and the variations of them are within a factor of about two [19]. To avoid the problem of not knowing what the value of ε_{OH} exactly is, Eq. (2.3) was reorganized in such a way that all measurable parameters are grouped on the right hand side. This leads to Eq. (2.5).

$$c_{H_2O} \cdot \varepsilon_{OH} = \frac{1}{2} \cdot \frac{A_g}{d_g} \cdot \frac{M_{H_2O}}{\rho_g} \tag{2.5}$$

If ε_{OH} is assumed to be constant, any water concentration variation is proportional to that of the product $c_{H_2O} \cdot \varepsilon_{OH}$. If ε_{OH} is not constant, c_{H_2O} will vary somewhat differently with the glass composition than the product $c_{H_2O} \cdot \varepsilon_{OH}$ does.

2.3.3 Density Measurements

A glass pycnometer was used to measure the densities of as-received glasses using the Archimedean method. First, the pycnometer was filled with de-ionized water at approximately 22 °C and then its mass, m_{pw}, was measured using an analytical laboratory balance to a resolution of 0.1 mg. Thereafter, glass sample material was put into the pycnometer, the pycnometer was again filled with de-ionized water and its mass thereafter was recorded as m_{pws}. The mass of the glass sample in air was m_s. The density of the glass sample can then be calculated using Eq. (2.6).

$$\rho_g = \rho_w \cdot \frac{m_s}{m_s + m_{pw} - m_{pws}} \tag{2.6}$$

ρ_w is the density of water at 22 °C.

2.3.4 Tracer Diffusion Experiments

To study the diffusion of sodium in glass samples the radioactive isotope Na-22 was used. The energies associated with the γ-radiation resulting from the decay of Na-22 are 0.51 and 1.28 MeV [20]. The tracer was applied as a thin film. After diffusion-annealing residual radioactivities were measured as a function of the distance from the original sample surface by using a high resolution, high-purity Ge detector (EG&G Ortec). The data obtained were used to determine values of sodium tracer diffusion coefficients. Details of the experiments and of the evaluation of the measured data are given below.

2.3.4.1 Experimental Details

Before applying the radioactive tracer, each glass sample was pre-heated in an oven at 130 °C. Then small droplets of an aqueous solution containing Na-22 as a chloride were applied to the original sample surface by using a syringe. The use of pre-heated samples led to a rapid removal of water applied with the tracer solution and kept the time of interaction between water and the glass sample at a minimum. Thereafter the glass sample was transferred to a tube furnace with the side containing the radioactive tracer facing up for diffusion-annealing at a preset temperature in most cases in dry air at 1 atm total pressure. In very few cases, diffusion-annealing was performed in wet air to check for any possible influence of water taken up by a glass sample during diffusion-annealing on the sodium tracer diffusion. After removing the sample from the furnace, to eliminate any influence of surface diffusion on the measured residual radioactivity profiles, about 1 mm of sample material was ground off from each edge perpendicular to the surface where the tracer had been applied earlier. The sample was thereafter ultrasonically cleaned in water, dried and then glued onto a plane-parallel stainless steel sample holder with the surface onto which the tracer was applied facing up in preparation for measuring residual radioactivity profiles.

To obtain normalized residual radioactivity profiles, $A(x)/A(x=0)$ vs. x, first the initial radioactivity of a sample, $A(x=0)$, was measured using the detector denoted

before. This detector allows to measure the radiation related to the two energies denoted above separately. Then, the position of the original sample surface relative to the top surface of the sample holder onto which the sample was glued before was determined by using a digital indicator. To remove several micrometer thick layers from samples by grinding using a diamond wheel, a high precision grinding machine was used. This machine is equipped with a vacuum chuck that allows to hold a plane-parallel sample holder with a plane-parallel sample glued onto it in such a way that plane-parallel layers can be removed from the sample by grinding. Water is used as a coolant and to remove debris from the grinding area. After removing a layer, the sample was ultrasonically cleaned in water, dried and inserted into the chamber of the detector for measuring values for the residual radioactivity A(x) after removing material with the thickness x. The value of x was determined after the radioactivity measurement was completed and not before to allow the sample holder to adapt to the temperature present in the laboratory. This was done to avoid errors in length measurements related to thermal expansion. After measuring the location of the sample surface relative to that of the sample holder the value of x was determined. By stepwise removing layers from the sample a set of values for x and A(x) was determined allowing to calculate values for the sodium tracer diffusion coefficient as described in the next section.

2.3.4.2 Diffusion Mathematics

The thin film solution of Fick's second law applies for the diffusion of a tracer in a homogenous glass sample. The tracer concentration, $c_i(\xi,t)$, at a distance ξ from the surface after diffusion-annealing for the time, t, is given by Eq. (2.7) [21].

$$c_i(\xi,t) = \frac{Q_i}{\sqrt{\pi \cdot D_i^* \cdot t}} \cdot \exp\left(- \frac{\xi^2}{4\, D_i^* \cdot t} \right) \tag{2.7}$$

D_i^* is the tracer diffusion coefficient of the diffusing species i, in this study Na-22, and Q_i is the initial concentration of this tracer per unit area.

In principle, the intensity of the radiation measured by a detector is reduced due to absorption and scattering within the matter considered when radiation from the decay of a radioactive isotope passes through matter. In residual radioactivity measurements, the radiation emitted at different depths within a sample is absorbed by the matter between the surface and the location of the emission. The absorption coefficient, μ, is a measure of the degree of the absorption per unit length. The intensity of radiation decreases with the distance between the location of the emission and the surface of the sample following the Beer-Lambert law,

$$I = I_0 \cdot \exp(-\mu \cdot \xi), \tag{2.8}$$

where I and I_0 are the intensities of the radiation measured with and without passing through the material of interest and ξ is the distance between the location of the emission and the surface of the material.

In cases where the tracer penetration length and the absorption coefficient are both sufficiently small, the absorption of the radiation related to the decay of the radioactive isotope used in a tracer experiment within the sample is negligibly small and can be ignored for the data analysis. Based on previous experimental work on calcium aluminosilicate glasses [22] it is expected that μ has values on the order of 0.5 cm^{-1} for the type of glasses considered in this study. Such values, in combination with the profile lengths considered in this study, are sufficiently small to ignore absorption in the analysis of the results of the sodium tracer diffusion experiments performed in this study. Therefore an equation describing the normalized residual radioactivity, A(x,t)/A(x=0,t), as a function of the diffusion-annealing time, t, and the tracer diffusion coefficient of the species i, D_i^*, can be easily derived by departing from Eq. (2.7), ignoring any absorption and integrating as described in the first part of Eq. (2.9).

$$\frac{A(x,t)}{A(x=0,t)} = \frac{\int_x^\infty c_i(\xi,t) \cdot d\xi}{\int_0^\infty c_i(\xi,t) \cdot d\xi} = 1 - \mathrm{erf}\left(\frac{x}{2\sqrt{D_i^* \cdot t}} \right) \tag{2.9}$$

In order to determine values for the tracer diffusion coefficient of the species i, D_i^*, one can in principle fit Eq. (2.9) to experimental data for A(x,t)/A(x=0,t). However, to achieve a higher precision by more emphasizing the influence of data points obtained for larger penetration depths on the final result, it is better to fit the inverse function of the error function, erfi, to experimental data, see Eq. (2.10). This was done for all tracer diffusion experiments performed in this study.

$$\mathrm{erfi}\left(1 - \frac{A(x,t)}{A(x=0,t)}\right) = \frac{x}{2\sqrt{D_i^* \cdot t}} \qquad (2.10)$$

When a = erf(b), then b = erfi(a).

2.4 Results

2.4.1 Initial Water Content

Fig. 2.2 shows the values determined for the water content of as-received samples in the form of the product $c_{H_2O} \cdot \varepsilon_{OH}$ (in $(g_{H_2O}/kg_{glass}) \cdot (\ell/(mol_{OH} \cdot cm))$) as a function of the glass composition parameter x. For determining the data shown for the water content, density values corresponding to Eq. (2.11), see Section 4.2., were used. The standard deviations of the results obtained $c_{H_2O} \cdot \varepsilon_{OH}$ from the water concentration measurements, usually four for each glass composition, did not exceed about 5 %. Additional errors resulting from thickness measurements and from density data used to calculate values for $c_{H_2O} \cdot \varepsilon_{OH}$ are estimated to be of the order of 1 %, keeping the overall errors below about 6 %.

2.4.2 Densities of Glass Samples

The values determined pycnometrically for the densities of glasses of the type $(Na_2O)_{0.2}[(BO_{1.5})_x(SiO_2)_{1-x}]_{0.8}$ are listed in Table 2.1. The standard deviations obtained from the results of three density measurements for each glass composition were between about $2 \cdot 10^{-3}$ and $2 \cdot 10^{-2}$ g/cm^3, corresponding to between about ± 0.1 and ± 0.9 %. Although the laboratory balance used for determining densities was calibrated before the measurements, the true errors of

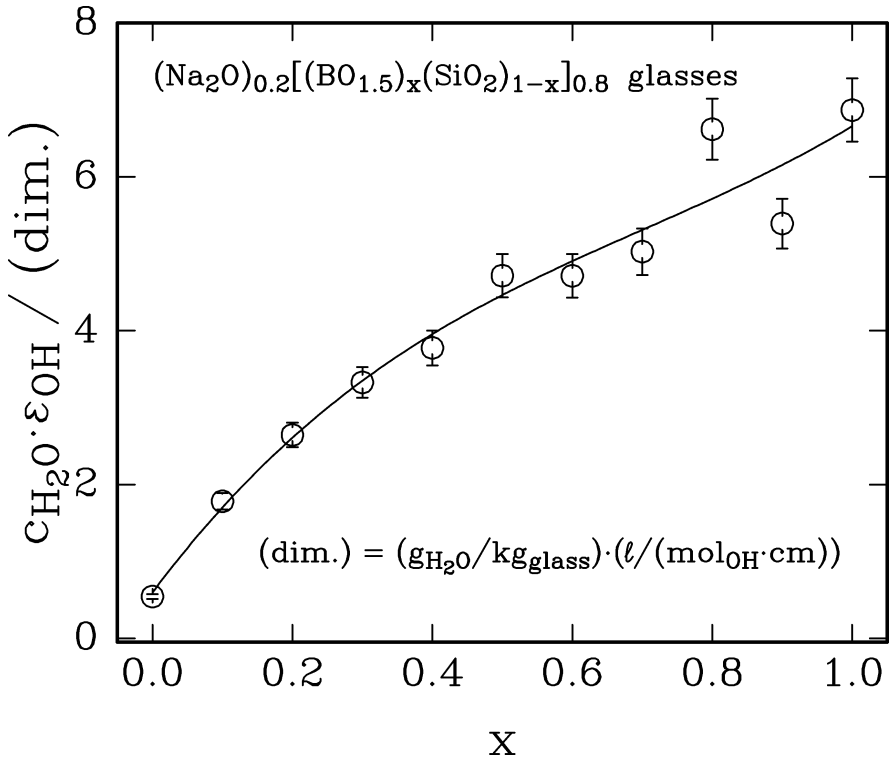

Fig. 2.2: Initial water contents of the sodium borosilicate glasses of the type $(Na_2O)_{0.2}[(BO_{1.5})_x(SiO_2)_{1-x}]_{0.8}$ obtained from Corning Inc. and considered in this article. The concentrations were determined by FTIR measurements. One unit of the y-axis corresponds to an OH concentration of about 0.02 mol% if it is assumed that $\varepsilon = 40\ \ell/(mol_{OH} \cdot cm)$ for all glass compositions. The errors for the results of the water concentration were estimated to be smaller than ± 6 %.

the density values obtained are probably a little larger than those given above, probably up to about ± 1 % due to systematic errors. These density data are shown in Fig. 2.3 in comparison with density values from the literature [23] and some values determined recently by collaborators at Iowa State University on similar samples from the same batches of glass provided by Corning Inc. [24]. The density as a function of the composition parameter x has a maximum near x = 0.5.

2.4.3 Sodium Tracer Diffusion

A typical residual radioactivity profile of Na-22 obtained for an as-received glass sample of the composition $(Na_2O)_{0.2}[(BO_{1.5})_{0.3}(SiO_2)_{0.7}]_{0.8}$ after diffusion-annealing in dry air for about 68 h at 241 °C is shown in Fig. 2.4a. The curves displayed in this figure were obtained by fitting Eq. (2.9) to experimental data for A(x,t)/A(x=0,t). Values for the tracer diffusion coefficient of sodium, D^*_{Na}, were derived by fitting the inverse function of the error function, erfi, see Eq. (2.10), to experimental data as shown in Fig. 2.5a. The values determined for tracer diffusion coefficients of sodium diffusing in the sodium borosilicate glasses considered in this study in dry air are listed in Table 2.2. The errors reported in Table 2.2 are those obtained from fitting Eq. (2.10) to the normalized residual radioactivities. Additional errors related to the measurement of diffusion-annealing times, temperatures, profile lengths and net counts make the actual errors of the tracer diffusion coefficient values larger than those listed in Table 2.2. Based on past experiences, the real errors are estimated to be about 5 %. Fig. 2.4b shows a residual radioactivity diffusion profile of Na-22 obtained for a glass sample of the same composition as that considered in Fig. 2.4a, $(Na_2O)_{0.2}[(BO_{1.5})_{0.3}(SiO_2)_{0.7}]_{0.8}$, diffusion-annealed in wet air (with P_{H_2O} = 474 mbar) for about 103 h at 241 °C. Measured tracer diffusion coefficients for the diffusion of sodium in the glasses of interest in dry air at different temperatures between 208 and 508 °C are shown in Fig. 2.6 as a function of the glass composition.

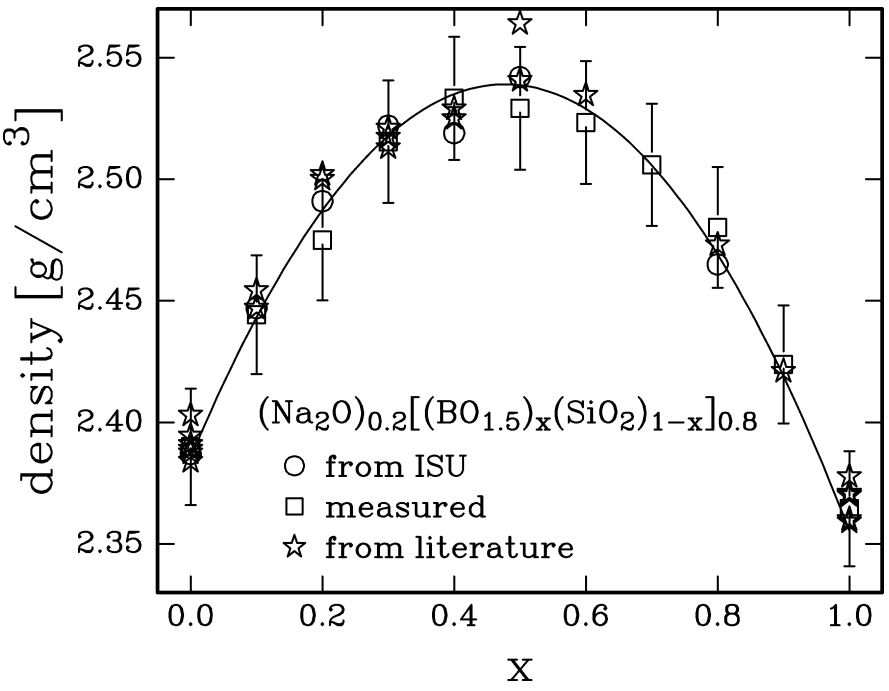

Fig. 2.3: Densities of glasses of the type $(Na_2O)_{0.2}[(BO_{1.5})_x(SiO_2)_{1-x}]_{0.8}$, measured in this study in comparison with data from the literature [23] and data recently measured by collaborators at Iowa State University [24]. The solid line has been generated by using Eq. (2.11). The error bars shown correspond to the upper error limit of ± 1 %, see Section 2.4.2.

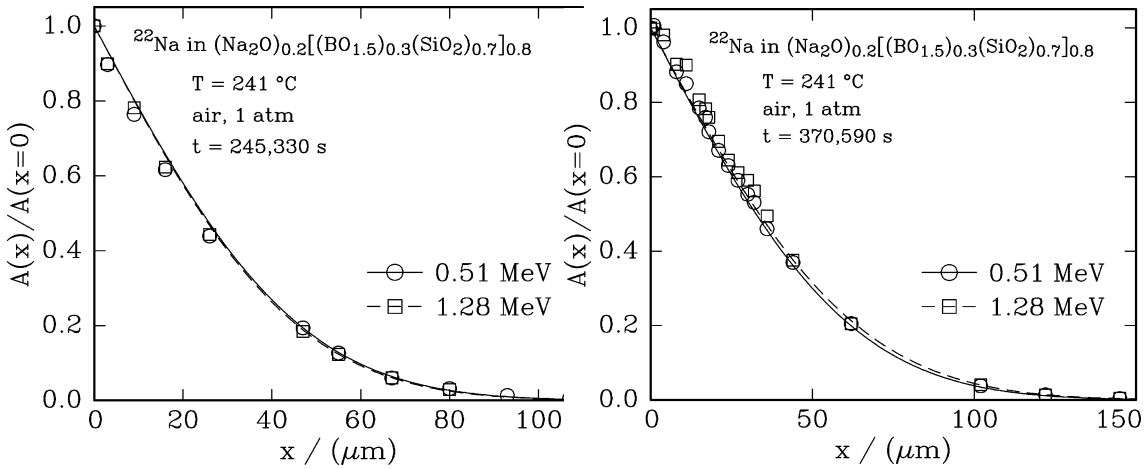

Fig. 2.4: Normalized residual radioactivity profiles of Na-22 observed in glass of the composition $(Na_2O)_{0.2}[(BO_{1.5})_{0.3}(SiO_2)_{0.7}]_{0.8}$ after diffusion-annealing for about 68 h in dry air at 241 °C (a) and after diffusion-annealing for about 103 h in wet air at 241 °C (b). The lines are from fits of Eq. (2.9) to the experimental data for different γ-energies.

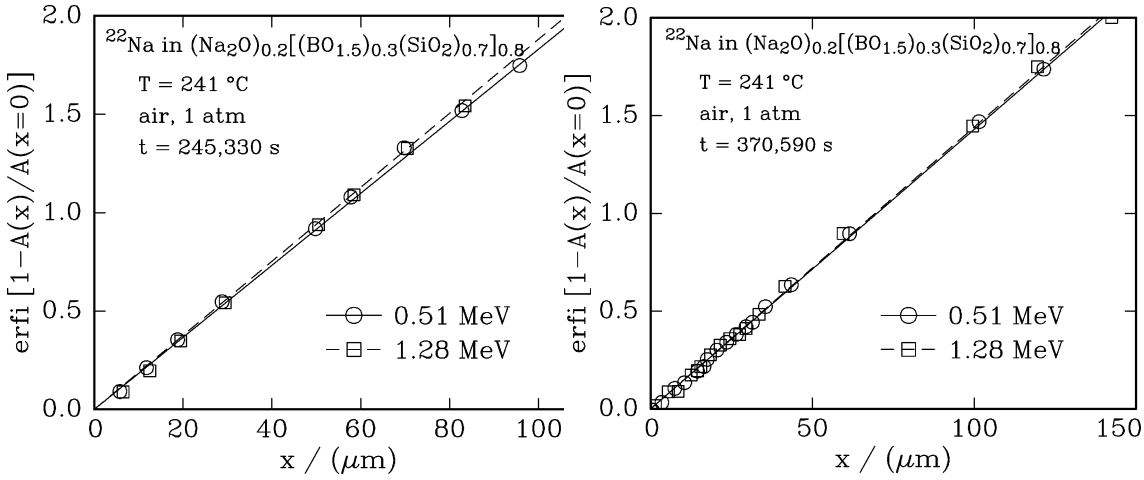

Fig. 2.5: Fits of Eq. (2.10) to normalized residual radioactivity data obtained (a) after diffusion-annealing for about 68 h in dry air at 241 °C and (b) after diffusion-annealing for about 103 h in wet air at 241 °C for glass of the composition $(Na_2O)_{0.2}[(BO_{1.5})_{0.3}(SiO_2)_{0.7}]_{0.8}$ to determine values for sodium tracer diffusion coefficients.

Table 2.2: Data for sodium tracer diffusion coefficients for sodium borosilicate glasses of the type $(Na_2O)_{0.2}[(BO_{1.5})_x(SiO_2)_{1-x}]_{0.8}$ at different temperatures and compositions. "– LD" stands for "$-\log_{10}(D^*_{Na}/(cm^2/s))$". Empty fields indicate that tracer diffusion data were not determined for the conditions the fields refer to. The errors reported in the table are from least squares fits of Eq. (2.10) to normalized residual radioactivity profiles. The overall errors are estimated to be on the order of 5 %, see also Section 3.3. Data in columns marked by * are weighted averages from several experiments.

T = 208 °C											
x	0	0.1	0.2	0.3	0.4	0.5	0.6	0.7	0.8	0.9	1
- LD	10.421	10.634	10.794	10.959	11.143	11.231	11.347	11.434	11.410	11.336	11.300
error ±	0.011	0.009	0.017	0.037	0.010	0.025	0.017	0.038	0.011	0.018	0.005

T = 241 °C											
x	0	0.1	0.2	0.3*	0.4	0.5	0.6	0.7	0.8	0.9	1*
- LD	9.822	10.147	10.316	10.536	10.646	10.779	10.831	10.879	10.831	10.733	10.776
error ±	0.013	0.004	0.007	0.006	0.010	0.003	0.006	0.009	0.027	0.009	0.008

T = 274 °C											
x	0	0.1	0.2	0.3*	0.4	0.5	0.6	0.7	0.8*	0.9*	1*
- LD	9.561	9.756	9.907	10.062	10.234	10.300	10.394	10.326	10.382	10.323	10.177
error ±	0.010	0.006	0.006	0.006	0.006	0.008	0.009	0.005	0.006	0.005	0.010

T = 308 °C											
x	0	0.1	0.2	0.3*	0.4	0.5*	0.6*	0.7*	0.8*	0.9	1*
- LD	9.106	9.327	9.495	9.635	9.778	9.924	9.967	9.952	9.927	9.948	9.814
error ±	0.010	0.008	0.003	0.005	0.014	0.004	0.005	0.011	0.006	0.010	0.007

T = 343 °C											
x	0	0.1	0.2	0.3	0.4	0.5	0.6	0.7	0.8	0.9	1
- LD	8.733	8.938	9.069	9.271	9.375	9.503			9.524	9.444	9.496
error ±	0.003	0.003	0.005	0.005	0.004	0.004			0.005	0.004	0.010

T = 378 °C											
x	0	0.1	0.2	0.3	0.4	0.5	0.6	0.7	0.8	0.9	1
- LD	8.379	8.549	8.794	8.834	9.021	9.119		9.083	9.171	9.027	9.129
error ±	0.002	0.005	0.008	0.011	0.004	0.006		0.006	0.003	0.006	0.004

T = 452 °C											
x	0	0.1	0.2	0.3	0.4	0.5	0.6	0.7	0.8	0.9	1
- LD	7.789	7.987	8.155	8.295	8.418				8.510		
error ±	0.002	0.001	0.004	0.005	0.002				0.009		

T = 503 °C											
x	0	0.1	0.2	0.3	0.4	0.5	0.6	0.7	0.8	0.9	1
- LD	7.260				8.047				7.994		
error ±	0.003				0.002				0.003		

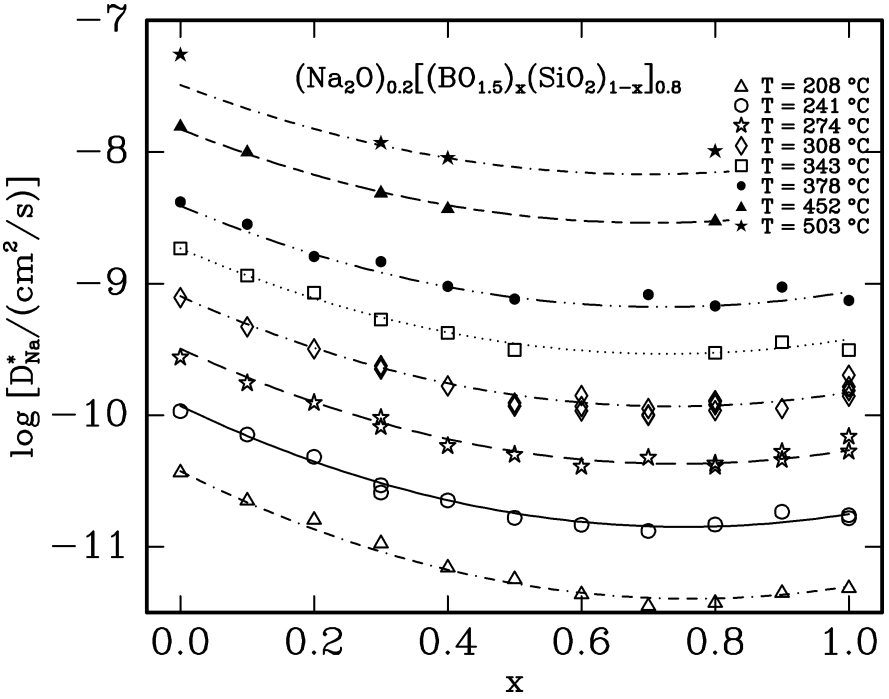

Fig. 2.6: Composition and temperature dependences of sodium tracer diffusion coefficients determined for sodium borosilicate glasses of the type $(Na_2O)_{0.2}[(BO_{1.5})_x(SiO_2)_{1-x}]_{0.8}$: experimental data in comparison with lines for isotherms derived by using an empirical equation, see Eq. (2.17). The errors obtained by fitting Eq. (2.10) to the experimental data are reported in Table 2.2 and are significantly smaller than the symbols used in the figure. The overall errors of the data points shown are estimated not to exceed ± 5 % corresponding to ± 0.021 in log [D^*_{Na}/(cm²/s)], i.e., approximately to the size of the symbols used in the figure.

2.5 Discussion

2.5.1 Initial Water Content

A molar absorption coefficient value typical for borosilicate glasses, about 40 $\ell/(mol_{OH} \cdot cm)$ [68], and data for the glass density given by Eq. (2.11) in Section 4.2. were used to estimate absolute values for the water content in the glasses investigated for all glass compositions. The concentration of water in these glasses was found to increase from about 13 weight ppm H_2O in the sodium silicate glass to about 170 weight ppm H_2O in the sodium borate glass. The water concentration is higher in boron-rich glasses compared to silica-rich ones and increases approximately linearly with the composition parameter x.

2.5.2 Densities and Molar Volume of Glass Samples

As shown in Fig. 2.3, the densities of glasses of the type $(Na_2O)_{0.2}[(BO_{1.5})_x(SiO_2)_{1-x}]_{0.8}$ measured in this study are in good agreement with densities from the literature [23] and also with such data recently determined by collaborators at Iowa State University [24]. The density data from the literature scatter to some extent due to the fact that different glass samples were used by different authors, e.g., glass samples with different thermal histories. The density of glasses of the type $(Na_2O)_{0.2}[(BO_{1.5})_x(SiO_2)_{1-x}]_{0.8}$ first increases when silicon is replaced by boron, goes through a maximum around x = 0.5, and then decreases. The line shown in Fig. 2.3 gives a good description of the density as a function of the composition parameter x; it was generated by using an empirical equation, Eq. (2.11).

$$\rho_{glass} = 2.38 + 0.64 \cdot x - 0.67 \cdot x^2 \qquad (2.11)$$

By considering the ratio between the molar mass and the density, the molar volume of the glass can be obtained. The resulting composition dependence of the molar volume shown in Fig. 2.7 was obtained by dividing the molar mass by density values corresponding to Eq. (2.11). It is found that the molar volume continuously decreases when x increases from 0 to 1. This indicates that the

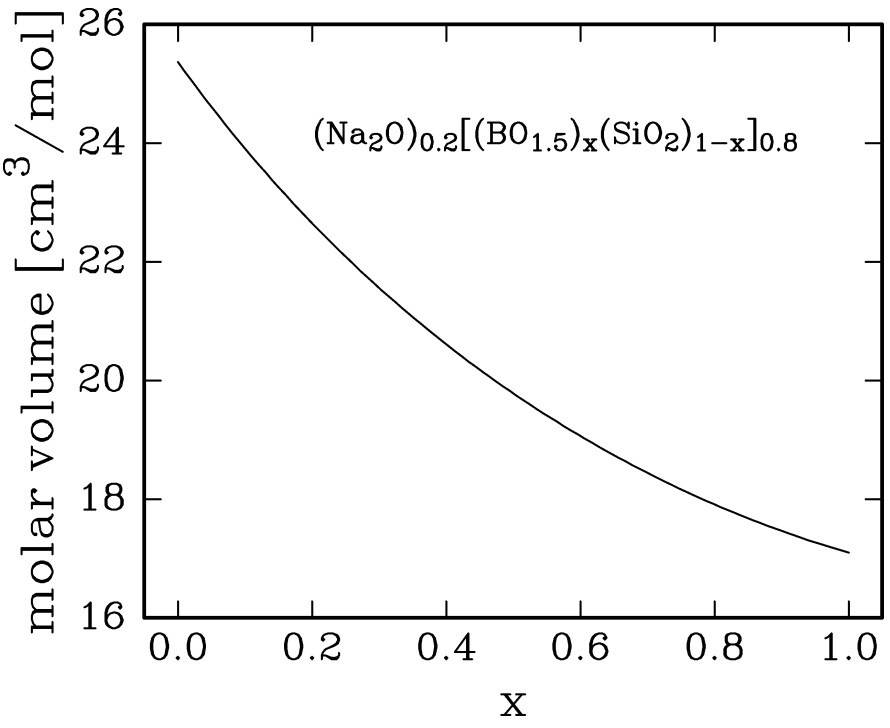

Fig. 2.7: Composition dependence of the molar volume of glasses of the type $(Na_2O)_{0.2}[(BO_{1.5})_x(SiO_2)_{1-x}]_{0.8}$.

structure of the glasses considered in this study becomes more compact when the glass former silicon is replaced by boron.

2.5.3 Sodium Tracer Diffusion

2.5.3.1. Influence of Variations in the Moisture Level Present in the Environment During Diffusion-Annealing

If water is taken up from the environment during diffusion-annealing, it is expected that the diffusivity of sodium near the surface decreases as observed earlier for the diffusion of sodium in other silicate glasses [22,25]. As an approximation for analyzing experimentally obtained residual radioactivity profiles in such situations, a two-layer model has been developed [25]. In this model it is assumed that one can describe the diffusion of an isotope by using one tracer diffusion coefficient for the near-surface region and a second one for the underlying bulk. This model has been successfully used to analyze residual radioactivity profiles obtained for the tracer diffusion of sodium in Corning Code 1737 glass diffusion-annealed in wet air [25], in Type I silica pre-annealed at higher temperatures in moist air and diffusion-annealed at significantly lower temperatures [26], and in model glasses of the type $(CaO{\cdot}Al_2O_3)_x(2SiO_2)_{1-x}$ diffusion-annealed in wet air [22]. For the sodium borosilicate glasses considered in this study, no such effect has been found, see the profiles shown in Fig. 2.4. The residual radioactivity profile obtained after diffusion-annealing in wet air, see Fig. 2.4b, looks very similar as that obtained after diffusion-annealing in dry air, see Fig. 2.4a. From fitting Eq. (2.10) to experimental data as shown in Fig. 2.5b, a value of $3.25{\cdot}10^{-11}$ cm^2/s was obtained for the sodium tracer diffusion coefficient after diffusion-annealing in wet air. This value is within the limits of error identical to the value of $3.10{\cdot}10^{-11}$ cm^2/s obtained for the sodium tracer diffusion coefficient after diffusion-annealing in dry air. Experiments to detect a possible uptake of water by glasses of the type $(Na_2O)_{0.2}[(BO_{1.5})_x(SiO_2)_{1-x}]_{0.8}$ upon annealing in wet air were also performed. The results obtained suggest that there is no significant uptake of water when annealing in wet air with a water vapor pressure of 474 mbar at a temperature of 241°C. At higher temperatures, when annealed in wet air,

some of the glasses investigated, especially those with higher boron contents, were found to be unstable. For example, glasses with x = 0.8 and 1 became non-transparent and looked white after annealing for one day at 300 °C in wet air; this observation is most likely related to recrystallization and/or phase separation.

2.5.3.2 Temperature Dependence of the Sodium Tracer Diffusion

When analyzing the temperature dependence of the sodium tracer diffusion it was found that an Arrhenius-type equation describes the temperature dependence of sodium tracer diffusion coefficients at temperatures sufficiently far below the glass transition temperature. At higher temperatures deviations occur, which are believed to be caused by structural changes at temperatures not far from T_g. Therefore, an Arrhenius-type equation, see Eq. (2.12), was fitted to sodium tracer diffusion coefficients only for temperatures up to about 310 °C, see Fig. 2.8.

$$D_{Na}^{*} = D_{Na}^{\circ} \cdot \exp\left(- \frac{\Delta E_a}{R \cdot T} \right) \qquad (2.12)$$

The values of the activation energy, ΔE_a, and pre-exponential factor, D_{Na}°, obtained from the fitting are shown in Table 2.3. It was found that the activation energy increases almost linearly from about 70 to about 80 kJ/mol when x increases from 0 to 1, see Fig. 2.9, and that the pre-exponential factor varies from about $3 \cdot 10^{-4}$ to about $2 \cdot 10^{-3}$ cm^2/s with a minimum around x = 0.4, see Fig. 2.10.

Many investigators [2-5] have reported that they found that variations of activation energies with the composition control changes of the ionic conductivity with the composition in several mixed glass former glasses. However, Carette et al. [27] reported that the variation of the ionic conductivity with composition in mixed anion glasses of the system $(Li_2S)_{0.24}(GeS_2)_{0.36}[(LiBr)_t(LiI)_{1-t}]_{0.4}$ with $0 \leq t \leq 0.6$ is mainly governed by the variations of the pre-exponential factor. For the sodium borosilicate glasses considered in this study it was found that the composition dependences of the activation energy and of the pre-exponential factor both affect the rate of the diffusion of sodium in the glass and that variations

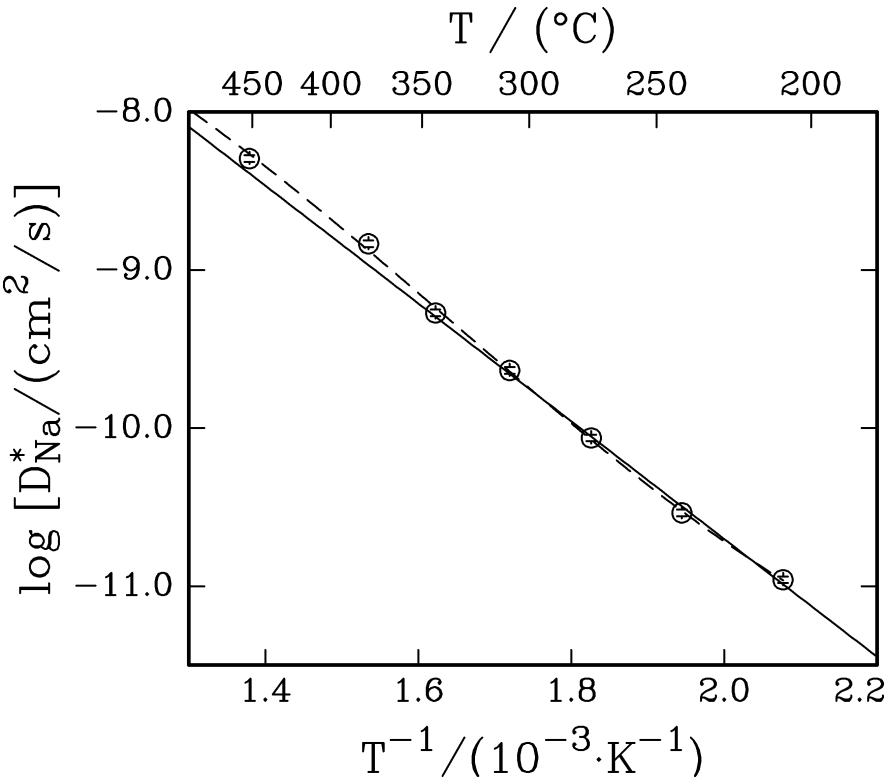

Fig. 2.8: Temperature dependence of sodium tracer diffusion coefficients for sodium borosilicate glasses of the type $(Na_2O)_{0.2}[(BO_{1.5})_x(SiO_2)_{1-x}]_{0.8}$. The solid line is a fit of Eq. (2.12) to the data for temperatures up to 310 °C; the dashed line was obtained by a spline fit and is for guiding the eye.

Table 2.3: Activation energies and pre-exponential factors for the tracer diffusion of Na-22 in glasses of the type $(Na_2O)_{0.2}[(BO_{1.5})_x(SiO_2)_{1-x}]_{0.8}$. The data shown were derived by considering experimental data for temperatures up to 310 °C. "ΔE_A" stands for "ΔE_A / (kJ/mol)" and "$-$ LD°" stands for "$-\log_{10}(D^\circ_{Na}/(cm^2/s)$". The errors of the data are based on the diffusion coefficients reported in Table 2.2 and attributing an estimated error of ± 5 % to these data. The errors of all values for ΔE_A listed below are ± 1.52 kJ/mol and those for $-$ LD° are all ± 0.15.

x	0	0.1	0.2	0.3	0.4	0.5	0.6	0.7	0.8	0.9	1
ΔE_A	69.78	69.27	68.46	71.30	72.35	70.70	73.88	78.92	79.38	79.82	81.40
$-$ LD°	2.87	3.12	3.36	3.25	3.30	3.57	3.33	2.86	2.79	2.67	2.47

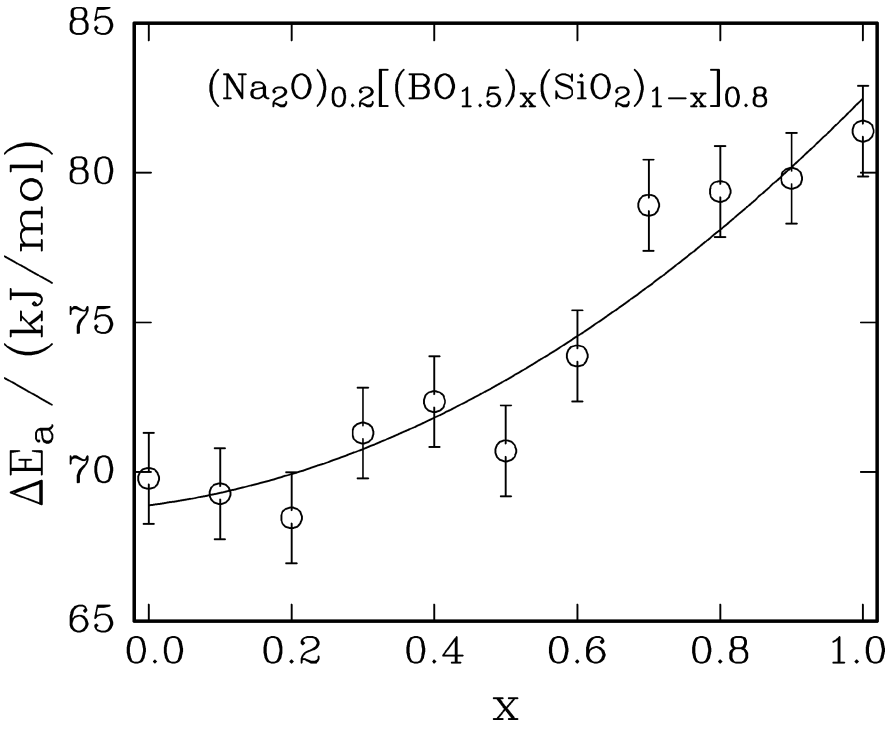

Fig. 2.9: Activation energy for the sodium tracer diffusion in sodium borosilicate glasses of the type $(Na_2O)_{0.2}[(BO_{1.5})_x(SiO_2)_{1-x}]_{0.8}$ as a function of the glass composition.

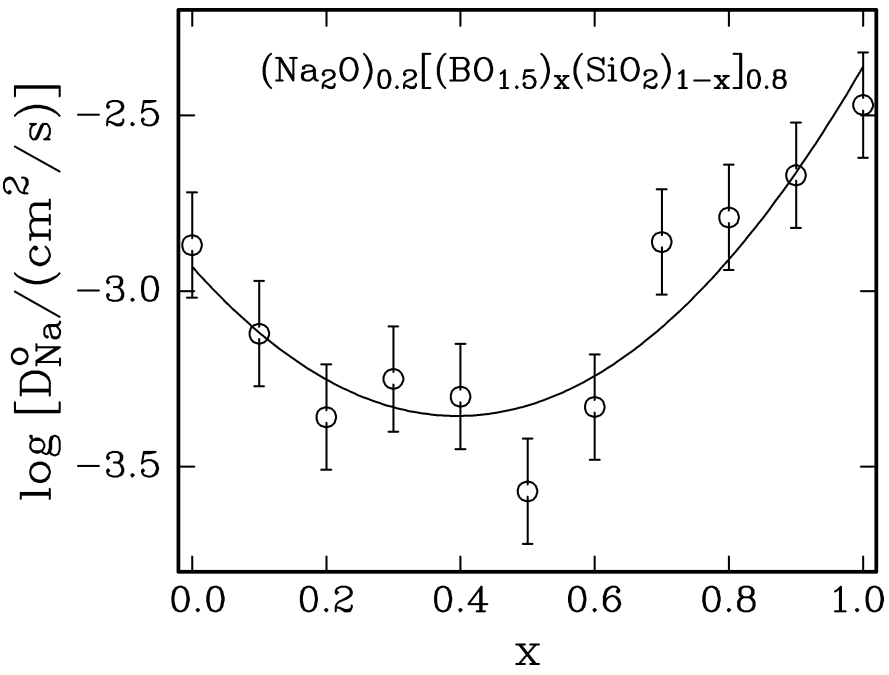

Fig. 2.10: Pre-exponential factors of sodium tracer diffusion coefficients for sodium borosilicate glasses of the type $(Na_2O)_{0.2}[(BO_{1.5})_x(SiO_2)_{1-x}]_{0.8}$ as a function of the glass composition.

in the pre-exponential factor have a relatively larger influence than variations of the activation energy. The increase of the activation energy with increasing x shifts the minimum in the tracer diffusion coefficient as a function of the composition parameter x to x around 0.7, i.e., to a composition which is different from the composition x = 0.4 where the pre-exponential factor shows a minimum.

2.5.3.3 Haven-Ratio

The tracer diffusion coefficient of a species i, D_i^*, is related to the component diffusion coefficient of this species, D_i, by the Haven-ratio, H_R, which is related to correlation effects:

$$D_i^* = D_i \cdot H_R \tag{2.13}$$

The Haven-ratio is one when an atomic/ionic species follows a random motion. In crystalline materials this is the case if diffusion occurs by a direct interstitial mechanism. In the same type of materials the value of H_R deviates from one when an atomic/ionic species diffuses via a vacancy mechanism or by an indirect interstitial mechanism, also called interstitialcy mechanism. In glasses this holds for any diffusion mechanisms which are similar to vacancy and interstitialcy diffusion processes in crystalline materials.

The field-induced drift of a single ionic species i can be described by a partial electrical conductivity, σ_i. The electrical conductivity of the species i is related to the tracer diffusion coefficient of that species, D_i^*, via the Nernst-Einstein relation given in Eq. (2.14).

$$\sigma_i = \frac{z_i^2 \cdot F^2 \cdot D_{i,\sigma} \cdot c_i}{R \cdot T} = \frac{z_i^2 \cdot F^2 \cdot D_i^* \cdot c_i}{H_R \cdot R \cdot T} \tag{2.14}$$

z_i is the ionic charge number of the diffusing species i, F is the Faraday constant, c_i is the concentration of the species i, R is the gas constant and T is the temperature in K. The tracer diffusion coefficient, D_i^*, is related to the conductivity diffusion coefficient $D_{i,\sigma}$ via the Haven-ratio H_R as denoted in Eq. (2.15).

$$D_i^* = D_{i,\sigma} \cdot H_R \tag{2.15}$$

For the sodium borosilicate glasses considered in this study, values for the Haven-ratio were calculated using Eqs. (2.14) and (2.15) with values for the conductivity diffusion coefficient, $D_{i,\sigma}$, obtained from ionic conductivity data determined by collaborators at Iowa State University [24] and density data given by Eq. (2.11). As it is shown in Fig. 2.11, the value of the Haven-ratio first decreases and later increases slightly when silicon is replaced by boron. All values obtained for the Haven-ratio in this study are smaller than one, i.e., they suggest that the diffusion of sodium tracer corresponds to a correlated motion. Without knowing what the actual transport mechanisms in the glasses considered are, the shallow minimum in the Haven-ratio indicates that there is a stronger diffusion correlation at x around 0.75 than at larger or smaller values of x. If the sodium diffusion should occur by a vacancy-like mechanism, the minimum in H_R suggests that the number of equivalent sites around a sodium ion in the glass decreases and has a shallow minimum as a function of x near x = 0.75. The correlation factor can be simply approximated as (1 – 2/z), where z is the number of equivalent neighboring sites [28]. This simple approximation produced estimates for values of correlation factors for several crystal lattices which were in reasonably good agreement with more accurate values reported in Ref. [29]. The occurrence of a minimum in the Haven-ratio as a function of x must be related to structural changes of the glasses with their composition. Currently, the details of these relationships remain unclear.

2.5.3.4 Composition Dependence of the Sodium Tracer Diffusion

Fig. 6 shows that the sodium tracer diffusion coefficient as a function of the composition parameter x has a minimum at around x = 0.7 at constant temperatures between 208 and 378 °C. To enable estimates for values of sodium tracer diffusion coefficients at other temperatures and glass compositions than experimentally studied in this work, an empirical equation for describing the values of sodium tracer diffusion coefficients as a function of the composition parameter x and the temperature T in Kelvin was derived, see Eq. (2.16).

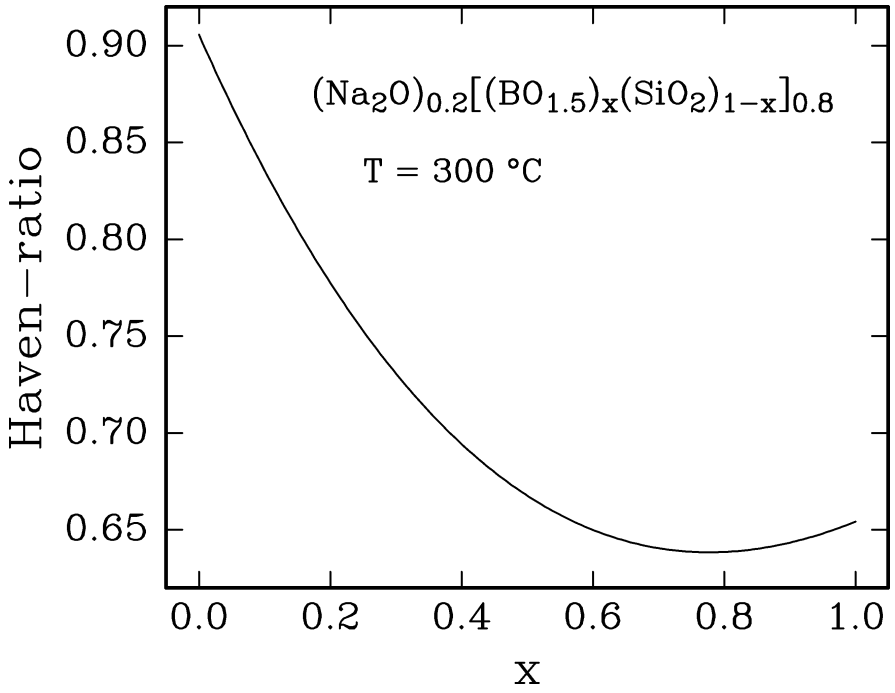

Fig. 2.11: Haven-ratios for the diffusion of sodium in sodium borosilicate glasses of the type $(Na_2O)_{0.2}[(BO_{1.5})_x(SiO_2)_{1-x}]_{0.8}$.

$$\log\left[D^{*}_{Na}/(cm^2/s)\right] = \left(\frac{338.4}{T/(K)} + 0.96\right)\cdot x^2 - \left(\frac{750.1}{T/(K)} + 0.98\right)\cdot x - \frac{3713}{T/(K)} - 2.71 \quad (2.16)$$

Lines for isotherms derived by using Eq. (2.16) in comparison with experimentally determined data points for sodium tracer diffusion coefficients are shown in Fig. 2.6. As it can be seen in this figure, Eq. (2.16) describes the experimental data very well for temperatures between about 200 and 450 °C. Some deviations occur at small and large values of x at 503 °C.

As mentioned before, the Haven-ratio shows a shallow minimum around x = 0.75, a composition similar to that at which the minimum in the tracer diffusion coefficient is observed. This indicates a stronger diffusion correlation at this composition than at others. A simple approach to partially explain this finding is to use elements of the atomistic theory of the diffusion of matter in crystalline materials, i.e., the fact that a tracer diffusion coefficient at a given defect concentration is proportional to the square of an elementary jump length, a, and the Haven-ratio, H_R. For the diffusion of cations in glasses, the situation is much more complicated than that in crystalline materials because of the lack of a periodic structure. The diffusional jumps in glasses have different jump lengths and heights of diffusion barriers. To overcome this difficulty, average quantities need to be introduced when considering the diffusion of ions in glass. A value proportional to an average jump distance, $\bar{a}$, was calculated by taking the cube root of a free volume, V_f. This free volume was obtained by subtracting the volume of the ions being present from the molar volume V_m, see Eq. (2.17).

$$V_f = V_m - \frac{4}{3}\cdot\pi\cdot N_A\cdot\left[0.4\cdot r^3_{Na^+} + 0.8\,x\cdot r^3_{B^{3+}} + 0.8\,(1-x)\cdot r^3_{Si^{4+}} + (1.8-4\,x)\cdot \right. \quad (2.17)$$

Values for the molar volume were calculated from molar masses and density values obtained by making use of Eq. (2.11). In Fig. 2.12, the logarithm of the product between H_R and the square of a quantity being proportional to the average jump distance $\bar{a}$ is shown as a function of the composition parameter x. The plot

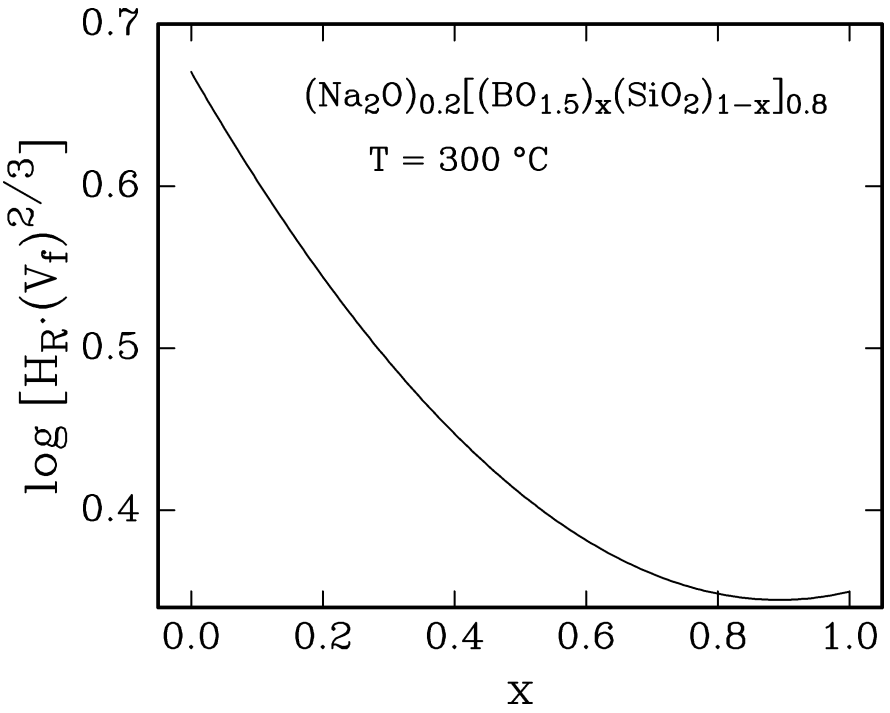

Fig. 2.12: Logarithm of the product between H_R and the square of a factor being proportional to a mean jump length $\bar{a}$ as a function of the composition parameter x in glasses of the type $(Na_2O)_{0.2}[(BO_{1.5})_x(SiO_2)_{1-x}]_{0.8}$.

shows a very shallow minimum at x around 0.9.

By considering experimental tracer diffusion data for about 300 °C, divided by values determined for the Haven-ratio and the square of a factor being proportional to a mean jump length, one finds that the maximum variation related to the product between the mean jump frequency of sodium ions and the number of sites available for a sodium ion to jump into, varies by a factor of about 3 with x; a minimum of this product occurs at x about 0.65. This product corresponds to an effective mean jump frequency. The variation by a factor of about 3 denoted above compared with that of about 2 observed for the Haven-ratio suggests that about 60 % of the compositional variation of the sodium tracer diffusion coefficient must be related to changes in the effective mean jump frequency with the composition parameter x. This effective mean jump frequency includes a mean jump frequency and the number of sites available for sodium ions to jump into. Interestingly, the compositional variation of the Haven-ratio increases the degree of compositional variation observed for the sodium tracer diffusion coefficient compared to the variations resulting from changes in the mean jump frequency and/or sites available for sodium ions to jump into.

To further explore the compositional dependence of the sodium tracer diffusion coefficient, structural information is needed. First, the two end compositions of the glasses investigated are considered. For $(Na_2O)_{0.2}(SiO_2)_{0.8}$ glass, according to ^{29}Si nuclear magnetic resonance (MAS-NMR) spectroscopy results reported by Maekawa et al. [30], half of the silicon atoms are bonded to one non-bridging and three bridging oxygen atoms (BO) and half of the silicon atoms are bonded to four BO. From their ^{11}B NMR study on sodium borosilicate glasses Yun and Bray [11] found for glass of the composition $(Na_2O)_{0.2}(BO_{1.5})_{0.8}$, being equivalent to $(Na_2O)_{0.33}(B_2O_3)_{0.67}$, that the glass mainly consists of diborate units. Each of such units contains two fourfold and two threefold coordinated boron atoms.

The structure of sodium borosilicate glasses with compositions between the two end compositions just discussed is more complicated and far from being well known. Although several studies have been performed related to this subject

[1,11-13,31-35], a unified picture, especially regarding the distribution of sodium between different structural units, does not yet exist. In glasses of the type $(Na_2O)_{0.2}[(BO_{1.5})_x(SiO_2)_{1-x}]_{0.8}$ with $0 < x < 1$ sodium can in principle be present near negatively charged NBO bonded to Si or B, near negatively charged BO_4^--units, and near more complex negatively charged structural units containing Si and B in different configurations. For possibly relating the observed decrease and shallow minimum in the tracer diffusion coefficient and in the Haven-ratio as a function of x at x around 0.7 to 0.75, it is of interest to identify species which could be present with a maximum concentration at x around 0.7 to 0.75 and lead to an increase of the number of structural units which cause a reduction of the number of equivalent sites in the vicinity of the site of a given sodium ion located at such structural units. Since the conclusions made in different studies of the structure of sodium borosilicates differ to some extent, it is currently not possible to relate any structural units discussed in the literature in an unequivocal way to the minima observed for sodium tracer diffusion coefficients and for the Haven-ratio as a function of x.

2.6 Conclusions

Sodium tracer diffusion coefficients, D^*_{Na}, have been measured in sodium borosilicate glasses of the type $(Na_2O)_{0.2}[(BO_{1.5})_x(SiO_2)_{1-x}]_{0.8}$ as a function of temperature and the composition parameter x. At constant temperature, the tracer diffusion coefficient of sodium as a function of x has a shallow minimum at about $x = 0.7$. At temperatures below about 310 °C the temperature dependences of the measured tracer diffusion coefficients are of Arrhenius-type; at higher temperatures one observes an increase in the temperature dependence with increasing temperature. Values derived for the Haven-ratio by comparing tracer diffusion and electrical conductivity data are smaller than one and show a shallow minimum as a function of x at around $x = 0.75$. Based on density data and information on the volume of different ions one finds that the molar volume of the glasses investigated decreases with x. The compositional variation of the Haven-ratio in combination with that of the molar volume allows to conclude that the

effective mean jump frequency of sodium ions varies only by a factor of about 3 as a function of x in glasses of the type $(Na_2O)_{0.2}[(BO_{1.5})_x(SiO_2)_{1-x}]_{0.8}$ at 300 °C. Further details how structural changes related to glass composition variations influence the diffusion of sodium remain unclear.

2.7 Acknowledgments

This work was supported by the National Science Foundation under Award Number DMR-0710564. The work made use of the Cornell Center for Materials Research Facilities supported by the National Science Foundation under Award Number DMR-0520404. The authors thank CCMR shared facility staff, Paul Bishop and John Hunt, for assistance related to a variety of topics. The authors thank Dr. Adam J. Ellison and Shari E. Koval from Corning Inc. for preparing and providing all glass samples considered in this study and also for determining T_g data for the glasses provided. Thanks are due to collaborators in the NSF-sponsored Materials World Network “An International Collaborative Research Program in the Study of Mixed Glass Former Phenomena in Materials”, including Steve Martin and Valeri Petkov, for many insightful discussions and Steve Martin also for many valuable suggestions related to this article. Finally, the authors thank all undergraduate researchers who helped in experimental work.

REFERENCES

[1] D. Manara, A. Grandjean and D.R. Neuville, “Structure of Borosilicate Glasses and Melts: A Revision of the Yun, Bray and Dell Model,” Journal of Non-Crystalline Solids, **355** (50-51) [2009] 2528-2531.

[2] A. Magistris, G. Chiodelli and M. Duclot, “Silver Borophosphate Glasses: Ion Transport, Thermal Stability and Electrochemical Behavior,” Solid State Ionics, **9/10** (Pt.1) [1983] 611-615.

[3] M. Tatsumisago, T. Minami and M. Tanaka, “Properties of Highly Ionic Conducting Li_4SiO_4-Li_3BO_3 Glasses Prepared by Rapid Quenching,” Glastechnische Berichte, **56** (Pt.2) [1983] 945-950.

[4] M. Tatsumisago, N. Machida and T. Minami, “Mixed Anion Effect in Conductivity of Rapidly Quenched Li_4SiO_4-Li_3BO_3 Glasses,” (in Japanese) Yogyo Kyokaishi, **95** (2) [1987] 197-201.

[5] L.F. Maia and A.C.M. Rodriguez, “Electrical Conductivity and Relaxation Frequency of Lithium Borosilicate Glasses,” Solid State Ionics, **168** (1-2) [2004] 87-92.

[6] H. Wakabayashi and R. Terai, “Effect of Trivalent Oxide on Electrical Conductivity of Alkali-silicate Glasses (Part 1) Borosilicate Glasses,” (in Japanese) Yogyo Kyokaishi, **93** (1) [1985] 13-19.

[7] H. Wakabayashi, R. Terai and H. Yamanaka, “Effect of Trivalent Oxide on Electrical Conductivity in Alkali-silicate Glasses (Part 2) Similarity of Various Network Forming Trivalent Ions,” (in Japanese) Yogyo kyokaishi, **93** (4) [1985] 209-216.

[8] C. Kaps, F. Schirrmeister and P. Stefanski, “On the Na^+ Self-diffusion and Electrical Conductivity of Na_2O_3-B_2O_3-SiO_2 Glasses Derived from the $Na_2O{\cdot}SiO_2$ Glass,” Journal of Non-Crystalline Solids, **87** (1-2) [1986] 159-170.

[9] J. Krogh-Moe, “Interpretation of the Infra-Red Spectra of Boron Oxide and Alkali Borate Glasses,” Physics and Chemistry of Glasses, **6** (2) [1965] 46-54.

[10] A.H. Silver and P.J. Bray, “Nuclear Magnetic Resonance Absorption in Glass: I. Nuclear Quadrupole Effects in Boron Oxide, Soda-Boric Oxide and Borosilicate Glasses,” Journal of Chemical Physics, **29** (5) [1958] 984-990.

[11] Y.H. Yun and P.J. Bray, “Nuclear Magnetic Resonance Studies of Glasses in the System Na_2O-B_2O_3-SiO_2," Journal of Non-Crystalline Solids, **27** (3) [1978] 363-380.

[12] Y.H. Yun, S.A. Feller and P.J. Bray, “Correction and Addendum to 'Nuclear Magnetic Resonance Studies of Glasses in the System Na_2O-B_2O_3-SiO_2'," Journal of Non-Crystalline Solids, **33** (2) [1979] 273-277.

[13] W.J. Dell, P.J. Bray and S.Z. Xiao, “^{11}B NMR Studies and Structural Modeling of Na_2O-B_2O_3-SiO_2 Glasses of High Soda Content,” Journal of Non-Crystalline Solids, **58** (1) [1983] 1-16.

[14] A.K. Varshneya, “Fundamentals of Inorganic Glasses,” Academic Press, Inc., San Diego, CA, [1994].

[15] M.E. Milberg and J.G. O’Keefe, R.A. Verhelst and H.O. Hooper, “Boron Coordination in Sodium Borosilicate Glasses,” Physics and Chemistry of Glasses, **13** (3) [1972] 79-84.

[16] T.F. Soules and A.K. Varshneya, “Molecular Dynamic Calculations of a Sodium Borosilicate Glass Structure,” Journal of the American Ceramic Society, **64** (3) [1981] 145-150.

[17] J.E. Shelby, “Introduction to Glass Science and Technology,” 2nd Ed., [2005], The Royal Society of Chemistry, Cambridge.

[18] R.H. Doremus, “Diffusion of Water in Silica Glass,” Journal of Materials Research, **10** (9) [1995] 2379-2389.

[19] C. Peuker, W. Bessau, K.W. Brzezinka, A. Kohl, U. Reinholz and H. Geibler, “IR and Raman Study of Calcium Aluminosilicate Glasses of the Composition $xCaO{\cdot}xAl_2O_3{\cdot}(100-2x)SiO_2$,” Glass Science and Technology, **75** (6) [2002] 313-322.

[20] B.J. Wilson, The Radiochemical Manual, 2nd Ed., [1966], The Radiochemical Centre, Amersham.

[21] J. Crank, The Mathematics of Diffusion, 2nd Ed., [1975], Clarendon Press, Oxford.

[22] H. Lu, "Diffusion of Sodium in Calcium Aluminosilicate Glasses with a 1:1 Molar Calcia-to-Alumina Ratio and the Influence of Water Taken up from the Environment," Ph.D. Thesis, Cornell University [2006].

[23] O.V. Mazurin, M.V. Streltsina and T.P. Shvaiko-Shvaikovskaya, Handbook of Glass Data, [1987], Elsevier Science Publ. Co., New York, NY.

[24] R. Christensen and S. Martin, Iowa State University, personal communication; data to be published.

[25] L. Tian, R. Dieckmann, C.Y. Hui and J.G. Couillard, "Effect of Water Incorporation on the Diffusion of Sodium in an Alkaline-Earth Boroaluminosilicate Glass," Journal of Non-Crystalline Solids, **296** (1-2) [2001] 123-134.

[26] L. Tian, R. Dieckmann, C.Y. Hui, Y.Y. Lin and J.G. Couillard, "Effect of Water Incorporation on the Diffusion of Sodium in Type I Silica Glass," Journal of Non-Crystalline Solids **286** (3) [2001] 146-161.

[27] B. Carette, M. Ribes and J.L. Souquet, ”The Effects of Mixed Anions in Ionic Conductive Glasses,” Solid State Ionics, **9-10** (Pt. 1) [1983] 735-737.

[28] P. Shewmon, Diffusion in Solids, 2nd Ed., [1989], The Minerals, Metals & Materials Society, Warrendale, PA.

[29] K. Compaan and Y. Haven, “Correlation Factors for Diffusion in Solids,” Transactions of the Faraday Society, **52** [1956] 786-801.

[30] H. Maekawa, T. Maekawa, K. Kawamura and T. Yokokawa, “The Structural Groups of Alkali Silicate Glasses Determined from Silicon-29 MAS-NMR,” Journal of Non-Crystalline Solids, **127** (1) [1991] 53-64.

[31] B.C. Bunker, D.R. Tellant, R.J. Kirkpatrick and G.L. Turner, “Multinuclear Nuclear Magnetic Resonance and Raman Investigation of Sodium Borosilicate Glass Structures,” Physics and Chemistry of Glasses, **31** (1) [1990] 30-41.

[32] S. Wang and J.F. Stebbins, “On the Structure of Borosilicate Glasses: A Triple-Quantum Magic-Angle Spinning ^{17}O Nuclear Magnetic Resonance Study,” Journal of Non-Crystalline Solids, **231** (3) [1998] 286-290.

[33] B.G. Parkinson, D. Holland, M.E. Smith, C. Larson, J. Doerr, M. Affatigato, S.A. Feller, A.P. Howes and C.R. Scales, “Quantitative Measurement of Q3 Species in Silicate and Borosilicate Glasses Using Raman Spectroscopy,” Journal of Non-Crystalline Solids, **354** (17) [2008] 1936-1942.

[34] S.W. Martin, J.W. Mackenzie, A. Bhatnagar, S. Bhowmik and S.A. Feller, “^{29}Si MAS NMR Study of the Short Range Order in Sodium Borosilicate Glasses,” Physics and Chemistry of Glasses, **36** (2) [1995] 82-88.

[35] L. Du and J.F. Stebbins, “Nature of Silicon-Boron Mixing in Sodium Borosilicate Glasses: A High-Resolution ^{11}B and ^{17}O NMR Study,” Journal of Physical Chemistry B, **107** (37) [2003] 10063-10076.

Section II

2.8 Structural Information from NMR Measurements

Nuclei which have even numbers of protons and of neutrons have a total spin of zero, while nuclei containing an odd number of protons and/or of neutrons have an intrinsic magnetic moment and angular momentum, in other words a non-zero spin [36]. The magnetic properties of nuclei of certain atoms can be used to obtain information related to the coordination of the atoms. Nuclear magnetic resonance (NMR) is a physical phenomenon which occurs when magnetic nuclei of atoms with a non-zero spin are placed in a static magnetic field and exposed to a second oscillating magnetic field, absorb and re-emit electromagnetic radiation [36]. NMR spectroscopy can provide detailed information about the chemical environment of atoms, like information about nearest neighbors. In any solid, a nuclear spin in a magnetic field experiences different interactions, like chemical shift anisotropy, dipolar, quadrupolar, etc., which cause very broad and featureless lines in NMR frequency domain spectra of the nuclei. At a magic angle, θ_m, the nuclear dipole-dipole interaction between magnetic moments of nuclei averages to zero. Therefore, the normally broad lines become narrower when spinning a sample (usually at a frequency between 1 and 70 kHz) at the magic angle with respect to the direction of the magnetic field. The so-called magic-angle-spinning (MAS) NMR method increases the resolution of NMR frequency domain spectra of nuclei.

^{11}B magic-angle-spinning (MAS) NMR spectra of sodium borosilicate glass samples of the type $(Na_2O)_{0.2}[(BO_{1.5})_x(SiO_2)_{1-x}]_{0.8}$ with x increasing from 0.1 to 1 were obtained by using a commercial NMR spectrometer (Chemagnetics/Varian) in conjunction with an 11.7 T wide-bore superconducting magnet. The resonance frequency of ^{11}B at this field strength is 160.34 MHz.

To prepare glass samples of the type $(Na_2O)_{0.2}[(BO_{1.5})_x(SiO_2)_{1-x}]_{0.8}$ for NMR investigation, an agate mortar and a pestle were used to finely crush glass samples of about 150 mg, which were subsequently packed into a 2.5 mm zirconia rotor and spun at 20 kHz. NMR Spectra were collected using a 2.5 mm double-

resonance T3 probe (Varian). Very short radio-frequency pulses widths of 0.6 μs and recycle delays of 2 seconds (in order to let the spins come to equilibrium [37]) are used in order to maintain accurate relative intensities of trigonal and tetrahedral boron resonances. ^{11}B MAS NMR data were obtained by averaging 2048 transients to improve the signal-to-noise ratio [37], Fourier-transformed with minimal line broadening, and referenced to aqueous boric acid at 19.6 ppm (relative to an external shift standard of BF_3-Et_2O at 0 ppm).

^{11}B MAS NMR spectra of sodium borosilicate glasses of the type $(Na_2O)_{0.2}[(BO_{1.5})_x(SiO_2)_{1-x}]_{0.8}$ with x increasing from 0.1 to 1 in steps of 0.1 are shown in Fig. 2.13. The relatively narrow symmetric peaks centered at about 1 ppm correspond to BO_4 units and the broad peaks at around 10 ppm correspond to the BO_3 units. By simulation of the observed ^{11}B MAS NMR lineshapes, the concentration of boron being present in a tetrahedral coordination relative to the total concentration of boron atoms, N_4, was determined; the values obtained for N_4 are reported in Fig. 2.13.

The change of the value of N_4 as a function of the glass composition is illustrated in Fig. 2.14. N_4 decreases with an increase of the boron concentration. The shift of the peak position of the 4-fold coordinated boron resonance to lower shielding (corresponding to larger ppm values) with increasing boron concentration indicates that there are more boron ions and less silicon ions present as the 2nd nearest neighbor cations.

Fig. 2.15 shows the concentrations of sodium ions, acting as charge compensators for boron-based oxide tetrahedra and for non-bridging oxygen (NBO), respectively, as a function of the glass composition. The concentration of sodium ions charge-compensating for BO_4 tetrahedra increases and that for NBO decreases with an increase of the boron content. As reported by Kaps and Kahnt [38], the interaction between sodium ions and NBO is stronger than that between sodium ions and BO_4 tetrahedra in sodium borosilicate glasses. This effect, competing with a decrease of the free volume discussed in Section 2.5.3.4, could

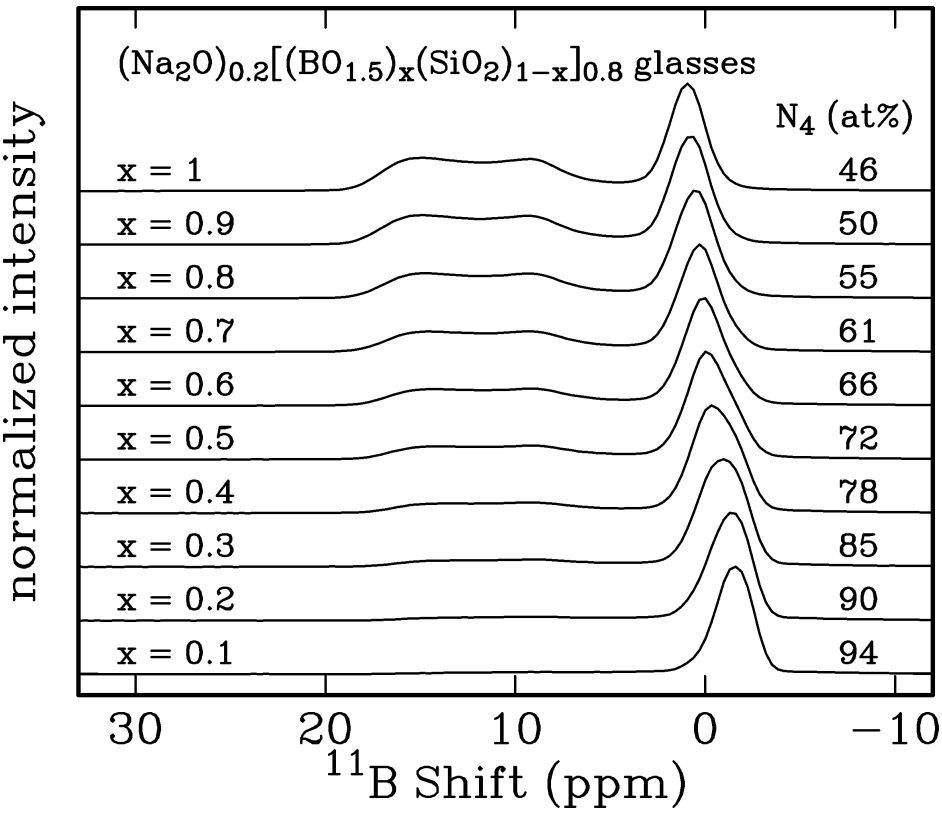

Fig. 2.13: ^{11}B MAS NMR spectra of sodium borosilicate glasses of the type $(Na_2O)_{0.2}[(BO_{1.5})_x(SiO_2)_{1-x}]_{0.8}$. The concentrations of 4-fold coordinated boron relative to the overall concentration of boron atoms, N_4, are listed at the right side of the figure.

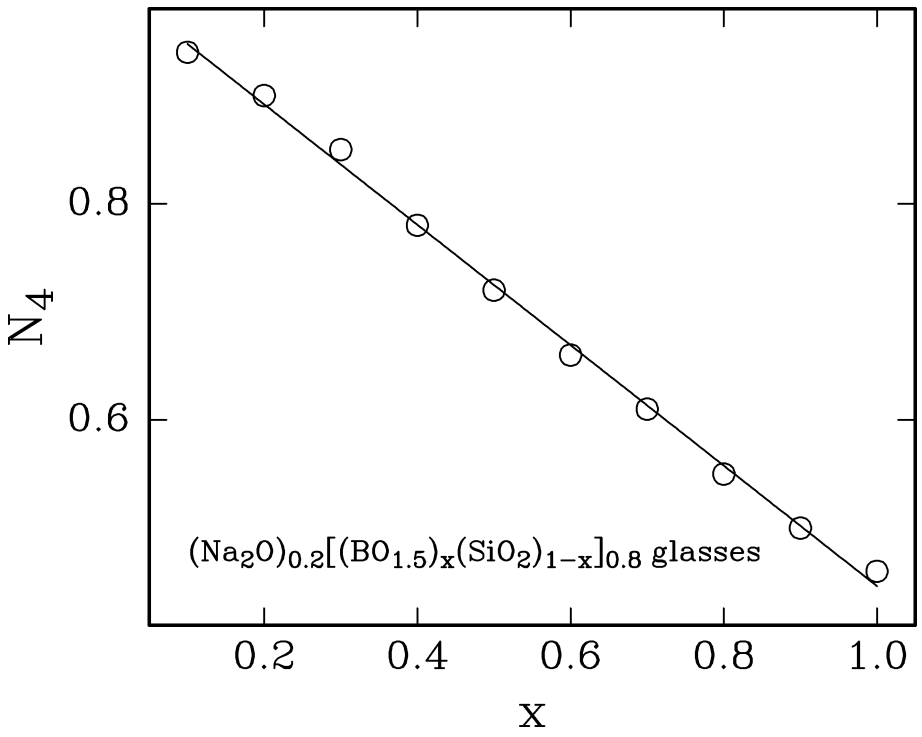

Fig. 2.14: Composition dependence of N_4-values found for $(Na_2O)_{0.2}[(BO_{1.5})_x(SiO_2)_{1-x}]_{0.8}$ glasses.

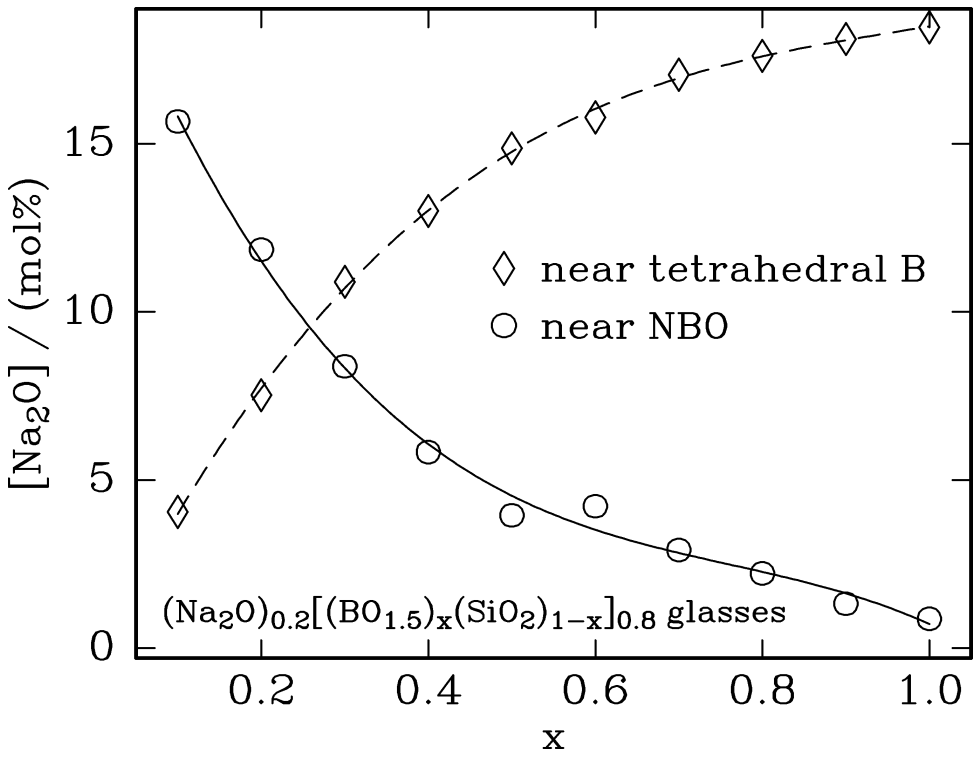

Fig. 2.15: Concentrations of sodium ions acting as charge compensators for boron-based oxide tetrahedra and non-bridging oxygen (NBO) as a function of the glass composition, respectively.

be to some extent the reason for the observed minima of sodium tracer diffusion coefficients with an increase of the boron concentration, see Fig. 2.6.

However, the strength of bonding between sodium ions and BO_4 tetrahedra can also change with different nearest neighbors of BO_4 tetrahedra, like isolated BO_4 units or BO_4 tetrahedra surrounded only by Si-containing units or by other B-containing units. The increase of the concentration of boron ions and the decrease of the concentration of silicon ions present as the 2nd nearest neighbor cations are confirmed by the shift of the peak position of the 4-fold coordinated boron resonance shown in Fig. 2.13. Du and Stebbins [39,40] have studied different environments of BO_4 tetrahedra in alkali borosilicate glasses by performing ^{11}B and ^{17}O NMR measurements. The observed change of the environment of BO_4 tetrahedra can also contribute to a modification of the sodium diffusivity with an increase of the B_2O_3 content. Unfortunately, the currently existing knowledge related to the structure of the considered sodium borosilicate glasses of the type $(Na_2O)_{0.2}[(BO_{1.5})_x(SiO_2)_{1-x}]_{0.8}$ does not allow any more firm conclusions with regard to the behavior of sodium ion mobilities as a function of the glass composition.

REFERENCES

[36] J.W. Akitt, “NMR and Chemistry,” 2nd Ed., [1983], Chapman and Hall, New York, NY, U.S.A.

[37] J. Keeler, “Understanding NMR Spectroscopy,” 2nd Ed., [2010], John Wiley & Sons, Chichester, U.K.

[38] C. Kaps and H. Kahnt, “Structure and Na^+ Transport in Borosilicate Glasses with a High Content of Na_2O ($\geq$10 mol%) – Studied by ^{22}Na Tracer Diffusion and Conductivity Measurements,” Acta Physica Slovaca, **38** (6) [1988] 366-369.

[39] L.-S. Du and J.F. Stebbins, “Solid-State NMR Study of Metastable Miscibility in Alkali Borosilicate Glasses,” Journal of Non-Crystalline Solids, **315** (3) [2003] 239-255.

[40] L.-S. Du and J.F. Stebbins, “Nature of Silicon-Boron Mixing in Sodium Borosilicate Glasses: A High-Resolution ^{11}B and ^{17}O NMR Study,” J. Phys. Chem B, **107** (37) [2003] 10063-10076.

CHAPTER THREE

SODIUM TRACER DIFFUSION IN GLASSES OF THE TYPE $(Na_2O)_{0.2}(B_2O_3)_y(SiO_2)_{0.8-y}$*

3.1 Abstract

Sodium tracer diffusion coefficients, D^*_{Na}, have been measured in sodium borosilicate glasses of the type $(Na_2O)_{0.2}(B_2O_3)_y(SiO_2)_{0.8-y}$ as a function of temperature and the composition parameter y. At constant temperature, the tracer diffusion coefficient of sodium decreases as y increases. The activation enthalpy derived from sodium tracer diffusion data for temperatures up to about 350 °C increases about linearly with increasing values of y from about 70 to 100 kJ/mol. The pre-exponential factor of the sodium tracer diffusion coefficient as a function of y varies by about one order of magnitude and has a minimum at near y = 0.3.

3.2 Introduction

Sodium borosilicate glasses are widely used in many applications including optical glasses, chemically resistant laboratory glassware, sealing materials and host materials for encapsulation of radioactive waste [1,2]. Despite the wide use of such glasses, the current understanding of their structure is only relatively limited. This is mainly because they contain two glass network formers, B and Si, which leads to the presence of a larger number of basic structural units than found in binary sodium borate or silicate glasses. Often, when one network former is replaced by another one, a non-additive variation of transport properties as a function of the glass former composition is observed. Such a non-additive behavior is attributed to the so-called “mixed glass former effect” (MGFE) [3]. In order to study the effect of the variation of the glass former composition on the transport of a selected type of ion, experimental data related to the transport of this ion as

---

* Reprinted with permission from Xinwei Wu, Arun K. Varshneya and Rüdiger Dieckmann, Journal of Non-Crystalline Solids, 357 (21) [2011] 3661-3669.

a function of the network former composition are needed.

In 1966, Otto [4] measured the electrical conductivities of one set of sodium borate glasses, one set of sodium borosilicate glasses with 25 mol% SiO_2 and one set of sodium borosilicate glasses with 50 mol% SiO_2. The Na_2O content of samples of each of these sets was varied from 5 to 25 mol% in steps of 5 mol%. It was found that, for any of the three types of glasses with identical Na_2O contents, the electrical conductivity decreased with an increase in the B_2O_3 content. The three electrical conductivity data points reported by Otto for sodium borosilicate glasses with 20 mol% Na_2O are for 350 °C. These conductivity data most likely refer to the diffusion of sodium and suggest that the diffusivity of sodium strongly decreases with an increasing content of B_2O_3. Any firm conclusions with regard to non-linearities of transport properties as a function of the network former composition, however, cannot be made based on the data reported in Ref. [4]. As discussed more in detail in Ref. [5], Wakabayashi and Terai [6,7] found that for glasses of the type $2Na_2O{\cdot}yB_2O_3{\cdot}(8-y)SiO_2$ both the ionic conductivity and the sodium tracer diffusion coefficient decrease with an increasing content of B_2O_3 until a molar ratio of B_2O_3/Na_2O equal to about one is reached and remain almost unchanged when the B_2O_3 content increases further. Kaps et al. [8] published ionic conductivities and sodium tracer diffusion coefficients for two types of sodium borosilicate glasses. For two samples with identical concentrations of Na_2O, the one with a higher B_2O_3 concentration had a lower ionic conductivity and a smaller sodium tracer diffusivity. This trend was also observed in more recent study by Ehrt and Keding [9] (published in 2009) for the electrical conductivity in four sodium borosilicate and two sodium silicate glasses. The compositions of these glasses varied over a wide range: Na_2O between 3 and 33.3 mol%, SiO_2 between 25 and 85 mol% and B_2O_3 between 0 and 62.5 mol% [9]. Of the glasses studied, one sodium silicate and one sodium borosilicate glass sample had identical concentrations of Na_2O of 15 mol%. The sodium silicate glass showed a higher ionic conductivity than the sodium borosilicate glass. Additional data for the ionic conductivity of sodium borosilicate glasses were found in Refs. [10-12]. The

data reported in these articles refer to variations of the ionic conductivity as a function of the sodium concentration or of the molar Na_2O/B_2O_3-ratio and do not allow any significant conclusions with regard to the influence of variations of the network former composition on the ionic conductivity. To study non-linearities of transport properties as a function of the network former composition in glasses, ion transport-related data as a function of network former composition variations for glasses with constant sodium oxide concentration or one tied to the boron oxide content and different molar SiO_2/B_2O_3- or $SiO_2/BO_{1.5}$-ratios are needed

Since there is a lack of such data in the literature, Wu and Dieckmann [5] have investigated the tracer diffusion of sodium in glasses of the type $(Na_2O)_{0.2}[(BO_{1.5})_x(SiO_2)_{1-x}]_{0.8}$. In Fig. 3.1 the compositions of these glasses are denoted by a dashed line. Wu and Dieckmann [5] found that, at constant temperatures between 208 and 378 °C, the tracer diffusion coefficient of sodium as a function of x has a shallow minimum at around x = 0.7. The compositions of glasses considered in this work, $(Na_2O)_{0.2}(B_2O_3)_y(SiO_2)_{0.8-y}$, correspond to a different join in the composition triangle for the Na_2O-B_2O_3-SiO_2 system; in Fig. 3.1 this join is denoted by a solid line.

The latter type of glasses denoted above has been used earlier in cation exchange studies. In 1974 Varshneya and Milberg [13] published the results of an investigation of the replacement of K^+ against Na^+ ions in sodium borosilicate glasses of the type $(Na_2O)_{0.2}(B_2O_3)_y(SiO_2)_{0.8-y}$ with y varying from 0.15 to 0.6 in steps of 0.15. By determining the distribution of potassium in these glasses after an ion exchange in molten KNO_3 by using an electron microprobe, values of interdiffusion coefficients were derived as a function of the glass composition. If it is assumed that the local electroneutrality in the interdiffusion zone is maintained by replacing Na^+ ions by an equal amount of K^+ ions and if any changes occurring due to the ion exchange in the molar volume and in the thermodynamics are sufficiently small so that they can be ignored, then the relationship between the interdiffusion coefficient, $\tilde{D}$, and the component diffusion coefficients of K^+ and

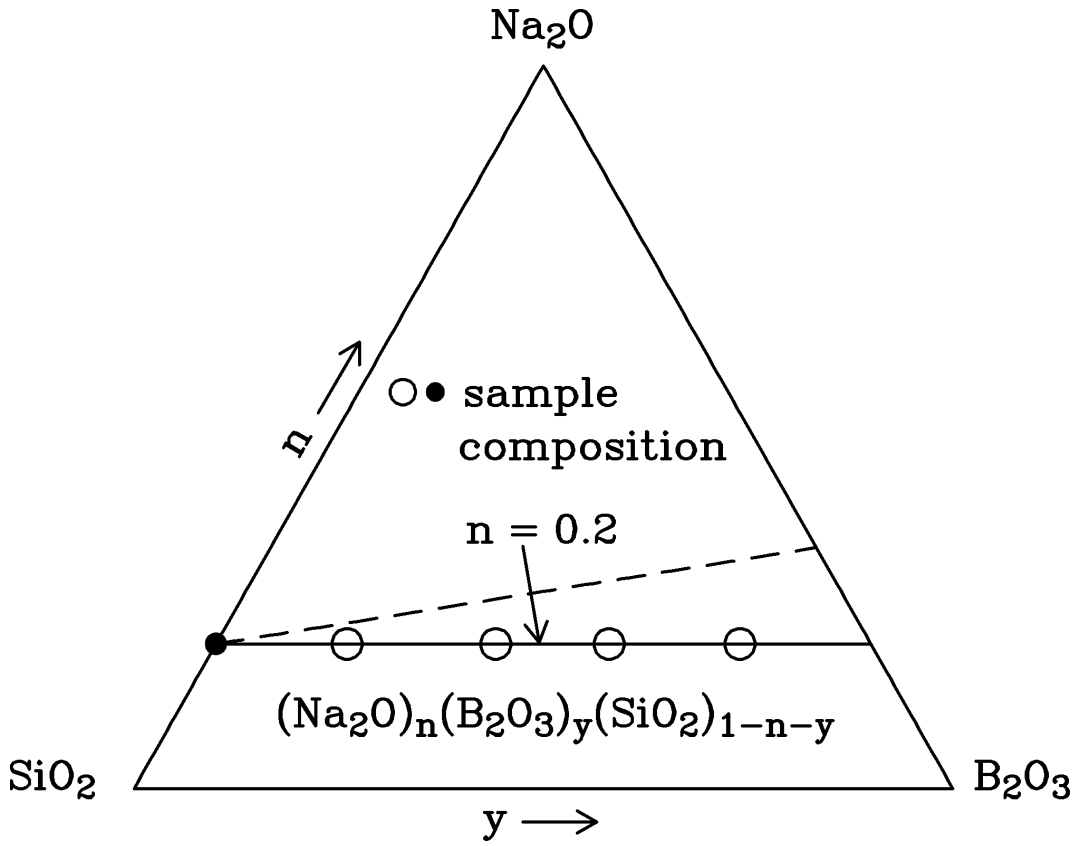

Fig. 3.1: Composition triangle for the system Na_2O-B_2O_3-SiO_2. The hollow circles in the diagram denote the compositions of the sodium borosilicate glasses of the type $(Na_2O)_{0.2}(B_2O_3)_y(SiO_2)_{0.8-y}$ considered in this article and the dashed line denotes the compositional join $(Na_2O)_{0.2}[(BO_{1.5})_x(SiO_2)_{1-x}]_{0.8}$ along which the sodium tracer diffusion was studied in Ref. [5]. The solid symbol refers to the sodium silicate glass $(Na_2O)_{0.2}(SiO_2)_{0.8}$ described in Ref. [5].

Na^+ ions, D_{K^+} and D_{Na^+}, is given by the Nernst-Planck equation [14], see Eq. (3.1), in its most simple form.

$$\tilde{D} = \frac{D_{Na^+} \cdot D_{K^+}}{m \cdot D_{K^+} + (1-m) \cdot D_{Na^+}} \tag{3.1}$$

In this equation, m is the fraction of the alkali ions in the glass which are K^+ ions. According to Eq. (3.1), when m approaches a value of zero, the interdiffusion coefficient becomes equal to the component diffusion coefficient of K^+. Since the radius of K^+ ions of about 140 pm is much larger than that of Na^+ of about 100 pm, the component diffusion coefficient of K^+ is expected to be significantly smaller than that of Na^+ in glasses with m being close to zero. This expectation is in agreement with the results from a comparison of interdiffusion coefficients obtained for the exchange of Na^+ ions by K^+ ions in $Na_2O{\cdot}3SiO_2$ glass by Varshneya [15] with tracer diffusion coefficients for Na^+ and K^+ ions reported by Fleming and Day [16]. Later in this article, sodium tracer diffusion coefficients will be compared with interdiffusion coefficients obtained for the exchange of Na^+ by K^+ ions reported in Ref. [13] and extrapolated to m = 0 for the sodium borosilicate glasses of interest in this study.

It is well known that impurities can affect properties of glasses. On an atom-for-atom basis, the effect of oxide impurities is most pronounced when the impurity species is water. Water exists in glass in the form of hydroxyl (OH) bonded to the glass network former atoms and as molecular water dispersed in the interstices of the glass network [17]. Molecular water is the mobile diffusing species in glasses while hydroxyl groups are almost immobile [18]. Details of the incorporation of water molecules from a surrounding, moisture-containing gas atmosphere into oxide glasses can be found in Ref. [5]. Water incorporated into oxide glasses has a large effect on some structure-sensitive properties of such glasses, like the density, the viscosity, the glass transition temperature [17] and the diffusivity of sodium in silicate glasses [19].

This article has two main goals. One is to determine experimentally the composition and temperature dependencies of sodium tracer diffusion coefficients for sodium borosilicate glasses of the type $(Na_2O)_{0.2}(B_2O_3)_y(SiO_2)_{0.8-y}$. The second one is to examine the composition dependence of the activation enthalpy of the sodium tracer diffusion and of the pre-exponential factor of the sodium tracer diffusion coefficient.

3.3 Experiments

The following sections provide details of the glass samples used in this study, their original water content and of the sodium tracer diffusion experiments performed.

3.3.1 Glass Samples

Samples of glasses of the type $(Na_2O)_{0.2}(B_2O_3)_y(SiO_2)_{0.8-y}$ with y varying from 0.15 to 0.6 in steps of 0.15 were prepared almost 40 years ago by Varshneya and Milberg [13]; for details see their publication. A composition triangle for the system Na_2O-B_2O_3-SiO_2 is shown in Fig. 3.1. In this diagram, hollow circles indicate the glass compositions experimentally investigated in this study and the solid bullet denotes the composition of sodium silicate glass samples described in Ref. [5] and considered in this study for comparison. The nominal and the actual compositions of the sodium borosilicate glasses used in this study are reported in Table 3.1.

As received, the sodium borosilicate glass samples with y = 0.15 and 0.32 were rods with a diameter of about 1.6 cm and a length of about 7 cm. Disks with thicknesses of around 2 mm were cut from these rods and ground to be plane-parallel for later use in tracer diffusion experiments. Samples with compositions of y = 0.45 and 0.6 were received in the form of square plates with dimensions of about 8×8×3 mm. Each of these samples was cut parallel to its large surfaces to obtain two sheets with thicknesses of about 1.2 mm. These sheets, starting from the two new surfaces generated by cutting, were ground to make them plane-parallel to the original large sample surfaces so that they could be used for tracer

Table 3.1: Nominal and actual compositions, R- and K-ratios ($R = n_{Na_2O}/n_{B_2O_3}$ and $K = n_{SiO_2}/n_{B_2O_3}$ determined based on the actual compositions), glass transition temperature (T_g) and density (ρ) values of the sodium borosilicate glasses of the type $(Na_2O)_{0.2}(B_2O_3)_y(SiO_2)_{0.8-y}$ considered in this study. All data except for densities for y > 0 are from Ref. [13] and those for y = 0 are from Ref. [5]. The densities listed in the table were measured using a glass pycnometer. Values for the fraction of boron in a fourfold coordination, N_4, and values for the fraction of non-bridging oxygen, f_{NBO}, were obtained by using the model proposed by Yun and Bray [25] in its revised form [26].

y	nominal mol%			actual mol%			R	K	N_4	f_{NBO}	T_g (°C)	ρ (g/cm^3)
	Na_2O	B_2O_3	SiO_2	Na_2O	B_2O_3	SiO_2						
0	20	0	80	20.2	0.1	79.7					500	2.39
0.15	20	15	65	19.7	15.0	65.3	1.3	4.4	0.75	0.09	600	2.51
0.32	20	30	50	19.2	32.0	48.8	0.6	1.5	0.60	0.00	577	2.50
0.45	20	45	35	19.7	45.0	35.3	0.4	0.8	0.44	0.00	545	
0.6	20	60	20	19.8	60.5	19.7	0.3	0.3	0.33	0.00	508	

diffusion experiments. All glass samples were washed ultrasonically in de-ionized water, acetone and ethanol to avoid any contamination by alkali and alkaline-earth compounds introduced by fingerprints. Tweezers were used thereafter to handle the glass samples for tracer diffusion and initial water content measurements.

3.3.2 Water Content Measurements

According to the literature, almost all water in silicate glasses is accommodated (at least at room temperature) in the form of hydroxyl groups as long as the concentrations of water are relatively small, see, e.g., Ref. [17]. To determine the initial water content of all glass samples by measuring at room temperature the IR absorbance related to the presence of OH groups at wavelengths between 3500 and 3700 cm^{-1}, depending on the glass composition, a Bruker Optics Equinox 55 Fourier Transform Infrared (FTIR) Spectrometer was used. Details about such water content measurements can be found in Ref. [5].

According to the Beer-Lambert law, the average water concentration in the area of a glass plate through which the IR beam travels is

$$c_{H_2O} = \frac{1}{2} \cdot \frac{A_g}{\varepsilon_{OH} \cdot d_g} \cdot \frac{M_{H_2O}}{\rho_g} = \frac{A_g}{\varepsilon_{H_2O} \cdot d_g} \cdot \frac{M_{H_2O}}{\rho_g} \tag{3.2}$$

with

$$A_g = -\log_{10}\left(\frac{I}{I_0}\right), \tag{3.3}$$

where A_g is the measured absorbance of the glass, ε_{OH} (in $\ell/(mol_{OH} \cdot cm)$) is the molar absorption coefficient related to the overall concentration of Si-OH and B-OH groups present in the glass, d_g (in cm) is the thickness of the glass sample, c_{H_2O} is the mass fraction of H_2O in the glass, M_{H_2O} is the molar mass of H_2O (= 18.02 g/mol), ρ_g (in g/cm^3) is the density of the glass and I/I_0 is the ratio between the integral intensities of the transmitted and the initial IR signal. The molar absorption coefficient of OH groups is approximately one half of that related to the overall water present in the glass, i.e., $2\ \varepsilon_{OH} \approx \varepsilon_{H_2O}$; both coefficients correspond

to the stretching of OH groups.

Values for the molar absorption coefficient of the sodium borosilicate glasses considered in this study as a function of the glass composition are not available. Eq. (3.2) was therefore reorganized to avoid the problem of not knowing what the value of ε_{OH} exactly is, leading to Eq. (3.4).

$$c_{H_2O} \cdot \varepsilon_{OH} = \frac{1}{2} \cdot \frac{A_g}{d_g} \cdot \frac{M_{H_2O}}{\rho_g} \tag{3.4}$$

If ε_{OH} is assumed to be constant, regardless of changes in the glass composition, any water concentration variation is proportional to that of the product $c_{H_2O} \cdot \varepsilon_{OH}$.

3.3.3 Sodium Tracer Diffusion Experiments

3.3.3.1 Diffusion Mathematics

In a homogenous glass sample the tracer diffusion coefficient of a tracer i is constant and the thin film solution of Fick's second law applies. If the tracer is applied to one surface of a sample as a thin film, the sodium tracer concentration, $c_i(\xi,t)$, at a distance ξ from the surface after diffusion-annealing for the time, t, is

$$c_i(\xi,t) = \frac{Q_i}{\sqrt{\pi \cdot D_i^* \cdot t}} \cdot \exp\left(- \frac{\xi^2}{4\, D_i^* \cdot t} \right) \tag{3.5}$$

given by Eq. (3.5), see Ref. [20].
Q_i is the initial concentration of the radioactive tracer per unit area and D_i^* is the tracer diffusion coefficient of the tracer i, in this study the radioactive isotope Na-22.

Since the tracer penetration length and the absorption coefficient in the experiments performed in this study are both sufficiently small, the absorption of the radiation from the decay of the radioactive isotope used within the sample is negligibly small and can be ignored for the data analysis. Therefore the normalized residual radioactivity, A(x,t)/A(x=0,t), as a function of the diffusion-annealing time, t, and the tracer diffusion coefficient of the species i, D_i^*, is described by Eq. (3.6),

in which x is the distance from the original surface where the tracer was applied. This equation was obtained by integration departing from Eq. (3.5).

$$\frac{A(x,t)}{A(x=0,t)} = \frac{\int_{x}^{\infty} c_i(\xi,t)\cdot d\,\xi}{\int_{0}^{\infty} c_i(\xi,t)\cdot d\,\xi} = 1 - \mathrm{erf}\left(\frac{x}{2\sqrt{D_i^{*}\cdot t}}\right) \tag{3.6}$$

To achieve a higher precision by more emphasizing the influence of data points obtained for larger penetration depths on the final result, the inverse function of the error function, erfi, is used to analyze experimental data. This was done by fitting Eq. (3.7) to experimental data.

$$\mathrm{erfi}\left(1 - \frac{A(x,t)}{A(x=0,t)}\right) = \frac{x}{2\sqrt{D_i^{*}\cdot t}} \tag{3.7}$$

When a = erf(b), then b = erfi(a).

3.3.3 Experimental Details

Tracer diffusion coefficients for the radioactive isotope Na-22 diffusing in as-received glass samples were obtained by measuring residual radioactivities as a function of the distance from the surface initially containing all tracer material. A high resolution, high-purity Ge detector (EG&G Ortec) was used to measure separately residual radioactivities related to the two energies associated with the γ-radiation resulting from the decay of Na-22, 0.51 and 1.28 MeV [21]. Residual radioactivity profiles, A(x)/A(x=0) as a function of x were obtained by measuring the initial radioactivity of a sample, A(x=0), and residual radioactivities of this sample, A(x), after removing layers parallel to the surface where the tracer was originally applied. A normalized residual radioactivity profile, A(x)/A(x=0) vs. x, where x is the distance from the original surface, was obtained by sequentially removing material from the sample and measuring residual radioactivities for different values of x. More details about such measurements can be found in Ref. [5].

3.4 Results

3.4.1 Initial Water Content

The shapes of the infrared absorption peaks observed for the sodium borosilicate glasses considered in this study are similar to those observed for B_2O_3-SiO_2-glasses [22]. The observed broad absorption peaks can be attributed to two partially overlapping peaks related to the IR-absorption by B-OH and Si-OH groups. Therefore, it was attempted to use two Gaussian functions corresponding to the absorption of two types of OH groups for an analysis analogous to that performed by Bandyopadhyai et al. [22] for infrared spectra for B_2O_3-SiO_2-glasses. Figs. 2a and 2b show the result of fits produced by assuming two Gaussian individual absorption peaks and their sum in comparison with experimenally observed absorption peaks for two typical spectra for sodium borosilicate glasses with y = 0.15 and 0.32. The Si-OH absorption peak appears at around 3600 cm^{-1} and is sharper than the B-OH peak located at around 3430 cm^{-1}. With an increase of the boron content, the height of the B-OH absorption peak relative to that of the Si-OH peak increases.

The values determined for the water content of as-received samples in the form of the product $c_{H_2O}\cdot\varepsilon_{OH}$ (in $(g_{H_2O}/kg_{glass})\cdot(\ell/(mol_{OH}\cdot cm))$) as a function of the glass composition parameter y are shown in Fig. 3.2b in comparison with a value reported in Ref. [5] for a glass with y = 0. For determining the data shown for the water content, density values corresponding to Eq. (3.8), see Section 4.2. The standard deviations of the results obtained for water contents, usually from three water concentration measurements for each glass composition, were smaller than about 5 %. Additional errors related to the density data used and from thickness measurements to calculate values for $c_{H_2O}\cdot\varepsilon_{OH}$ are estimated to be of the order of 1 %, leading to overall errors below about 6 %.

3.4.2 Sodium Tracer Diffusion

Fig. 3.3a shows a typical residual radioactivity profile for Na-22 obtained by measuring residual radioactivities using an as-received glass sample of the

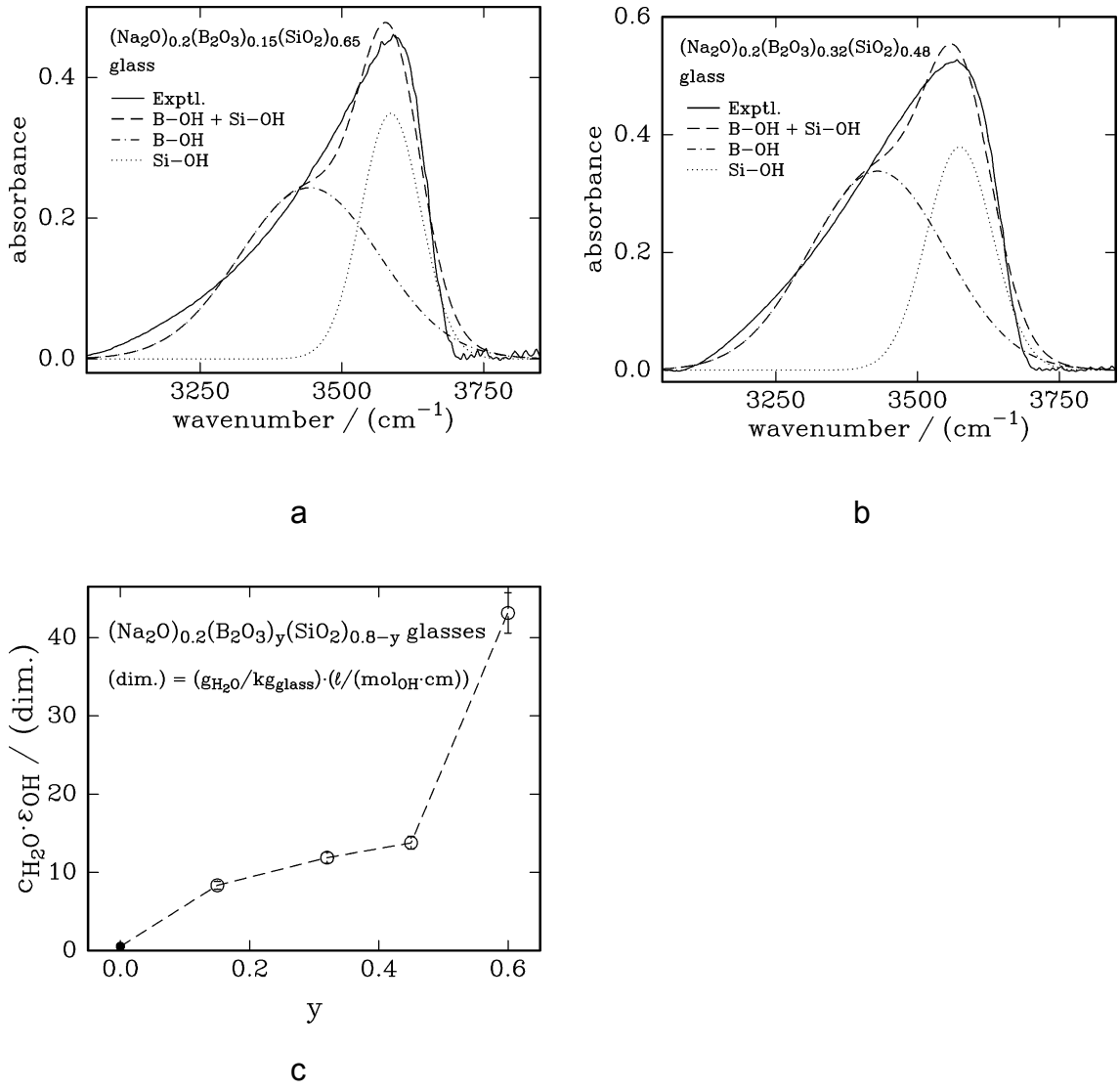

Fig. 3.2: Infrared spectra obtained for sodium borosilicate glasses with y = 0.15 (a) and 0.3 (b). Gaussian-shape peaks are shown, which are attributed to the presence of B-OH and Si-OH groups, as well as the sum of these peaks and the experimentally obtained peak. The latter peak was used for determining the overall concentration of OH groups. Part (c) of the figure shows the initial water contents of the sodium borosilicate glasses of the type $(Na_2O)_{0.2}(B_2O_3)_y(SiO_2)_{0.8-y}$ considered in this article. The concentrations were determined by FTIR measurements. One unit of the y-axis corresponds to an OH concentration of about 0.02 mol% if it is assumed that ε_{OH} = 43 ℓ/(mol_{OH}·cm) for all glass compositions. The

initial water content for the glass with y = 0 denoted by a solid symbol is from Ref. [5]. The errors for the results of the water concentration were estimated not to exceed ± 6 %.

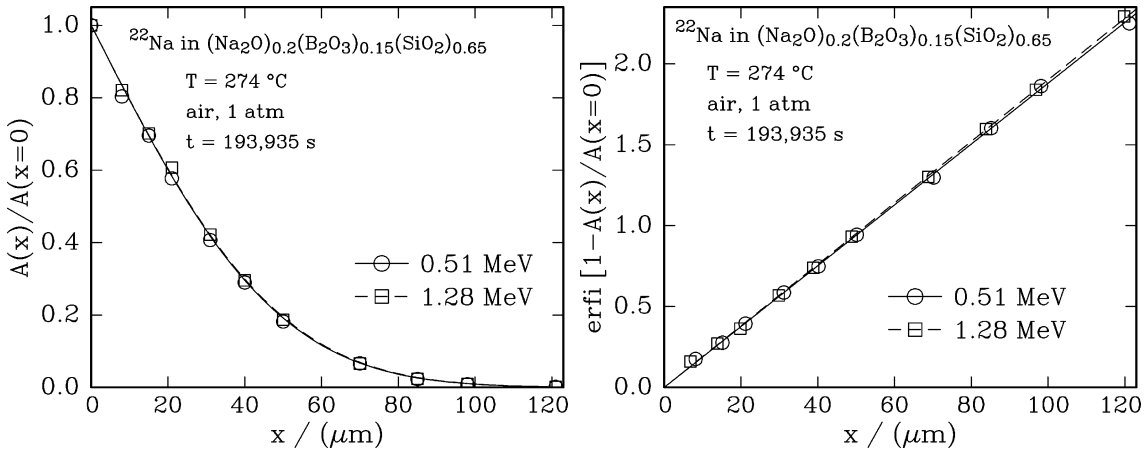

Fig. 3.3: Example for experimental data: (a) Normalized residual radioactivity profile of Na-22 observed in a glass of the composition $(Na_2O)_{0.2}(B_2O_3)_{0.15}(SiO_2)_{0.65}$ after diffusion-annealing for about 54 h in dry air at 274 °C and at atmospheric pressure. (b) Results of fits of Eq. (3.7) to the normalized residual radioactivity data shown in part (a) to determine values for sodium tracer diffusion coefficients.

composition $(Na_2O)_{0.2}(B_2O_3)_{0.15}(SiO_2)_{0.65}$ after diffusion-annealing in dry air for about 54 h at 274 °C. The curves displayed in this figure were obtained by fitting Eq. (3.6) to experimental data for A(x,t)/A(x=0,t). By fitting the inverse function of the error function, erfi, see Eq. (3.7), to the same experimental data as shown in Fig. 3.3b, values for the tracer diffusion coefficient of sodium, D^*_{Na}, were derived. Table 3.2 reports the values determined for tracer diffusion coefficients of sodium diffusing in the sodium borosilicate glasses considered in this study in dry air in comparison with some data for y = 0 from Ref. [5]. The errors reported in Table 3.2 are those obtained from fitting Eq. (3.7) to the normalized residual radioactivities obtained from experiments. Additional errors related to the measurement of temperatures in the annealing furnace, profile lengths during profile determinations, diffusion-annealing times and of net counts make the actual errors of the tracer diffusion coefficient values significantly larger than those listed in Table 3.2. The real errors are estimated to be about 5 % based on past experiences and the individual errors involved in determining the different parameters used to derive values for tracer diffusion coefficients. Measured tracer diffusion coefficients for the diffusion of sodium in the glasses of interest in dry air at different temperatures between 208 and 346 °C are shown in Fig. 3.4a as a function of the glass composition in comparison with data for y = 0 and temperatures up to 308 °C from Ref. [5].

3.5 Discussion

3.5.1 Initial Water Content

Values reported for the molar absorption coefficient for OH-groups in borosilicate glasses vary between about 38 and 47 $\ell/(mol_{OH} \cdot cm)$ for different glass compositions [17]. To estimate absolute values for the water content in the glasses investigated, a molar absorption coefficient with a mean value of 43 $\ell/(mol_{OH} \cdot cm)$ and data for the density summarized by Eq. (3.8), see the next section, were used. The concentration of water in the glasses considered was found to increase from about 13 weight ppm H_2O in the sodium silicate glass investigated in Ref. [5] to about 1000 weight ppm H_2O in the glass of the type $(Na_2O)_{0.2}(B_2O_3)_y(SiO_2)_{0.8-y}$ with

Table 3.2: Data for sodium tracer diffusion coefficients obtained for sodium borosilicate glasses of the type $(Na_2O)_{0.2}(B_2O_3)_y(SiO_2)_{0.8-y}$ at different temperatures and compositions. "– LD" stands for "– $\log_{10}$ $(D^*_{Na}/(cm^2/s))$. The data listed for y = 0 are from Ref. [5], except those for T = 346 °C. Data in columns marked by * are weighted averages from two experiments. The errors reported in the table are from least squares fits of Eq. (3.7) to normalized residual radioactivity profiles. The overall errors are estimated to be on the order of 5 %, as stated in Section 3.2.

T = 208 °C					
y	0	0.15	0.32	0.45	0.6
– LD	10.421	11.486	11.983	12.665	13.056
error ±	0.011	0.017	0.004	0.013	0.024

T = 241 °C					
y	0	0.15*	0.32	0.45*	0.6
– LD	9.822	10.923	11.437	12.088	12.473
error ±	0.013	0.004	0.011	0.008	0.083

T = 274 °C					
y	0	0.15	0.32	0.45*	0.6*
– LD	9.561	10.431	10.965	11.434	11.633
error ±	0.013	0.006	0.011	0.017	0.016

T = 308 °C					
y	0	0.15*	0.32	0.45	0.6
–LD	9.106	9.966	10.468	10.866	11.200
error ±	0.017	0.006	0.008	0.027	0.007

T = 346 °C					
y	0	0.15	0.32	0.45	0.6
– LD	8.701	9.559	10.020	10.458	10.650
error ±	0.004	0.017	0.010	0.005	0.011

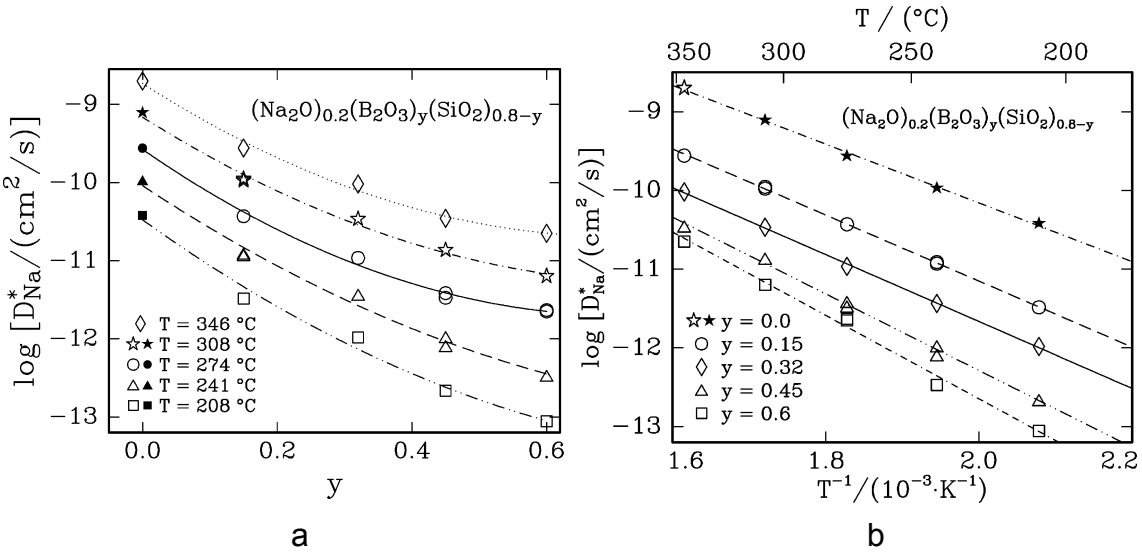

Fig. 3.4: (a) Composition and (b) temperature dependencies of sodium tracer diffusion coefficients determined for sodium borosilicate glasses of the type $(Na_2O)_{0.2}(B_2O_3)_y(SiO_2)_{0.8-y}$. The data shown for y = 0 and denoted by solid symbols are from Ref. [5], except those for T = 346 °C. The errors from fitting Eq. (3.7) to the experimental data are reported in Table 3.2 and are significantly smaller than the symbols used in the figure. The overall errors of the data points shown are estimated to be not larger than ± 5 % corresponding to ± 0.021 in $\log [D^*_{Na}/(cm^2/s)]$, which are also smaller than those corresponding to the sizes of the symbols shown in the figure.

y = 0.6. The water concentration is much larger in boron-rich glasses than in silica-rich ones and increases approximately linearly with the composition parameter y. Compared to the initial water contents of the sodium borosilicate glasses studied in Ref. [5], the glass samples considered in this study with y = 0.32, 0.45 and 0.6 have significantly larger water contents. This is not surprising in view of their age.

3.5.2 Densities and Free Volume of Glass Samples

Density values for glasses of the type $(Na_2O)_{0.2}(B_2O_3)_y(SiO_2)_{0.8-y}$ from the literature [5,13,23] and measured by using a glass pycnometer are shown in Fig. 3.5a. Details related to the density measurements can be found in Ref. [5]. The densities of glasses with y = 0.45 and 0.6 were not measured due to not having a sufficient amount of sample material available. The errors of the density values are about ± 1 % due to systematic errors. The density data from the literature scatter to some extent because glass samples used by different authors were different, e.g., glass samples with different thermal histories. The density of glasses of the type $(Na_2O)_{0.2}(B_2O_3)_y(SiO_2)_{0.8-y}$ increases first, goes through a maximum around y = 0.2, and then decreases when the concentration of boron increases. The line shown in Fig. 3.5a was generated by using an empirical equation, Eq. (3.8), and allows a good description of the density as a function of the composition parameter y.

$$\rho_{glass} = 2.38 + 1.58 \cdot y - 5.37 \cdot y^2 + 4.03 \cdot y^3 \qquad (3.8)$$

The molar volume of the glasses can be obtained by dividing the molar masses by density values corresponding to Eq. (3.8). It is found that the molar volume goes through a shallow minimum around y = 0.18 when y increases from 0 to 0.6. This indicates that the structure of the glasses considered in this study is most compact around y = 0.18.

3.5.3 Sodium Tracer Diffusion

3.5.3.1 Composition Dependence of the Sodium Tracer Diffusion

Fig. 3.4a shows that the sodium tracer diffusion coefficient decreases as the

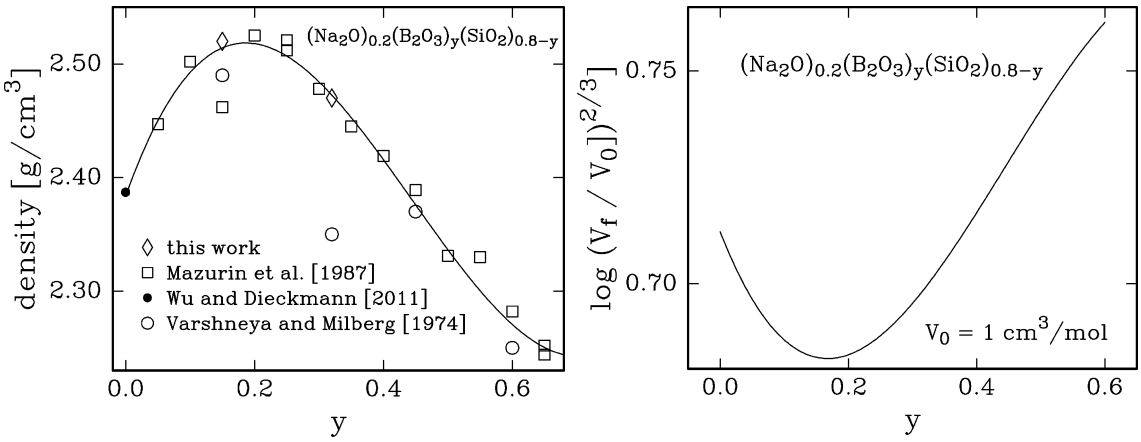

Fig. 3.5: (a) Densities of glasses of the type $(Na_2O)_{0.2}(B_2O_3)_y(SiO_2)_{0.8-y}$ measured and from the literature [5,13,23]. The solid line has been generated by using Eq. (3.8). (b) The logarithm of the square of the cube root of the ratio of a free volume, V_f, normalized to a standard volume, V_0 (= 1 cm^3/mol), as a function of the composition parameter y of glasses of the type $(Na_2O)_{0.2}(B_2O_3)_y(SiO_2)_{0.8-y}$.

composition parameter y increases at constant temperatures between 208 and 346 °C. This trend is different from the composition dependence of the sodium tracer diffusion coefficients for $(Na_2O)_{0.2}[(BO_{1.5})_x(SiO_2)_{1-x}]_{0.8}$ glasses, which showed a shallow minimum near x = 0.7 [5]. The decrease of the sodium tracer diffusion coefficients with the increase of the boron content found in the present study is in agreement with the trends reported in the literature for the decrease of ionic conductivity with the increase of boron concentration in different types of sodium borosilicate glasses [4-9]. The continuous decrease of the sodium tracer diffusion coefficients with y may to some extent also be related to the higher water concentration in the boron-rich glass samples used in this study.

According to the atomistic theory of the diffusion of matter in crystalline materials, a tracer diffusion coefficient is at a given defect concentration proportional to the square of an elementary jump length, a. Because of the lack of a periodic structure in glasses, the situation of the cation diffusion in glasses is much more complicated than that in crystalline materials. Instead of being fixed by a crystal structure, the lengths of diffusional jumps in glasses vary due to local variations of the glass structure. To overcome this difficulty, a value proportional to an average jump distance, $\bar{a}$, was calculated by taking the cube root of a free volume, V_f, which was obtained by subtracting the ionic volume from the molar volume V_m:

$$V_f = V_m - \frac{4}{3} \cdot \pi \cdot N_A \cdot \left[0.4 \cdot r_{Na^+}^3 + 2\,y \cdot r_{B^{3+}}^3 + (0.8 - y) \cdot r_{Si^{4+}}^3 + (1.8 + y) \cdot r_{O^{2-}}^3 \right]. \quad (3.9)$$

In Fig. 3.5b, the logarithm of the square of a quantity being proportional to the average jump distance $\bar{a}$ is shown as a function of the composition parameter y. This plot indicates that the maximum variation of the logarithm of the sodium tracer diffusion coefficient due to variations of $\bar{a}$ when varying y between 0 and 0.6 is smaller than 0.1 and cannot be an important factor for the experimentally observed variation of the sodium tracer diffusion coefficient. According to Fig. 3.5b the square of the parameter $\bar{a}$ has a minimum at around y = 0.19 and varies by not

more than 20 % in the composition range considered in this article. This composition variation is much smaller than that of the sodium tracer diffusion coefficient which is at all temperatures significantly larger than one order of magnitude.

The composition dependence of the transport properties of the considered sodium borosilicate glasses is therefore anticipated to be mostly related to structural changes. In sodium borosilicate glasses, added sodium may associate either with silicon, generating non-bridging oxygen atoms (NBO), i.e., SiO^-Na^+, or with boron, creating NBO at trigonal BO_3 units, i.e., BO^-Na^+, or converting trigonal BO_3 units to tetrahedral BO_4 units, the latter not generating any NBO, depending on the values of R (= $n_{Na_2O}/n_{B_2O_3}$; n = number of moles) and K (= $n_{SiO_2}/n_{B_2O_3}$) [24]. The fraction of boron atoms in fourfold coordination, N_4, for each glass compositions with y > 0 was calculated based on models proposed by Yun and Bray [25], Yun et al. [26] and by Dell et al. [27]. It was found that the value of N_4, for values see Table 3.1, decreases as y increases from 0.15 to 0.6. The concentration of B_2O_3 in BO_4 tetrahedra increases from about 11 to about 20 mol%. The fraction of sodium attached to NBO, f_{NBO}, was calculated based on values for N_4 and was found to decrease to almost zero when y reaches a value of 0.32, i.e., practically all sodium ions act as charge compensators for tetrahedral BO_4 units in glass samples with y = 0.32, 0.45 and 0.6. This behavior is in agreement with earlier observations by Milberg et al. [28] and by Kaps and Kahnt [29]. It seems that just looking at values of N_4 and of f_{NBO} is insufficient for possibly understanding the observed composition dependence of the sodium tracer diffusion. The strength of bonding of Na^+ to units of units of $BO_{4/2}^-$ may vary, depending on the different environments of such units, whether one has isolated units of $BO_{4/2}^-$ surrounded only by Si-containing units or units of $BO_{4/2}^-$ having other B-containing units next to them. Some information on differences in the environment of units of $BO_{4/2}^-$ has been obtained by Du and Stebbins [30,31]. These authors confirmed that different environments exist and that their fractions change with the content of B_2O_3. Such changes could also contribute to the

experimentally observed decrease of the sodium diffusivity with increasing values of y at higher B_2O_3 contents although the overall concentration of $BO^-_{4/2}$ remains almost unchanged. Unfortunately, the currently existing knowledge related to the structure of the considered sodium borosilicate glasses does not allow any more firm conclusions with regard to the behavior of ion mobilities as a function of the glass composition. To an unknown extent the observed decrease of the tracer diffusion coefficient with increasing values of y may also be related to structural changes caused by the observed very significant increase of the water content with increasing values of y, see Fig. 3.2c. Systematic studies using glasses with identical values of y and varying water concentrations are desirable to better understand the composition dependence observed in this study for larger values of y.

As discussed before, several factors may contribute to the observed variation of the sodium tracer diffusion coefficient with the composition parameter y. As discussed above, one of them is the variation of the average jump distance, $\overline{a}$, in the glass structure. Based on the preceding data analysis this factor can be only of minor importance. Another factor, which may contribute, is the strong increase in the concentration of water with an increasing content of B_2O_3. An increase of the water content in glasses usually leads to a reduction of sodium diffusivities and ionic conductivities. For the sodium tracer diffusion data presented in this article it is unknown how large the influence of the water content on the sodium diffusivity is. It is also unknown how large the influence of variations in the glass structure due to an increasing B_2O_3 concentration is. Currently it remains unclear how much the different factors denoted above contribute to the observed reduction of the sodium diffusivity in the glasses considered in this article.

3.5.3.2 Temperature Dependence of the Sodium Tracer Diffusion

An Arrhenius-type equation was used to analyze the temperature dependence of the sodium tracer diffusion coefficients obtained at temperatures sufficiently far below the glass transition temperature. To derive Fig. 3.4b, an Arrhenius-type equation, see Eq. (3.10), was fitted to sodium tracer diffusion coefficients for

temperatures up to about 350 °C.

$$D^{*}_{Na} = D^{o}_{Na} \cdot \exp\left(- \frac{\Delta E_a}{R \cdot T} \right) \tag{3.10}$$

The values of the activation enthalpy, ΔE_a, and of the pre-exponential factor, D°_{Na}, determined from the fitting are listed in Table 3.3. It was found that the activation enthalpy, ΔE_a, increases almost linearly from about 70 to 100 kJ/mol when y increases from 0 to 0.6, see Fig. 3.6a, and that the pre-exponential factor varies from about $7 \cdot 10^{-4}$ to about $9 \cdot 10^{-3}$ cm^2/s with a minimum at y around 0.32, see Fig. 3.6b.

In addition to analyzing the tracer diffusion data from this work, it was also attempted to compare these with data from the literature. For the temperature range covered by the experiments performed such data were not found. However, for 600 °C, a temperature above T_g, sodium tracer diffusion data measured by Wakabayashi and Terai [6] are available. These data are not for the specific compositions considered in this study, except for y = 0. To enable a comparison, an interpolation of the tracer diffusion data from Ref. [6] to y = 0.15, 0.32 and 0.45 was performed. Then the tracer diffusion data for 600 °C were compared in an Arrhenius plot with diffusion data from this study for y = 0, 0.15, 0.32 and 0.45. This comparison showed that the tracer diffusion coefficients for 600 °C are somewhat larger than those obtained by extrapolating the data shown in Fig. 3.4b to 600 °C, at maximum by a factor of about 4. This suggests that the temperature dependence of the sodium tracer diffusion coefficient is at higher temperatures, beginning near T_g, larger than at lower temperatures.

3.5.3.3 Comparison with Ionic Conductivities and Haven-Ratio

In a previous study of transport in glasses of the type $(Na_2O)_{0.2}[(BO_{1.5})_x(SiO_2)_{1-x}]_{0.8}$ Wu and Dieckmann [5] have compared sodium tracer diffusion data with sodium diffusion coefficients calculated departing from ionic conductivity data and derived values for Haven-ratios for 300 °C. Such a comparison was also attempted for the glasses considered in this study but could

Table 3.3: Activation enthalpies and pre-exponential factors for the tracer diffusion of Na-22 in glasses of the type $(Na_2O)_{0.2}(B_2O_3)_y(SiO_2)_{0.8-y}$. The data shown were derived by considering experimental data for temperatures up to 346 °C. "ΔE_a" stands for "ΔE_a / (kJ/mol)" and "$-$ LD°" stands for "$-\log_{10}$ (D°_{Na} / (cm^2/s)". Attributing an estimated error of ± 5 % to the diffusion coefficients, the errors of all values listed below, calculated based on the diffusion coefficients listed in Table 3.2, for ΔE_a are ± 1.11 kJ/mol and those for $-$ LD° are all ± 0.11.

y	0	0.15	0.32	0.45	0.6
ΔE_a	70.47	80.07	81.36	93.78	101.30
$-$ LD°	2.79	2.79	3.17	2.50	2.08

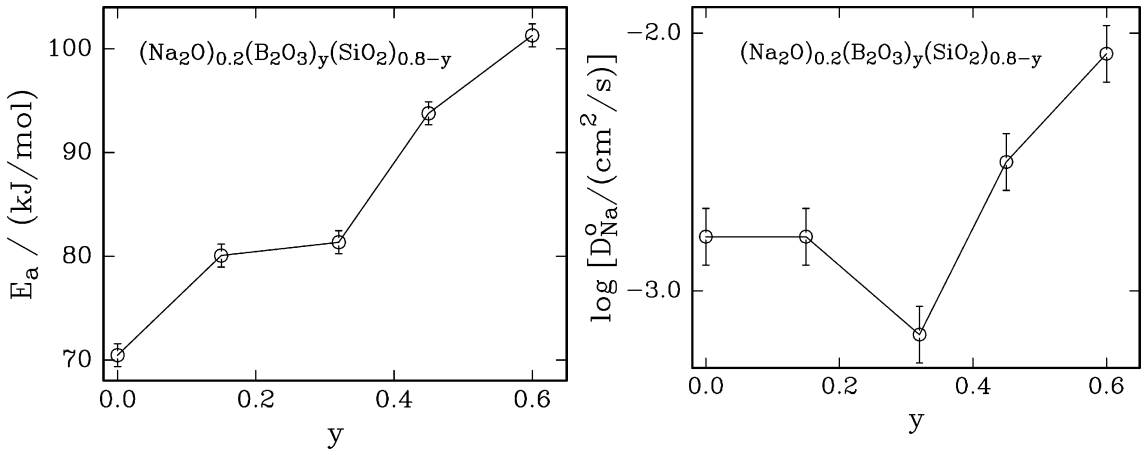

Fig. 3.6: (a) Activation enthalpies and (b) pre-exponential factors for the sodium tracer diffusion in sodium borosilicate glasses of the type $(Na_2O)_{0.2}(B_2O_3)_y(SiO_2)_{0.8-y}$ as a function of the glass composition.

not go very far due to a lack of a sufficient number of suitable ionic conductivity data. As stated in the introduction, Otto [4] has reported a few conductivity data for sodium borosilicate glasses with 20 mol% Na_2O. Two of his data points for about 350 °C can be used to calculate values for component diffusion coefficients of sodium, D_σ, which then can be compared with tracer diffusion coefficients from this study. For calculating values for D_σ Eq. (3.11) was used.

$$D_\sigma = \frac{\sigma_i \cdot R \cdot T}{z_i^2 \cdot F^2 \cdot c_i} \tag{3.11}$$

In this equation σ_i is the ionic conductivity attributed to the electrical conduction by Na^+ ions, R is the gas constant, T is the temperature, z_i (=1) is the charge number of Na^+, F is the Faraday constant and c_i is the concentration of Na^+ ions. The calculated values of D_σ for y = 0.3 and y = 0.55 are shown in Fig. 3.7 together with a value calculated for D_σ for y = 0 using ionic conductivity data denoted in Ref. [5] and extrapolated to 350 °C and with values for sodium tracer diffusion coefficients from this work for about 350 °C. The electrical conductivity value for y = 0.8 from Ref. [4] was ignored due to a lack of reliable density data for the density close to y = 0.8 and the non-availability of any sodium tracer diffusion data for y = 0.8 which could be used for comparison. The D^*_{Na}-value shown for y = 0.55 was obtained by interpolating. At all values of y the tracer diffusion coefficients are smaller than the sodium component diffusion coefficients. This means that the Haven-ratio, H_R (= D^*_{Na}/D_σ), is at all compositions considered smaller than one, as expected for a correlated motion of the tracer. Values calculated for H_R are also shown in Fig. 3.7. The values vary between about 0.3 and 0.85. One of the lines drawn in the figure with the intent to guide the eye suggests that there may be a minimum in H_R as a function of y. The limited data available at this time are not sufficient to firmly support this suggestion.

3.5.3.4 Comparison with Interdiffusion Data

As stated in the introduction, the interdiffusion occurring when sodium in glasses of the type $(Na_2O)_{0.2}(B_2O_3)_y(SiO_2)_{0.8-y}$ is exchanged against potassium is

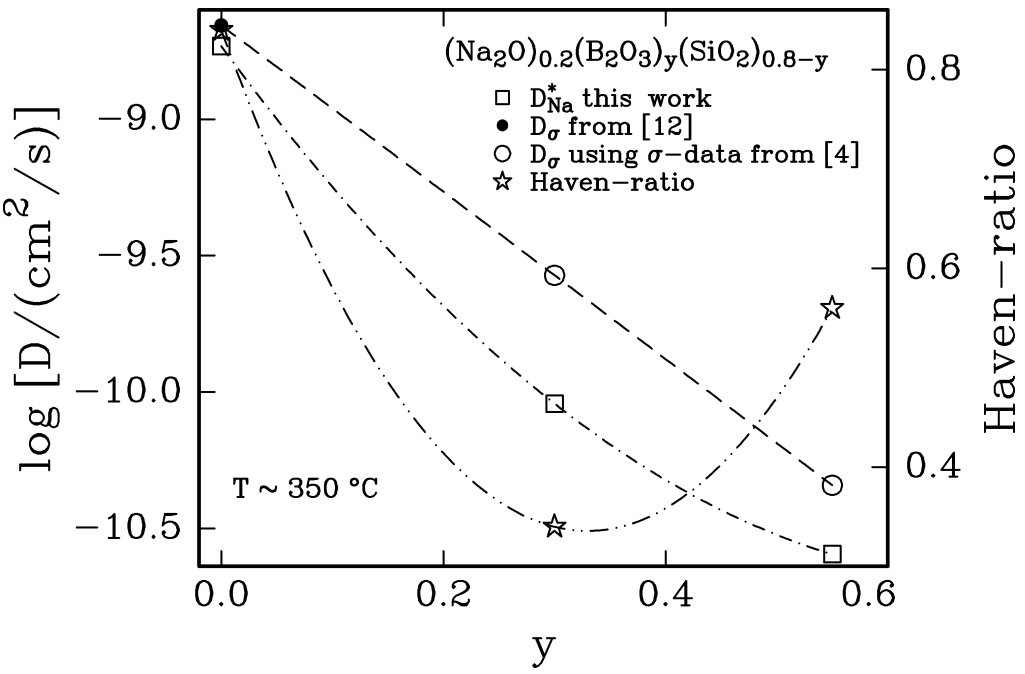

Fig. 3.7: Comparison between sodium tracer diffusion coefficients, D^*_{Na}, and component diffusion coefficients for sodium, D_σ, derived by using values for the ionic conductivities denoted in Ref. [5] and such from Ref. [4] and density data summarized by Eq. (3.8). In addition, resulting values for the Haven-ratio, H_R, are shown. All lines in the figure are for guiding the eye only.

governed by the diffusion of sodium and potassium. The interdiffusion coefficient, $\tilde{D}$, describing this interdiffusion varies with the fraction of the sodium replaced by potassium, m, and is linked via the Nernst-Planck equation, see Eq. (3.1), to the component diffusion coefficients of Na and K, D_{Na} and D_K. If m = 0, then $\tilde{D} = D_K$. As stated before, based on ion sizes it is expected that $D_K < D_{Na}$ when m approaches zero.

Using interdiffusion data obtained many years ago [13] by performing ion exchange experiments using the same boron oxide-containing glasses as considered in this work, one can determine whether the expectation $D_K < D_{Na}$ is fulfilled. For this purpose interdiffusion data reported in Ref. [13] were extrapolated to m = 0. For T = 343 °C values between about $6 \cdot 10^{-14}$ and $5 \cdot 10^{-13}$ cm^2/s were obtained for $\tilde{D} = D_K$, varying in a non-systematical way with the composition parameter of y between 0.15 and 0.6. These values can be compared with values for sodium tracer diffusion coefficients at 346 °C listed in Table 3.2. The values of the sodium tracer diffusion coefficients vary between about $3 \cdot 10^{-10}$ and $2 \cdot 10^{-11}$ cm^2/s when y increases from 0.15 to 0.6. Even when taking into account that extrapolating values for interdiffusion coefficients to m = 0 involves relatively large uncertainties and also that Haven-ratios with values smaller than one are contained in the sodium tracer diffusion coefficients, the comparison clearly shows that the expectation $D_K < D_{Na}$ is fulfilled for m = 0, i.e., for glasses of the type $(Na_2O)_{0.2}(B_2O_3)_y(SiO_2)_{0.8-y}$. Sodium and potassium tracer diffusion coefficients measured by Fleming and Day [16] for sodium silicate glasses of the type $Na_2O \cdot 3SiO_2$ at temperatures between 250 and 450 °C indicate that this expectation is also fulfilled for glasses of the composition $Na_2O \cdot 3SiO_2$.

3.6 Conclusions

Sodium tracer diffusion coefficients, D^*_{Na}, have been measured in sodium borosilicate glasses of the type $(Na_2O)_{0.2}(B_2O_3)_y(SiO_2)_{0.8-y}$ as a function of temperature and the composition parameter y. At constant temperature, the tracer diffusion coefficient of sodium decreases with an increasing value of the composition parameter y. Based on literature data the fraction of boron atoms in

fourfold coordination, N_4, was found to decrease when y increases from 0.15 to 0.6. However, at the same time the absolute value of the concentration of boron in tetrahedra increases to some extent while the environment of these tetrahedra varies too. Almost all of the sodium ions act as charge compensators for tetrahedral BO_4 units in glass samples with y = 0.32, 0.45 and 0.6. Firm conclusions to which extent variations in the glass structure are responsible for the observed decrease of the sodium diffusivity with an increasing boron oxide content cannot be made. The observed increase of the initial water concentrations with the value of y could be a second reason for the decrease of the sodium diffusivity with an increasing value of y. The pre-exponential factor of the sodium tracer diffusion coefficient varies by about one order of magnitude with a minimum at around y = 0.32 and the activation enthalpy increases about linearly with increasing y from about 70 kJ/mol to about 100 kJ/mol between y = 0 and y = 0.6.

3.7 Acknowledgments

This work was supported by the National Science Foundation under Award Number DMR-0710564. The work made use of the Cornell Center for Materials Research Facilities supported by the National Science Foundation under Award Number DMR-0520404. The authors thank CCMR shared facility staff, Paul Bishop, for assistance related to a variety of topics. Thanks are due to collaborators in the NSF-sponsored Materials World Network “An International Collaborative Research Program in the Study of Mixed Glass Former Phenomena in Materials”, including Steve Martin and Valeri Petkov, for many insightful discussions. Finally, the authors thank all undergraduate researchers who helped in experimental work.

REFERENCES

[1] G. El-Damrawi, W. Mueller-Warmuth, H. Doweidar and I.A. Gohar, "Structure and Heat Treatment Effects of Sodium Borosilicate Glasses as Studied by ^{29}Si and ^{11}B NMR," Journal of Non-Crystalline Solids, **146** (2-3) [1992] 137-144.

[2] D. Manara, A. Grandjean and D.R. Neuville, "Structure of Borosilicate Glasses and Melts: A Revision of the Yun, Bray and Dell Model," Journal of Non-Crystalline Solids, **355** (50-51) [2009] 2528-2531.

[3] A. Pradel, C. Rau, D. Bittencourt, P. Armand, E. Philippot and M. Ribes, "Mixed Glass Former Effect in the System $0.3Li_2S$-$0.7[(1-x)SiS_2$-$xGeS_2]$: A Structural Explanation," Chemistry of Materials, **10** (8) [1988] 2162-2166.

[4] K. Otto, "Electrical Conductivity of SiO_2-B_2O_3 Glasses Containing Lithium or Sodium," Physics and Chemistry of Glasses, **7** (1) [1966] 29-37.

[5] X. Wu and R. Dieckmann, "Sodium Tracer Diffusion in Glasses of the Type $(Na_2O)_{0.2}[(BO_{1.5})_x(SiO_2)_{1-x}]_{0.8}$," Journal of Non-Crystalline Solids, **357** (15) [2011] 2846-2856.

[6] H. Wakabayashi and R. Terai, "Effect of Trivalent Oxide on Electrical Conductivity of Alkali-silicate Glasses (Part 1) Borosilicate Glasses," (in Japanese) Yogyo Kyokaishi, **93** (1) [1985] 13-19.

[7] H. Wakabayashi, R. Terai and H. Yamanaka, "Effect of Trivalent Oxide on Electrical Conductivity in Alkali-silicate Glasses (Part 2) Similarity of Various Network Forming Trivalent Ions," (in Japanese) Yogyo kyokaishi, **93** (4) [1985] 209-216.

[8] C. Kaps, F. Schirrmeister and P. Stefanski, "On the Na^+ Self-diffusion and Electrical Conductivity of Na_2O_3-B_2O_3-SiO_2 Glasses Derived from the $Na_2O{\cdot}SiO_2$ Glass," Journal of Non-Crystalline Solids, **87** (1-2) [1986] 159-170.

[9] D. Ehrt and R. Keding, “Electrical Conductivity and Viscosity of Borosilicate Glasses and Melts,” Physics and Chemistry of Glasses: European Journal of Glass Science and Technology Part B, **50** (3) [2009] 165-171.

[10] R.M. Catchings, “Influence of Composition and Structure on the Ionic Conductivity of the Glass System Sodium Oxide-Boron Oxide-Silica,” Journal of Applied Physics, **52** (2) [1980] 1116-1117.

[11] A. Grandjean, M. Malki and C. Simonnet, “Effect of Composition on Ionic Transport in SiO_2-B_2O_3-Na_2O Glasses,” Journal of Non-Crystalline Solids, **352** (26-27) [2006] 2731-2736.

[12] A. Grandjean, M. Malki, V. Montouillout, F. Debruycker and D. Massiot, “Electrical Conductivity and ^{11}B NMR Studies of Sodium Borosilicate Glasses,” Journal of Non-Crystalline Solids, **354** (15-16) [2008] 1664-1670.

[13] A.K. Varshneya and M.E. Milberg, “Ion Exchange in Sodium Borosilicate Glasses,” Journal of the American Ceramic Society, **57** (4) [1974] 165-169.

[14] R.H. Doremus, “Exchange and Diffusion of Ions in Glass,” The Journal of Physical Chemistry, **68** (8) [1964] 2212-2218.

[15] A.K. Varshneya, “Kinetics of Ion Exchange in Glasses,” Journal of Non-Crystalline Solids, **19** [1975] 355-365.

[16] J.W. Fleming and D.E. Day, “Relation of Alkali Mobility and Mechanical Relaxation in Mixed-Alkali Silicate Glasses,” Journal of the American Ceramic Society, **55** (4) [1972] 186-192.

[17] J.E. Shelby, “Introduction to Glass Science and Technology,” 2nd Ed., [2005], The Royal Society of Chemistry, Cambridge.

[18] R.H. Doremus, “Diffusion of Water in Silica Glass,” Journal of Materials Research, **10** (9) [1995] 2379-2389.

[19] R.H. Doremus, Glass Science, 2nd Ed., John Wiley, New York, 1994.

[20] J. Crank, The Mathematics of Diffusion, 2nd Ed., [1975], Clarendon Press, Oxford.

[21] B.J. Wilson, The Radiochemical Manual, 2nd Ed., [1966], The Radiochemical Centre, Amersham.

[22] A.K. Bandyopadhyai, R. Jabra and J. Phalippou, "Association of Hydroxyl Groups with Boron and Silicon Atoms in SiO_2-B_2O_3 Glasses by Infrared Spectroscopy," Journal of Materials Science Letters, **8** (12) [1989] 1464-1467.

[23] O.V. Mazurin, M.V. Streltsina and T.P. Shvaiko-Shvaikovskaya, Handbook of Glass Data, [1987], Elsevier Science Publ. Co., New York, NY.

[24] A.K. Varshneya, "Fundamentals of Inorganic Glasses," Academic Press, Inc., San Diego, CA, [1994].

[25] Y.H. Yun and P.J. Bray, "Nuclear Magnetic Resonance Studies of Glasses in the System Na_2O-B_2O_3-SiO_2," Journal of Non-Crystalline Solids, **27** (3) [1978] 363-380.

[26] Y.H. Yun, S.A. Feller and P.J. Bray, "Correction and Addendum to 'Nuclear Magnetic Resonance Studies of Glasses in the System Na_2O-B_2O_3-SiO_2'," Journal of Non-Crystalline Solids, **33** (2) [1979] 273-277.

[27] W.J. Dell, P.J. Bray and S.Z. Xiao, "^{11}B NMR Studies and Structural Modeling of Na_2O-B_2O_3-SiO_2 Glasses of High Soda Content," Journal of Non-Crystalline Solids, **58** (1) [1983] 1-16.

[28] M.E. Milberg, J.G. O/keefe, R.A. Verhelst and H.O. Hooper, "Boron Coordination om Sodium Borosilicate Glass," Phys. Chem. Glasses, **13** (3) [1972] 79-84.

[29] C. Kaps and H. Kahnt, "Structure and Na^+ Transport in With a High Content of Na_2O ($\geq$ 10 mol%) - Studied by ^{22}Na Tracer Diffusion and Conductivity Measurements," Acta Phys. Slov., **38** (6) [1988] 366-369.

[30] L.-S. Du and J.F. Stebbins, “Solid-State NMR Study of Metastable Miscibility in Alkali Borosilicate Glasses,” Journal of Non-Crystalline Solids, **315** (3) [2003] 239-255.

[31] L.-S. Du and J.F. Stebbins, “Nature of Silicon-Boron Mixing in Sodium Borosilicate Glasses: A High-Resolution ^{11}B and ^{17}O NMR Study,” J. Phys. Chem B, **107** (37) [2003] 10063-10076.

CHAPTER FOUR

SODIUM TRACER DIFFUSION IN SODIUM BOROALUMINOSILICATE GLASSES*

4.1 Abstract

Sodium tracer diffusion coefficients, D^*_{Na}, have been measured using the radioactive isotope Na-22 in sodium boroaluminosilicate (NBAS) glasses containing either a small amount of As_2O_3 or of Fe_2O_3. The chemical compositions of the first type of glasses are given by the formula $[(Na_2O)_{0.71}(Fe_2O_3)_{0.05}(B_2O_3)_{0.24}]_{0.2}[(SiO_2)_x(Al_2O_3)_{1-x}]_{0.8}$ and those of the second type of glasses correspond to the formula $[(Na_2O)_{0.73}(B_2O_3)_{0.24}(As_2O_3)_{0.03}]_{0.18}[(SiO_2)_x(Al_2O_3)_{1-x}]_{0.82}$. Tracer diffusion measurements were performed at different temperatures between 198 and 350 °C. Pre-annealing of the glass samples at their glass transition temperatures in common air was found to lead to changes in the values of sodium tracer diffusion coefficients. For the NBAS glasses containing Fe_2O_3, after pre-annealing for 5 hours, the activation enthalpy derived for the sodium tracer diffusion increases almost linearly from 57.5 to 71.3 kJ/mol with a decrease in the alumina content while the pre-exponential factor of the sodium tracer diffusion coefficient increases from $2.1 \cdot 10^{-4}$ to $5.3 \cdot 10^{-4}$ cm^2/s. For the iron-free NBAS glasses pre-annealed for 5 hours, the activation enthalpy varies between 63.9 and 71.4 kJ/mol while the pre-exponential factor varies between $1.5 \cdot 10^{-4}$ and $1.2 \cdot 10^{-3}$ cm^2/s. In addition, it was observed that the considered glasses take up water when annealed at 300 °C in wet air with P_{H_2O} = 474 mbar.

4.2 Introduction

Multi-component boroaluminosilicate glasses are widely used in various

---

* Reprinted with permission from Xinwei Wu, Jeremy D. Moskowitz, John C. Mauro, Marcel Potuzak, Qiuju Zheng and Rüdiger Dieckmann, Journal of Non-Crystalline Solids, 358 (12-13) [2012] 1430-1437.

applications such as fiber glass in strengthened composites [1], substrate glasses in active matrix liquid crystal displays [2,3], high-level nuclear waste glasses [4-6] and as glass seals [7] due to their high chemical durability and mechanical strength [8]. Ion-exchanged alkali boroaluminosilicate glasses having high resistance to scratch damage are applied as protective covers for electronic displays in laptop computer screens and mobile devices.

In 1962, Kistler [9] and Acloque and Tochon [10] introduced chemical strengthening of glass through ion exchange. Glass samples are immersed in a molten alkali salt bath at a temperature below the glass transition temperature, T_g, during the ion exchange process. When the ionic radius of the invading ions like K^+ is larger than the ionic radius of the ions originally present in the glass samples such as Na^+, high surface compressive stress is generated through the thermally activated interdiffusion process and glasses are strengthened. The well developed chemical strengthening science and technology of glass has been reviewed by several authors [11-19]. Studying sodium tracer diffusion in alkali boroaluminosilicate glasses is important for better understanding ion diffusion in such glasses.

Sodium cations can play different roles in sodium boroaluminosilicate (NBAS) glasses. They can act as charge compensators for tetrahedral aluminum and/or boron and can form non-bridging oxygen (NBO) bonded to tetrahedral silicon and/or trigonal boron. To study how sodium tracer diffusion coefficients change with the structural roles that sodium ions play in the NBAS glasses considered in this article, the molar concentration ratio $[SiO_2]/[Al_2O_3]$ was varied while the concentrations of all other oxides were kept constant.

Water being present or incorporated into oxide glasses can cause a water-assisted structural relaxation via reactions such as denoted in Eq. (4.1) [20]. This relaxation often leads to changes of structure-sensitive glass properties such as the viscosity, the glass transition temperature, T_g, the density, the dielectric constant, and the refractive index of such glasses [21] and also of the diffusivity of sodium in silicate glasses [22].

$$R\text{-}O\text{-}R' + H_2O\,(glass) \rightleftharpoons R\text{-}O\text{-}H + H\text{-}O\text{-}R' \quad (4.1)$$

In Eq. (4.1) R and R' denote parts of the glass network. Since water can affect the diffusivity of sodium, it was also of interest to examine whether the NBAS glasses considered in this article take up water in directly measurable amounts.

4.3 Experiments

The following sections provide details of the glass samples used in this study, how these glass samples were made, their composition and their original water content. Furthermore, information is given on the experiments performed to investigate the uptake of water and the sodium tracer diffusion.

4.3.1 Glass Samples

The NBAS glass samples, produced at Corning Incorporated, were square plates received with dimensions of about 10×10×1 mm with both large sides well polished. The glasses were made by melting powder mixtures containing appropriate amounts of Na_2CO_3, H_3BO_3, Al_2O_3, SiO_2, Fe_2O_3 and As_2O_3 in a covered Pt crucible at different homogenization temperatures for 6 hours in air. In the case of iron-free glasses, about 0.1 mol% As_2O_3 was added as fining agent. To ensure chemical homogeneity, after the melts were quenched in water, the glass shards were remelted for another 6 hours at their homogenization temperatures and then the melted glass was poured in air onto stainless steel plates. After that, the glasses were annealed for 2 hours at different temperatures between 450 and 560 °C, depending on the chemical composition of the glasses. The compositions of the prepared NBAS glasses were determined by using wet chemistry analyses and are reported in Table 4.1.

At Cornell University samples with the dimensions denoted above were cut into quarters by using a diamond pen to have more samples available for tracer diffusion experiments. To avoid any contamination introduced by fingerprints, like alkali and alkaline-earth compounds, all glass samples were washed ultrasonically in de-ionized (DI) water, ethanol and acetone and thereafter tweezers were used

Table 4.1: Chemical compositions determined using a wet chemistry analysis, densities obtained at room temperature by employing an Archimedes' principle-based technique using a METTLER Toledo balance with ethanol as the immersion liquid, glass transition temperatures, T_g, defined as the temperatures at which the equilibrium viscosity equals 10^{12} Pa·s, and fractions of boron in tetrahedral coordination (N_4) determined by ^{11}B MAS NMR spectroscopy of the iron-free and iron-containing NBAS glasses investigated. The denotations used for glasses without Fe_2O_3 contain an "n" at the end. All data listed in this table were determined at Corning Incorporated and will be reported in Ref. [27].

glass	chemical composition (mol%)						density (g/cm^3)	T_g (°C)	N_4 (at%)
	Na_2O	B_2O_3	Al_2O_3	SiO_2	Fe_2O_3	As_2O_3			
Al 2.5n	14.4	4.7	2.0	78.8		0.1	2.40	549	90
Al 5n	13.6	4.2	4.0	78.1		0.1	2.42	564	87
Al 7.5n	13.0	4.3	5.7	76.9		0.1	2.42	578	77
Al 10n	12.3	4.3	7.5	75.9		0.1	2.43	598	68
Al 12.5n	13.1	4.4	10.4	72.0		0.1	2.40	614	39
Al 15n	13.5	4.6	12.7	69.2		0.1	2.38	626	17
Al 2.5	14.6	4.9	2.2	77.4	0.9		2.44	543	
Al 5	14.6	5.0	4.7	74.7	1		2.44	551	
Al 7.5	14.7	4.9	7.6	71.8	1		2.46	573	
Al 10	14.8	5.0	10.3	68.9	1		2.44	577	
Al 12.5	14.3	5.0	12.6	67.1	1		2.41	591	
Al 15	14.3	5.0	15.6	64.1	1		2.42	631	

to handle the glass samples for all types of measurements performed. Some preliminary values for sodium tracer diffusion coefficients for as-received glasses diffusion-annealed at 301 °C were already reported in Ref. [23]. These data were compared in Ref. [23] with transport-related data from different types of experiments involving the transport of sodium ions but in which the kinetics are limited by other factors.

4.3.2 Water Content and Uptake Measurements

Almost all water being present in silicate glasses is accommodated in the form of hydroxyl groups as long as the concentration of water is relatively small [21]. To determine the water content of glass samples, the IR absorbance related to the presence of hydroxyl groups at wavenumbers between 3500 and 3700 cm^{-1} was measured by using a Bruker Optics Equinox 55 Fourier Transform Infrared (FTIR) Spectrometer. Details about the procedures used for measuring water concentrations in glasses can be found in Ref. [24].

By making use of the Beer-Lambert law, the average water concentration in an area of a glass sample through which the IR beam travels can be obtained. Eq. (4.2) was used to convert measured absorbances of the glass, A_g, into values for the average mass fraction of H_2O in the glass, c_{H_2O}.

$$c_{H_2O} = \frac{1}{2} \cdot \frac{A_g}{\varepsilon_{OH} \cdot d_g} \cdot \frac{M_{H_2O}}{\rho_g} = \frac{A_g}{\varepsilon_{H_2O} \cdot d_g} \cdot \frac{M_{H_2O}}{\rho_g} \tag{4.2}$$

with

$$A_g = -\log_{10}\left(\frac{I}{I_0}\right), \tag{4.3}$$

In these equations I/I_0 is the integral intensity ratio between the transmitted and the initial IR signal, ε_{OH} is the molar absorption coefficient related to the overall concentration of hydroxyl groups present in the glass (in $L/(mol_{OH} \cdot cm)$), d_g (in cm) is the thickness of the glass sample, M_{H_2O} is the molar mass of H_2O (= 18.02 g/mol) and ρ_g is the density of the glass (in g/cm^3). The molar absorption

coefficient related to the stretching of hydroxyl groups is about one half of the molar absorption coefficient of the overall water present in the glass, i.e., $2\,\varepsilon_{OH} \approx \varepsilon_{H_2O}$.

Eq. (4.2) was reorganized to avoid the problem of not knowing the value of ε_{OH} for the NBAS glasses considered in this study, leading to Eq. (4.4),

$$c_{H_2O} \cdot \varepsilon_{OH} = \frac{1}{2} \cdot \frac{A_g}{d_g} \cdot \frac{M_{H_2O}}{\rho_g}. \qquad (4.4)$$

If the value of ε_{OH} does not change significantly with the variation of the water concentration in a glass, the water concentration variation is proportional to the product $c_{H_2O} \cdot \varepsilon_{OH}$.

To measure the water uptake by a NBAS glass, glass samples of the size of about 5×5 mm with thicknesses of about 0.2 mm, were held upright in a thin slot of an alumina sample holder and were annealed in moist air in a tube furnace at about 300 °C. These glass samples were used to determine the relationships between the overall uptake of water and the annealing time for samples with unchanged water contents within glass samples near their centers. Samples of the same type were also used to measure the solubility of water in glass samples and to follow the uptake of water as a function of the annealing time in order to determine values of effective chemical diffusion coefficients, $\tilde{D}_{eff}$. All glass samples were annealed in a furnace containing wet air for a sufficiently long time. The wet air was obtained by bubbling common air through DI water at 80 °C (P_{H_2O} = 474 mbar) and was pumped through the furnace at a rate of about 20 L/h. Overall water contents were determined using a Bruker Optics Equinox 55 FTIR Spectrometer after samples were taken out of the annealing furnace, washed using HPLC grade acetone, and dried for about ten minutes in an oven at 130 °C.

4.3.3 Tracer Diffusion Experiments

4.3.3.1 Experimental Details

Tracer diffusion coefficients for the radioactive isotope Na-22 diffusing in NBAS glass samples were obtained by measuring residual radioactivities as a function

of the distance from the surface where a thin film of solution containing isotope Na-22 was initially applied. The energies of γ-radiation associated with the decay of Na-22 are 0.51 and 1.28 MeV [25]. The initial radioactivity of a sample, A(x=0,t), and the residual radioactivities of this sample, A(x,t), after removing of material containing radioactive tracer with overall thicknesses of x parallel to the surface which originally contained all the tracer material were recorded by using a high resolution high-purity Ge detector (EG&G Ortec). Normalized residual radioactivity profiles, A(x,t)/A(x=0,t) vs. x, were obtained by stepwise removal of material from the samples and measuring residual radioactivities for different values of x. Further details about such experiments can be found in Ref. [24].

4.3.3.2 Diffusion Mathematics

For a homogenous glass sample in which the tracer diffusion coefficient of sodium is constant, the thin film solution of Fick's second law applies. The concentration of a tracer i, $c_i(\xi,t)$, at a distance ξ from the surface where the tracer i was applied before diffusion-annealing for the time, t, can be obtained by using Eq. (4.5) [26].

$$c_i(\xi,t) = \frac{Q_i}{\sqrt{\pi \cdot D_i^* \cdot t}} \cdot \exp\left(- \frac{\xi^2}{4\, D_i^* \cdot t} \right) \tag{4.5}$$

In this equation Q_i is the initial concentration of the tracer per unit area and D_i^* is the tracer diffusion coefficient of the species i, i.e., in the present work of radioactive Na-22.

By integration, departing from Eq. (4.5), Eq. (4.6) can be obtained to describe the normalized radioactivity of the tracer i, A(x,t)/A(x=0,t), as a function of the tracer diffusion coefficient of the species i, D_i^*, and the diffusion-annealing time, t, when the absorption of the radiation from the decay of the radioactive isotope used in the sample is sufficiently small so that it can be ignored for the data analysis. This is the case for the experiments performed in this study.

$$\frac{A(x,t)}{A(x=0,t)} = \frac{\int_{x}^{\infty} c_i(\xi,t)\cdot d\xi}{\int_{0}^{\infty} c_i(\xi,t)\cdot d\xi} = 1 - \mathrm{erf}\left(\frac{x}{2\sqrt{D_i^*\cdot t}}\right). \quad (4.6)$$

Instead of Eq. (4.6), an equation containing the inverse function of the error function, erfi, was used to analyze experimental data in order to achieve a higher precision by more emphasizing the influence of data points obtained for larger penetration depths on the results, see Eq. (4.7).

$$\mathrm{erfi}\left(1 - \frac{A(x,t)}{A(x=0,t)}\right) = \frac{x}{2\sqrt{D_i^*\cdot t}} \quad (4.7)$$

When a = erf(b), then b = erfi(a).

4.4 Results

4.4.1 Initial Water Content

An infrared absorption peak observed for an iron-containing, as-received NBAS glass sample containing about 7.5 mol% alumina is shown in Fig. 4.1a. The observed broad asymmetric absorption peak can be attributed to three partially overlapping peaks related to the IR-absorption by Al-OH, B-OH and Si-OH groups. By using the density values reported in Table 4.1, values determined for the initial water content of as-received glass samples in the form of the product $c_{H_2O}\cdot\varepsilon_{OH}$ (in $(g_{H_2O}/kg_{glass})\cdot(L/(mol_{OH}\cdot cm))$) as a function of the concentration difference $[Na_2O] - [Al_2O_3]$ are shown in Fig. 4.1b.

4.4.2 Water Uptake

To investigate how much water the considered NBAS glasses take up upon annealing in moist air and also how the amount of water taken up changes as a function of the annealing time, values for increases of water contents, $\Delta c_{H_2O}\cdot\varepsilon_{OH}$ (in $(g_{H_2O}/kg_{glass})\cdot(L/(mol_{OH}\cdot cm))$), were experimentally determined. Values for water contents obtained for about 0.2 mm thick samples of two types of iron-free glass

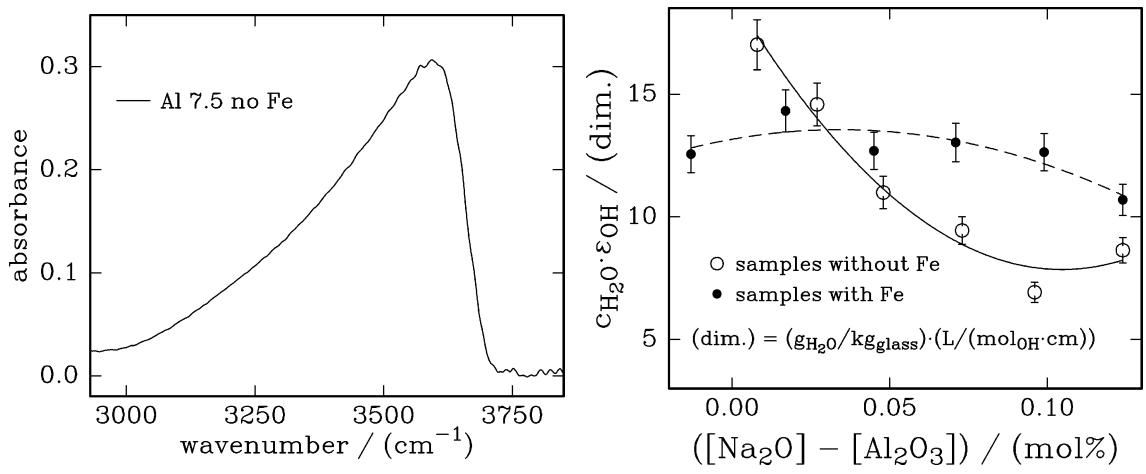

a b

Fig. 4.1: a) Infrared spectrum for an iron-free NBAS glass sample containing about 7.5 mol% alumina. The asymmetric shape of the absorption peak is due to the presence of B-OH, Al-OH and Si-OH groups. The experimentally obtained peak was used for determining the overall concentration of OH groups. b) Initial water contents of the NBAS glasses considered in this study as a function of the glass composition. The concentrations were determined based on the results of FTIR measurements. One unit of the y-axis corresponds to an OH concentration of about $2.6 \cdot 10^{-5}$ wt% if it is assumed that ε_{OH} = 38 L/(mol_{OH}·cm) for all glass compositions. The errors for the results of the water concentration were estimated not to exceed ± 6 %.

samples are shown in Fig. 4.2a as a function of the square root of the time of annealing in wet air. Density values listed in Table 4.1 were used to determine values for water contents. To study the solubility of water and to determine values for the effective chemical diffusion coefficient of water in glass samples, the variation of the ratio between the total water content after annealing for the time t, M_t, and the saturation water content at an infinite annealing time, M_∞, was analyzed as a function of the annealing time. An example for the time dependence of experimentally determined values for M_t, as a function of the initial water content, M_0, and the saturation water content after an infinite annealing time, M_∞, as a function of the annealing time is provided in Fig. 4.2b in the form of a plot of $(M_t - M_0)/(M_\infty - M_0)$ vs. t. The line shown in Fig. 4.2b is from a fit of Eq. (4.9) to these data, to obtain a value for the effective chemical diffusion coefficient of water, $\tilde{D}_{eff}$; for details see the discussion in Section 4.1. The data shown in Fig. 4.2b are for an iron-free NBAS glass sample containing about 15 mol% alumina annealed in air saturated with water at 80 °C at 1 atm total pressure.

4.4.3 Sodium Tracer Diffusion

Fig. 4.3a shows a typical normalized residual radioactivity profile of Na-22 observed in this work. The profile shown was obtained for an iron-free NBAS glass sample containing about 10 mol% alumina after diffusion-annealing for about 19 h in common air at 301 °C. The curve shown in this figure was generated by fitting Eq. (4.6) to experimental data for A(x,t)/A(x=0,t). By fitting the inverse function of the error function, erfi, see Eq. (4.7), to the same experimental data, a value for the tracer diffusion coefficient of sodium, D^*_{Na}, was obtained, see Fig. 4.3b.

As typical for glasses, all as-received glass samples were in metastable states, i.e., transport properties like the tracer diffusion coefficients may change with time upon annealing at conditions allowing structural changes to occur. To avoid large influences of rapidly occurring structural changes on measured tracer diffusion coefficients in many experiments, the influence of pre-annealing at the glass transition temperature, T_g, for different times on measured sodium tracer diffusion coefficient was investigated first. The water concentrations measured before and

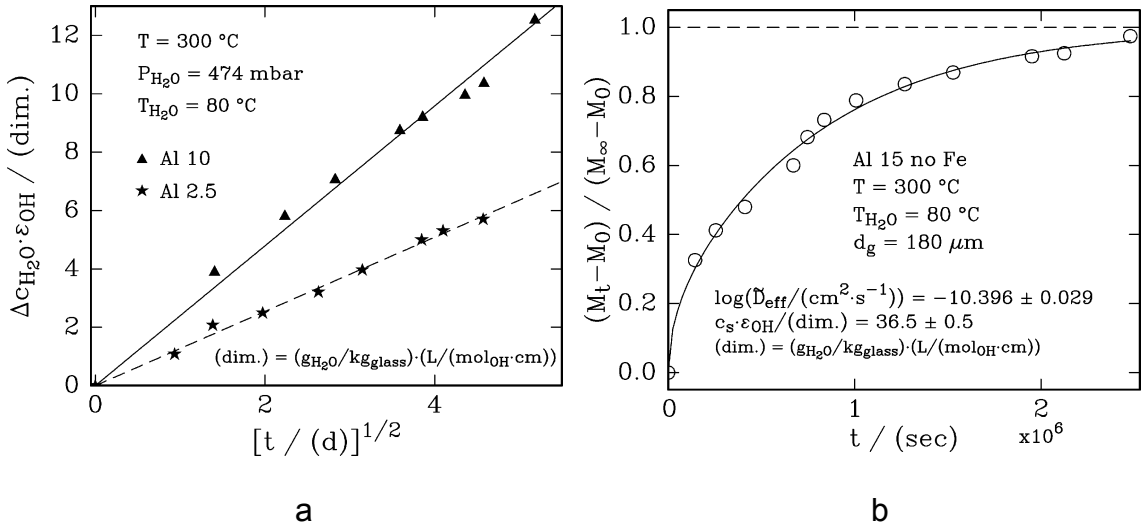

Fig. 4.2: a) Uptake of water by iron-containing NBAS glasses containing about 2.5 and 10 mol% alumina, respectively, annealed at 300 °C in wet air with P_{H_2O} = 474 mbar at atmospheric pressure. Straight lines are fitted to the amount of water taken up as a function of the square root of the annealing time. b) Time dependence of the uptake of water by an iron-free NBAS glass sample containing about 15 mol% alumina and being annealed in wet air (P_{H_2O} = 474 mbar) at 300 °C.

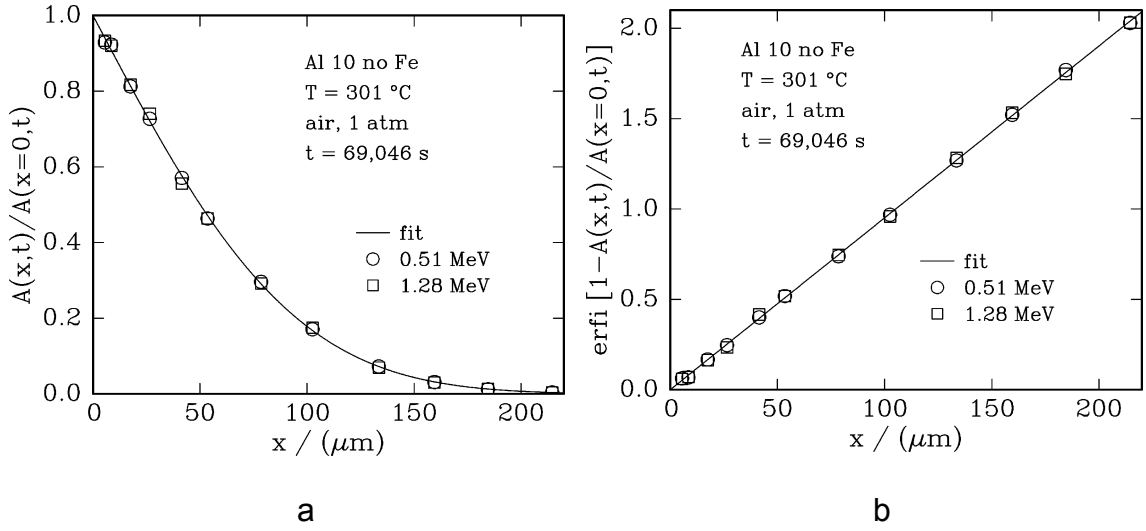

Fig. 4.3: Example for experimental sodium tracer diffusion data: a) Normalized residual radioactivity profile of Na-22 observed in an iron-free NBAS glass containing about 10 mol% alumina after diffusion-annealing for 19 h in common air at 301 °C. b) Results of fitting Eq. (4.7) to the normalized residual radioactivity data shown in part a) to determine values for sodium tracer diffusion coefficients.

after pre-annealing in common air 1 atm were compared and found to be unchanged. Therefore, common air was used for pre-annealing in this study. Values determined for tracer diffusion coefficients of Na-22 diffusing in different as-received NBAS glasses and in the same glasses after pre-annealing at T_g for different lengths of time in dry air at 301 °C are reported in Table 4.2. The results for six samples are summarized in Fig. 4.4a. It was found that after pre-annealing for about 5 hours, the sodium tracer diffusion coefficients became almost constant for all considered glass compositions. This suggests that the glass structures do not change very significantly after 5 hours additional pre-annealing for the diffusion annealing times used in this study. Based on this finding all glass samples were pre-annealed for 5 hours at their respective glass transition temperatures, T_g, before sodium tracer diffusion measurements were performed to establish composition and temperature dependencies of sodium tracer diffusion coefficients.

Table 4.3 reports the values obtained for tracer diffusion coefficients of Na-22 diffusing in NBAS glasses (obtained by pre-annealing as-received glass samples in common air at their respective T_g for 5 hours) after diffusion-annealing in dry air at different temperatures from 198 °C to 350 °C. The errors listed in Tables 4.2 and 4.3 are those obtained when fitting Eq. (4.7) to normalized residual radioactivities derived from experimental data. There are several additional errors related to determining temperatures of the annealing furnace, diffusion-annealing times, radioactivity net counts and to measuring lengths during profile determinations. Based on past experiences and estimates of individual errors, these errors in combination with those listed in Tables 4.2 and 4.3 result in errors of tracer diffusion coefficient values of about ± 5 %. Measured tracer diffusion coefficients for the diffusion of sodium in NBAS glasses pre-annealed at T_g for 5 hours are shown in Fig. 4.4b as a function of the glass composition, denoted by using the difference between the molar concentrations of Na_2O, $[Na_2O]$, and of Al_2O_3, $[Al_2O_3]$, for four different diffusion-annealing temperatures between 198 and 350 °C.

Table 4.2: Data for sodium tracer diffusion coefficients obtained at 301 °C in common air at 1 atm for NBAS glasses as-received and after being pre-annealed in common air at 1atm at their glass transition temperatures for different lengths of time. "– LD" stands for "$-\log_{10}(D^{*}_{Na}/(cm^2/s))$. The errors reported in the table are from least squares fits of Eq. (4.7) to normalized residual radioactivity profiles. The overall errors are estimated to be on the order of 5 %, as stated in Section 3.3. The denotations used for glasses without Fe_2O_3 contain an "n" at the end.

glass		Pre-annealing Time (hours)							
		0	2	5	9	14	15	24	48
Al 2.5n	- LD	10.33		9.78			9.82		9.87
	error ±	0.004		0.010			0.023		0.025
Al 5n	- LD	9.86		9.73					
	error ±	0.011		0.010					
Al 7.5n	- LD	9.64		9.55		9.56			9.48
	error ±	0.012		0.013		0.009			0.008
Al 10n	- LD	9.58		9.40					
	error ±	0.008		0.012					
Al 12.5n	- LD	9.32		9.10				9.18	
	error ±	0.008		0.014				0.008	
Al 15n	- LD	9.14		8.88	8.91			8.90	8.91
	error ±	0.008		0.010	0.012			0.005	0.007
Al 2.5	- LD	10.09	9.87	9.76			9.91		9.96
	error ±	0.003	0.013	0.017			0.007		0.020
Al 5	- LD	9.85		9.73					
	error ±	0.008		0.013					
Al 7.5	- LD	9.75		9.49		9.48			9.38

glass		Pre-annealing Time (hours)							
		0	2	5	9	14	15	24	48
	error ±	0.012		0.009		0.006			0.024
Al 10	- LD	9.47		9.25					
	error ±	0.008		0.019					
Al 12.5	- LD	9.26		9.09					
	error ±	0.010		0.010					
Al 15	- LD	9.11	8.99	8.86	8.91	8.92		8.95	8.91
	error ±	0.009	0.004	0.012	0.013	0.012		0.004	0.007

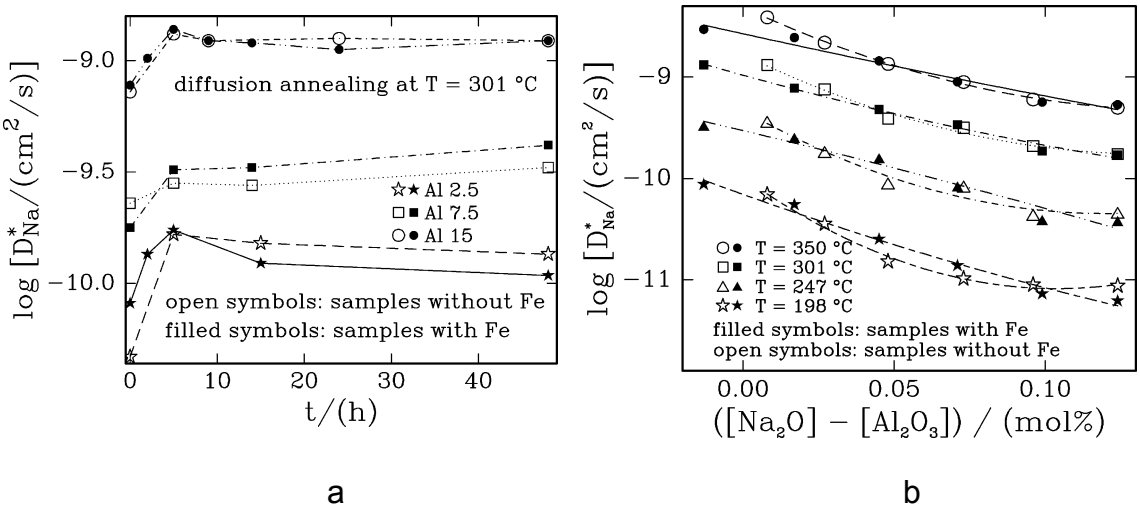

Fig. 4.4: a) Pre-annealing time and b) composition and temperature dependencies of sodium tracer diffusion coefficients determined for the considered NBAS glasses diffusion-annealed in common air at 1 atm. The errors obtained by fitting Eq. (4.7) to the experimental data are reported in Tables 4.2 and 4.3 and are significantly smaller than the size of the symbols used in the figure. The overall errors of the data points shown are estimated not to exceed ± 5 % corresponding to ± 0.021 in $\log [D^*_{Na}/(cm^2/s)]$, i.e., are approximately as large as corresponding to the size of the symbols used in the figure.

Table 4.3: Data for sodium tracer diffusion coefficients for different temperatures between 198 and 350 °C in common air at 1 atm obtained for NBAS glasses after being pre-annealed in common air at their glass transition temperatures for 5 hours. Corresponding values for sodium tracer diffusion coefficients at 301 °C can be found in Table 4.2. "– LD" stands for "– $\log_{10}$ (D^*_{Na}/(cm^2/s)). The errors reported in the table are from least squares fits of Eq. (4.7) to normalized residual radioactivity profiles. The overall errors are estimated to be on the order of 5 %, as stated in Section 3.3. The denotations used for glasses without Fe_2O_3 contain an "n" at the end.

T = 198 °C						
glass	Al 2.5n	Al 5n	Al 7.5n	Al 10n	Al 12.5n	Al 15n
– LD	11.06	11.05	10.99	10.82	10.45	10.16
error ±	0.017	0.016	0.010	0.012	0.017	0.015

T = 198 °C						
glass	Al 2.5	Al 5	Al 7.5	Al 10	Al 12.5	Al 15
– LD	11.21	11.14	10.86	10.60	10.26	10.06
error ±	0.019	0.027	0.008	0.013	0.015	0.024

T = 247 °C						
glass	Al 2.5n	Al 5n	Al 7.5n	Al 10n	Al 12.5n	Al 15n
– LD	10.45	10.42	10.16	9.93	9.63	9.41
error ±	0.004	0.03	0.007	0.025	0.016	0.014

T = 247 °C						
glass	Al 2.5	Al 5	Al 7.5	Al 10	Al 12.5	Al 15
– LD	10.39	10.40	10.11	9.86	9.60	9.47
error ±	0.019	0.015	0.013	0.012	0.018	0.013

T = 350 °C						
glass	Al 2.5n	Al 5n	Al 7.5n	Al 10n	Al 12.5n	Al 15n
- LD	9.30	9.22	9.05	8.87	8.66	8.41
error ±	0.014	0.002	0.017	0.029	0.018	0.027

T = 350 °C						
glass	Al 2.5	Al 5	Al 7.5	Al 10	Al 12.5	Al 15
- LD	9.27	9.25	9.05	8.84	8.61	8.53
error ±	0.024	0.003	0.011	0.020	0.015	0.015

4.5 Discussion

4.5.1 Water Uptake

If the incorporation of water into a glass is diffusion-controlled, the increase of the water content is expected to follow a parabolic rate law, i.e., the change in the concentration of water, Δc_{H_2O}, multiplied with the molar absorption coefficient, ε_{OH}, will increase linearly with the square toot of the annealing time t, provided that ε_{OH} is constant, see Eq. (4.8).

$$\Delta c_{H_2O} \cdot \varepsilon_{OH} \propto \sqrt{t} \tag{4.8}$$

The changes in the water content after annealing in wet air (P_{H_2O} = 474 mbar) at 300 °C as a function of the annealing time t, multiplied by ε_{OH}, $\Delta c_{H_2O} \cdot \varepsilon_{OH}$, for two NBAS glasses with different compositions as a function of the square root of the annealing time t are shown in Fig. 4.2a. These data indicate that a parabolic relationship as described by Eq. (4.8) is followed for both glasses considered in the figure. Straight lines describe very well the relationship between $\Delta c_{H_2O} \cdot \varepsilon_{OH}$ and the annealing time t. This indicates that the uptake of water by the considered NBAS glasses is diffusion-controlled.

Since the values of the molar absorption coefficient for the considered NBAS glasses are unknown, a typical value of ε_{OH} for aluminosilicate glasses, 38 L/(mol_{OH}·cm) [21], was used to estimate absolute values for the water content in the glasses. According to such an estimate, one unit of the y-axis of Fig. 4.1b corresponds to an OH concentration of $2.6 \cdot 10^{-5}$ wt%. The same type of estimate leads to the conclusion that the initial water concentration in the iron-containing NBAS glass samples varies around $3.3 \cdot 10^{-4}$ wt% and that the initial water concentration in the iron-free glass samples decreases from $4.4 \cdot 10^{-4}$ to $1.8 \cdot 10^{-4}$ wt% with a decreasing concentration of alumina.

In order to determine values for the effective chemical diffusion coefficient of water, $\tilde{D}_{eff}$, Eq. (4.9) was used.

$$\frac{M_t - M_0}{M_\infty - M_0} = 1 - \sum_{n=0}^{\infty} \frac{8}{(2n+1)^2 \cdot \pi^2} \cdot \exp\left[- \frac{\tilde{D}_{eff} \cdot (2n+1)^2 \cdot \pi^2 \cdot t}{4\, d^2} \right] \qquad (4.9)$$

This equation, taken from Ref. [26], describes the total content of water of a plane-parallel glass sample with the thickness d after the annealing time t, M_t, as a function of the initial water content, M_0, and the final water content after saturation is reached, M_∞, for the case that the effective chemical diffusion coefficient $\tilde{D}_{eff}$ is independent of the time and the water content. Eq. (4.9) was fitted to data for the water concentration measured by using an FTIR instrument after an iron-free NBAS glass sample containing about 15 mol% alumina was annealed in wet air for different lengths of time, as shown in Fig. 4.2b. The effective chemical diffusion coefficient of water obtained from this fitting is about $4 \cdot 10^{-11}$ cm^2/s. The ratio between the sodium tracer diffusion coefficient and the effective chemical diffusion coefficient of water in this type of glass at 300 °C is around 33. This indicates that for a given annealing time, the penetration length of the sodium tracer is much larger than that of water. This may be one reason why any significant influence of moisture being present in the atmosphere surrounding samples during diffusion annealing on the sodium tracer diffusion was not observed in the NBAS glass samples investigated.

4.5.2 Sodium Tracer Diffusion

4.5.2.1 Pre-annealing Time Dependence of the Sodium Tracer Diffusion

As shown in Fig. 4.4a, for both iron-free and iron-containing glass samples the tracer diffusion coefficients of sodium increase for the first 5 hours of pre-annealing at T_g and become almost constant afterwards for the times of pre-annealing used. The observed changes in the values of sodium tracer diffusion coefficients are attributed to structural changes occurring during pre-annealing. Most of these changes occur within about five hours of pre-annealing. Any changes that may take place thereafter occur so slowly that they do not significantly influence the diffusion of sodium. For all glasses considered in this study, structural changes occurring after pre-annealing at T_g for 5 hours when

continuing the pre-annealing for another 45 hours seem to be only minor so that they can be ignored.

4.5.2.2 Composition Dependence of the Sodium Tracer Diffusion

The values of the sodium tracer diffusion coefficients, D^*_{Na}, shown in Fig. 4.4b indicate that D^*_{Na} decreases at temperatures between 198 and 350 °C at a given concentration of Na_2O when the concentration of alumina decreases. There does not seem to be any significant influence of the presence of a small amount of iron oxide on the diffusion of sodium tracer in the NBAS glasses considered in this study.

Compared to the diffusion of cations in crystalline materials, the situation of cation diffusion in glasses is much more complicated due to the lack of periodicity in the structure. Diffusional jumps of cations in glasses have a distribution of different jump lengths and various heights of diffusion barriers. Average quantities can be introduced by considering the diffusion of ions in glasses to overcome this difficulty. By taking the cube root of a free volume, V_f, a value for a parameter which is proportional to an average jump distance, $\overline{a}$, can be obtained. A free volume was calculated by subtracting the total volume of all different ions being present from the molar volume V_m of a considered glass. Values for the molar volume were calculated from molar masses and the density values listed in Table 4.1. As shown in Fig. 4.5, the logarithm of the square of a quantity being proportional to the average jump distance $\overline{a}$ decreases as the alumina concentration decreases for both iron-free and iron-containing glasses. This indicates that the structure of the glasses becomes less open when the concentration of alumina decreases. The decrease of the value of the logarithm of the sodium tracer diffusion coefficient with a decrease of the concentration of alumina due to the decrease of the square of the average jump distance is only small, around 0.04. This translates into a change of up to about 10 % in the value of D^*_{Na} within the glass composition ranges considered in this work. For the iron-containing glasses, the decrease of the logarithm of the tracer diffusion coefficient with a decrease of the alumina concentration due to an increase of the activation

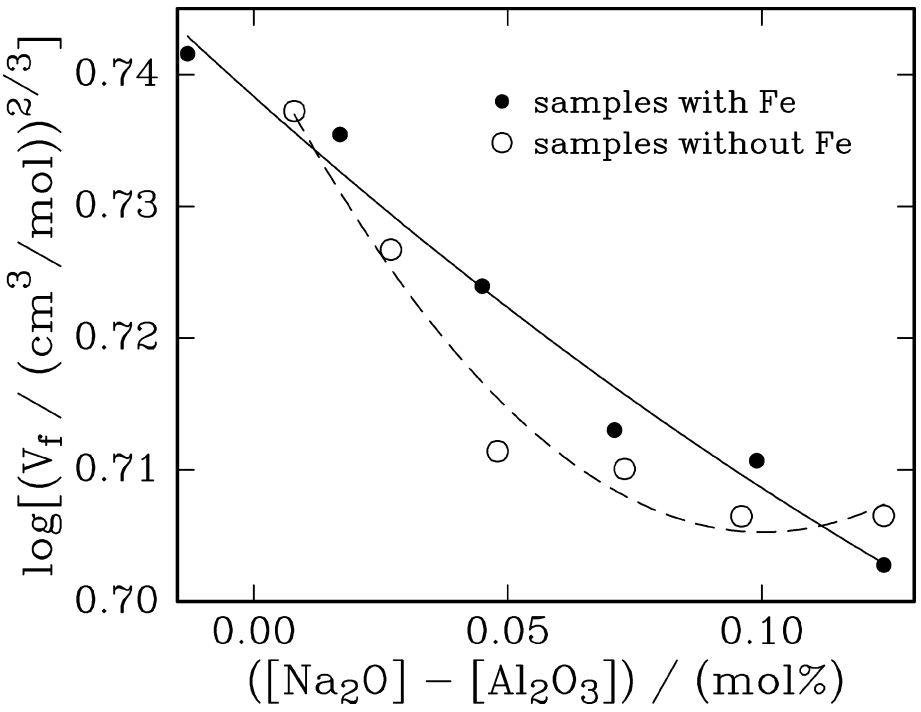

Fig. 4.5: Logarithm of the square of a factor being proportional to a mean jump length $\bar{a}$ as a function of the glass composition.

enthalpy, see Section 4.2.3, is about 0.9. Therefore the influence of the change of the activation enthalpy on the composition dependence of the sodium tracer diffusion is much more significant than that resulting from the variation of the square of the average jump length.

Some information related to the structure of the iron-free NBAS glasses considered in this article is available from a parallel MAS NMR spectroscopy study performed by using ^{27}Al and ^{11}B [27]. In this study, aluminum was found to be fourfold coordinated in all glass samples investigated. Values determined in Ref. [27] for the content of boron in tetrahedral coordination relative to the total content of boron, N_4, are listed in Table 4.1. Fig. 4.6 shows the change of the concentration distribution of Na_2O, acting as charge compensator for aluminum-based oxygen tetrahedra, for boron-based oxygen tetrahedra and for non-bridging oxygen present (NBO) at boron- and silicon-based oxygen tetrahedra, as a function of the glass composition. As one can see from Fig. 4.6, the environment of sodium ions in the glasses changes with the content of alumina. This is expected to influence the diffusivity of sodium as a function of the glass composition and must therefore be related to the observed glass composition dependence of D^*_{Na} shown in Fig. 4.4b.

In 1969, Terai [28] studied the tracer diffusion of sodium in sodium aluminosilicate glasses of the type $Na_2O{\cdot}2SiO_2{\cdot}xAl_2O_3$. The tracer diffusion coefficient of sodium shows a maximum value at a composition at which all aluminum-based oxide tetrahedra are anticipated to be charge balanced by sodium cations and where no NBO should exist. Kaps and Kahnt [29] found that in sodium borosilicate glasses the interaction between Na^+ and NBO is stronger than that between Na^+ and BO_4^-. As shown in Fig. 4.6, the Na_2O involved in the formation of NBO increases with a decreasing concentration of alumina. This could be, at least to some extent, the reason for the observed decrease of the sodium tracer diffusion coefficient with a decrease of the alumina concentration.

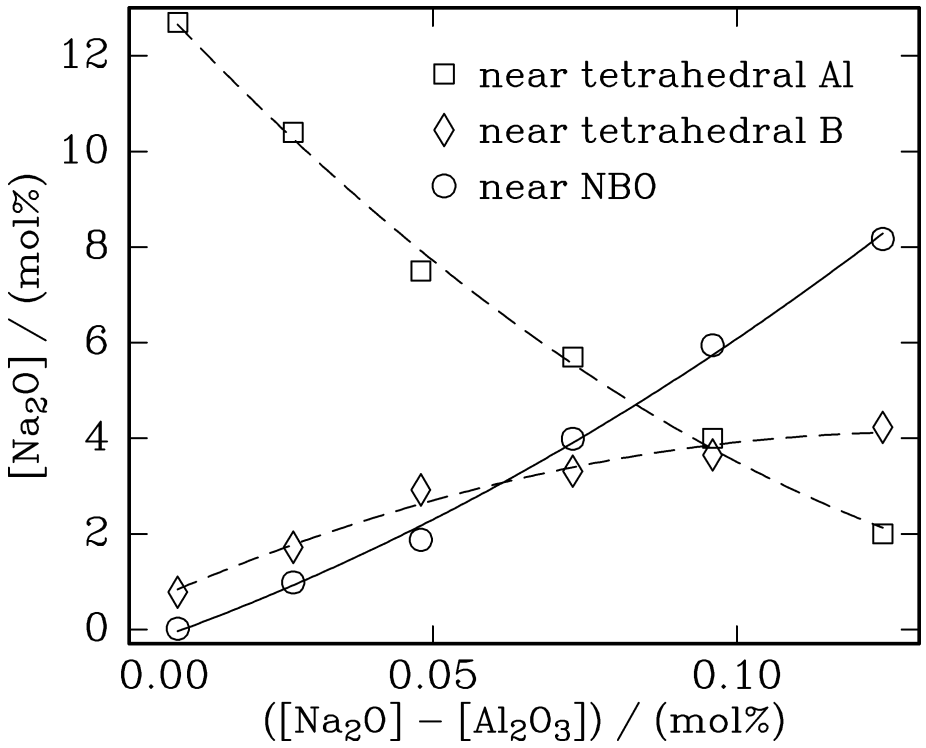

Fig. 4.6: Concentrations of sodium ions acting as charge compensator for aluminum-based oxide tetrahedra, boron-based oxide tetrahedra and non-bridging oxygen (NBO), respectively, as a function of the glass composition.

4.5.2.3 Temperature Dependence of the Sodium Tracer Diffusion

An Arrhenius-type equation, in which R is the gas constant, was used to analyze the temperature dependence of the sodium tracer diffusion coefficients, D^*_{Na}, obtained at temperatures far below the glass transition temperatures, T_g. Figs. 4.7a and 4.7b show the results of fitting an Arrhenius-type equation, see Eq. (4.10), to the sodium tracer diffusion coefficients obtained experimentally for temperatures up to 350 °C for both iron-free and iron-containing NBAS glasses, all pre-annealed for 5 hours at their respective glass transition temperatures.

$$D^*_{Na} = D^0_{Na} \cdot \exp\left(- \frac{\Delta E_a}{R \cdot T} \right) \tag{4.10}$$

Values for the activation enthalpy, ΔE_a, and for the pre-exponential factor, D^0_{Na}, for the diffusion of sodium tracer in the glasses considered and obtained from the fitting denoted above are listed in Table 4.4 and shown in Figs. 4.8a and 4.8b, respectively. It was found that the changes of the activation enthalpy and of the pre-exponential factor with the glass composition are relatively small for both iron-free and iron-containing glasses. For the iron-free glasses, the activation enthalpy varies between 63.9 and 71.4 kJ/mol and the pre-exponential factor varies between $1.5 \cdot 10^{-4}$ and $1.2 \cdot 10^{-3}$ cm^2/s. For the iron-containing glasses, the activation enthalpy increases from 57.5 to 71.3 kJ/mol and the pre-exponential factor increases from $2.1 \cdot 10^{-4}$ to $5.3 \cdot 10^{-4}$ cm^2/s almost linearly with a decreasing concentration of alumina.

4.5.2.4 Influence of Iron Oxide Additions on the Diffusion of Sodium

As indicated by the compositions reported in Table 4.1, one set of glass samples contained 1 mol% Fe_2O_3 while the other one did not contain any iron. As shown in Fig. 4.4b and stated in Section 4.2.2, sodium tracer diffusion coefficients measured for iron-free and iron-containing samples, when considered as a function of the concentration difference $[Na_2O] - [Al_2O_3]$, are very similar, i.e., they are not very significantly influenced by the small Fe_2O_3 additions present in one set of glass samples.

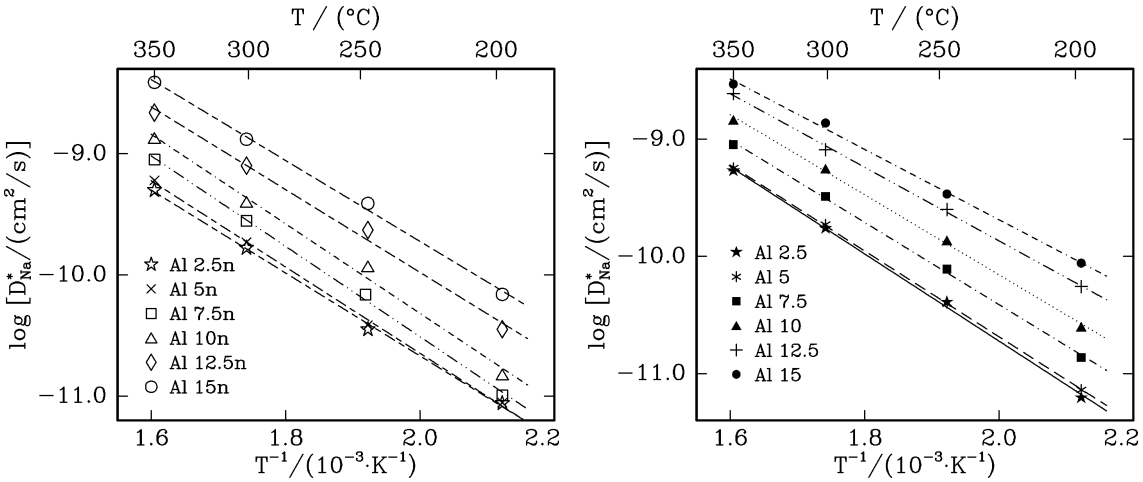

Fig. 4.7: Temperature dependencies of sodium tracer diffusion coefficients for NBAS glasses a) without iron and b) with iron. The straight lines are from fitting Eq. (4.10) to the data for temperatures up to 350 °C.

Table 4.4: Values for activation enthalpies and pre-exponential factors for the tracer diffusion of Na-22 in NBAS glasses. The data shown were derived by considering experimental data for temperatures up to 350 °C. "ΔE_a" stands for "ΔE_a / (kJ/mol)" and "$-$ LD°" stands for "$-\log_{10} (D^{\circ}_{Na} / (cm^2/s)$". Attributing an estimated error of ± 5 % to the individual tracer diffusion coefficients, the errors of all values listed below, calculated based on the tracer diffusion coefficients listed in Tables 4.2 and 4.3, are all ± 1.043 kJ/mol for ΔE_a and ± 0.101 for $-$ LD°. The denotations used for glasses without Fe_2O_3 contain an "n" at the end.

glass	Al 2.5n	Al 5n	Al 7.5n	Al 10n	Al 12.5n	Al 15n
ΔE_a	65.51	68.14	71.42	70.71	65.38	63.91
$-$ LD°	3.82	3.53	3.05	2.93	3.15	3.05

glass	Al 2.5	Al 5	Al 7.5	Al 10	Al 12.5	Al 15
ΔE_a	71.26	70.15	67.20	65.41	60.14	57.51
$-$ LD°	3.28	3.36	3.39	3.32	3.58	3.68

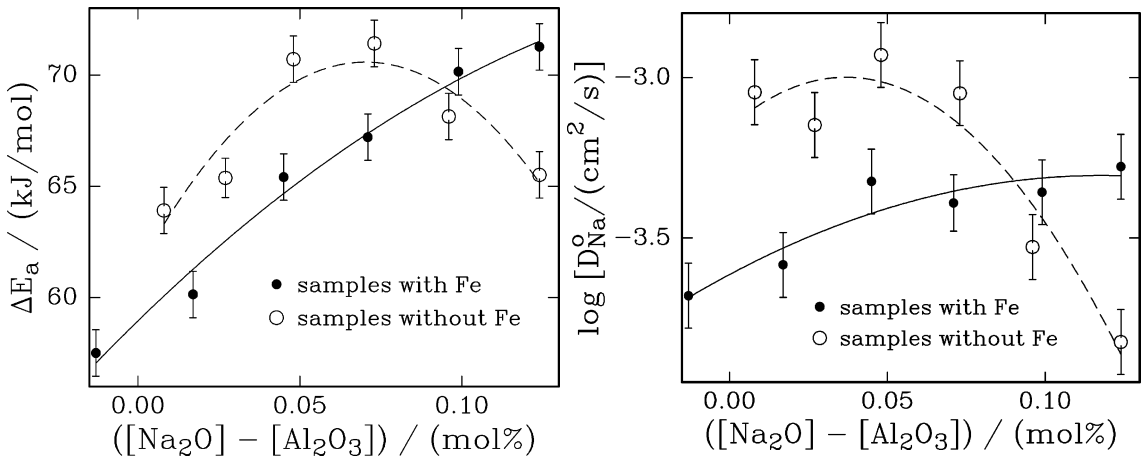

a b

Fig. 4.8: a) Activation enthalpies and b) pre-exponential factors for the sodium tracer diffusion in NBAS glasses as a function of the glass composition.

As indicated in Section 4.2.3. the values obtained for pre-exponential factors and activation enthalpies by analyzing the temperature dependencies of measured tracer diffusion coefficients are also not very different at fixed values of the composition parameter $[Na_2O] - [Al_2O_3]$. However, the trends observed for pre-exponential factors and activation enthalpies as a function of this composition parameter seem to differ to some extent.

In principle the addition of Fe_2O_3 during making glasses could lead to the presence of Fe^{2+} and Fe^{3+} ions in the glass matrix. The fraction of Fe being present in the form of Fe^{3+} is expected to vary with the processing conditions (temperature and oxygen activity) and possibly on conditions established during subsequent annealing. As reported in Ref. [23], most of the iron (between 78 and 95 at%) is present as Fe^{3+} in the iron-containing glasses considered here. At the Na_2O concentrations present in the glasses considered in this article Fe^{3+} ions are expected to act as network formers in a fourfold coordination. Comparing the relatively small concentration of Fe_2O_3 with the concentrations of the other network formers being present, the addition of Fe_2O_3 is not expected to lead to any very significant changes in the glass structure and of structure-sensitive properties.

Looking in detail at the composition data reported in Table 4.1 reveals that there exist some relatively large differences in the $Na_2O:B_2O_3:Al_2O_3:SiO_2$ concentration ratio at nominally constant contents of Al_2O_3, e.g., in samples denoted in Table 4.1 as Al 7.5 and Al 7.5n. Differences in the SiO_2 content at nominally constant contents of Al_2O_3 are in most cases significantly larger than the content of Fe_2O_3 in the iron-containing samples.

Due to the composition variations discussed above, i.e., of $Na_2O:B_2O_3:Al_2O_3:SiO_2$ concentration ratios, and not expecting any major influence of the addition of 1 mol% Fe_2O_3 it is unclear what the reasons for the seemingly different trends observed for pre-exponential factors and activation enthalpies as a function of the composition parameter $[Na_2O] - [Al_2O_3]$ are. To possibly identify these reasons additional experimental work using glasses with much more tight

composition control and also with higher concentrations of Fe_2O_3 would be required, which is outside of the scope of the current paper.

4.6 Conclusions

Sodium tracer diffusion coefficients, D^*_{Na}, have been measured in NBAS glasses at different temperatures between 198 and 350 °C. 5-hour pre-annealing at the glass transition temperature was performed on all glass samples used for establishing composition and temperature dependencies before tracer diffusion annealing. For both iron-free and iron-containing glasses, the sodium tracer diffusion coefficients decrease with a decreasing concentration of alumina. The changes of activation enthalpies and pre-exponential factors derived from sodium tracer diffusion coefficients as a function of the glass composition in both iron-free and iron-containing glasses are relatively small. The composition dependence of the diffusion of sodium tracer in the glasses depends much more strongly on activation enthalpy variations than on changes of the square of the average jump length with composition. The considered glasses were found to take up water at 300 °C in wet air with P_{H_2O} = 474 mbar. The effective chemical diffusion coefficient of water in an iron-free NBAS glass sample containing about 15 mol% alumina glass sample was found to be much smaller than the tracer diffusion coefficient of sodium and no influence of water on the diffusion of sodium tracer was observed in this study.

4.7 Acknowledgments

This work was supported by the National Science Foundation under Award Number DMR-0710564. The work made use of the Cornell Center for Materials Research Facilities supported by the National Science Foundation under Award Number DMR-1120296. The authors thank all undergraduate researchers at Cornell who helped in experimental work.

REFERENCES

[1] A.K. Varshneya, “Fundamentals of Inorganic Glasses,” Academic Press Inc., San Diego, CA, U.S.A., [1994].

[2] Y. Kato, H. Yamazaki, T. Watanabe, K. Saito and A.J. Ikushima, “Early Stage of Phase Separation in Aluminoborosilicate Glass for Liquid Crystal Display Substrate,” Journal of the American Ceramic Society, **88** (2) [2005] 473-477.

[3] A. Ellison and I.A. Cornejo, “Glass Substrates for Liquid Crystal Displays,” International Journal of Applied Glass Science, **1** (1) [2010] 87-103.

[4] T.M. Besmann and K.E. Spear, “Thermochemical Modeling of Oxide Glasses,” Journal of the American Ceramic Society, **85** (12) [2002] 2887-2894.

[5] B. Boizot, N. Ollier, F. Olivier, G. Petite, D. Ghaleb and E. Malchukova, “Irradiation Effects in Simplified Nuclear Waste Glasses,” Nuclear Instruments and Methods in Physics Research Section B, **240** (1-2) [2005] 146-151.

[6] C.M. Jantzen, K.G. Brown and J.B. Pickett, “Durable Glass for Thousands of Years,” International Journal of Applied Glass Science, **1** (1) [2010] 38-62.

[7] V.V. Gerasimov and O.V. Spirina, “Coordination State of Boron and Aluminum in Low-alkali Aluminoborosilicate Glasses,” Glass and Ceramics, **61** (5-6) [2004] 168-170.

[8] J. Ramkumar, V. Sudarsan, S. Chandramouleeswaran, V.K. Shrikhande, G.P. Kothiyal, P.V. Ravindran, S.K. Kulshreshtha and T. Mukherjee, “Structural Studies on Boroaluminosilicate Glasses,” Journal of Non-Crystalline Solids, **354** (15-16) [2008] 1591-1597.

[9] S.S. Kistler, “Stresses in Glass Produced by Nonuniform Exchange of Monovalent Ions,” Journal of the American Ceramic Society, **45** (2) [1962] 59-68.

[10] P. Acloque and J.D. Tochon, “Measurement of the Mechanical Strength of Glass after Reinforcement,” Symposium sur la Résistance Mécanique du Verre et les Moyens de l'Améliorer, Compte Rendu, [1962] 687-704.

[11] R.F. Bartholomew and H.M. Garfinkel, “Chemical Strengthening of Glass,” Glass Science and Technology, Vol. 5 [1980] 217-267, Academic Press, New York 1980.

[12] A.K. Varshneya and W.C. LaCourse, “Technology of Ion Exchange Strenthening of Glass: a Review,” Ceramic Transactions, **29** (Advances in Fusion and Processing of Glass) [1993] 365-376.

[13] A.K. Varshneya, “Chemical Strengthening of Glass Products,” Transactions of the Indian Ceramic Society, **60** (1) [2001] 1-6.

[14] R. Gy, “Ion Exchange for Glass Strengthening,” Materials Science & Engineering, B: Advanced Functional Solid-State Materials, **149** (2) [2008] 159-165.

[15] C.R. Kurkjian, P.K. Gupta and R.K. Brow, “The Strength of Silicate Glasses: What Do We Know, What Do We Need to Know?,” International Journal of Applied Glass Science, **1** (1) [2010] 27-37.

[16] K. Karlsson, B. Jonson and C. Stalhandske, “The Technology of Chemical Glass Strengthening - a Review,” Glass Technology: European Journal of Glass Science and Technology Part A, **51** (2) [2010] 41-54.

[17] A.K. Varshneya, “The Physics of Chemical Strengthening of Glass: Room for a New View,” Journal of Non-Crystalline Solids, **356** (44-49) [2010] 2289-2294.

[18] A.K. Varshneya, “Chemical Strengthening of Glass: Lessons Learned and Yet to Be Learned,” International Journal of Applied Glass Science, **1** (2) [2010] 131-142.

[19] M.E. Nordberg, E.L. Mochel, H.M. Garfinkel and J.S. Olcott, “Strengthening by Ion Exchange,” Journal of the American Ceramic Society, **47** (5) [1964] 215-219.

[20] R.H. Doremus, “Diffusion of Water in Silica Glass,” Journal of Materials Research, **10** (9) [1995] 2379-2389.

[21] J.E. Shelby, “Introduction to Glass Science and Technology,” 2nd Ed., [2005], The Royal Society of Chemistry, Cambridge.

[22] R.H. Doremus, Glass Science, 2nd Ed., [1994], John Wiley, New York.

[23] M.M. Smedskjaer, Q. Zheng, J.C. Mauro, M. Potuzak, S. Morup and Y. Yue, “Sodium Diffusion in Boroaluminosilicate Glasses,” Journal of Non-Crystalline Solids, **357** (22-23) [2011] 3744-3750.

[24] X. Wu and R. Dieckmann, “Sodium Tracer Diffusion in Glasses of the Type $(Na_2O)_{0.2}[(BO_{1.5})_x(SiO_2)_{1-x}]_{0.8}$,” Journal of Non-Crystalline Solids, **357** (15) [2011] 2846-2856.

[25] B.J. Wilson, The Radiochemical Manual, 2nd Ed., [1966], The Radiochemical Centre, Amersham.

[26] J. Crank, The Mathematics of Diffusion, 2nd Ed., [1975], Clarendon Press, Oxford.

[27] Q. Zheng, R.E. Youngman, C.L. Hogue, J.C. Mauro, M. Potuzak, A.J. Ellison, M.M. Smedskjaer and Y. Yue, ”Impact of $[Al_2O_3]/[SiO_2]$ on Structure of Boroaluminosilicate Glasses,” (in preparation)

[28] R. Terai, “Self-diffusion of Sodium Ions and Electrical Conductivity in Sodium Aluminosilicate Glasses,” Physics and Chemistry of Glasses, **10** (4) [1969] 146-152.

[29] C. Kaps and H. Kahnt, “Structure and Na^+ Transport in Borosilicate Glasses with a High Content of Na_2O ($\geq$ 10 mol%) – Studied by ^{22}Na Tracer Diffusion and Conductivity Measurements,” Acta Physica Slovaca, **38** (6) [1988] 366-369.

CHAPTER FIVE

SODIUM TRACER DIFFUSION IN A SODIUM ALUMINOSILICATE GLASS*

5.1 Abstract

Sodium tracer diffusion coefficients, D^{*}_{Na}, have been measured using the radioactive isotope Na-22 in a commercial, ion exchangeable sodium aluminosilicate glass at different temperatures between 195 and 400 °C. The activation enthalpy derived from sodium tracer diffusion data for the as-received glass samples was found to be 75.5 ± 1.2 kJ/mol and the value of the logarithm of the pre-exponential factor of the sodium tracer diffusion coefficient, $\log_{10}$ [$D^{\circ}_{Na}/(cm^2/s)$], is −2.58 ± 0.13. It was observed that pre-annealing the glass samples at the annealing point of 609 °C causes some reduction of the values of the sodium tracer diffusion coefficients. In addition, the glass samples investigated were found to take up water at 300 °C in wet air (P_{H_2O} = 474 mbar). However, an influence of the uptake of water during diffusion-annealing in wet air on the diffusivity of sodium was not observed.

5.2 Introduction

The diffusion of sodium in a commercial, ion exchangeable sodium aluminosilicate glass, which is used as a parent glass for producing chemically stengthened glass by ion-exchange, has been investigated in this study. Chemically strengthened glasses are widely used as protective covers for electronic displays, like laptop computer screens and mobile devices, as optical components and as high strength glass articles. Ion-exchanged alkali-aluminosilicate thin sheet glasses have a high compressive stress and a deep compression layer near the surface. Such glasses, for example Corning® Gorilla®

---

* Reprinted with permission from Xinwei Wu and Rüdiger Dieckmann, Journal of Non-Crystalline Solids, 357 (22-23) [2011] 3797-3802.

glass [1], have high resistance to scratch damage and high retained strength after use.

Chemical strengthening of glass by ion exchange was introduced in 1962 by Kistler [2] and Acloque and Tochon [3]. It is usually a process where glasses are immersed in a molten alkali salt bath at a temperature below the glass transition temperature, T_g. Provided that the ionic radius of the ions diffusing into the glass is larger than that of the ions which are simultaneously leaving the glass, glasses are strengthened during the thermally activated interdiffusion. The strengthening results in a high surface compressive stress that is created by inserting the penetrating larger alkali ion into sites occupied before by smaller host alkali ions and a lack of relaxation which would eliminate compressive stresses. Details of the chemical strengthening science and technology related to oxide glasses have been reviewed by several authors [4-11]. More complex chemical strengthening processes have also been discussed, for example, double and two-step ion exchanges. By re-introducing some of the initially replaced ions or by introducing another type of ion into the surface layer after a first ion exchange, the shape of residual stress profiles in glasses can be modified, potentially allowing to obtain strong glasses with low strength variability [12-14]. Compared to traditional thermal tempering, chemical strengthening generates a higher degree of surface compression without any significant optical distortion and can be applied to thinner glass products with complex geometry [6]. Chemically strengthened glasses exhibit higher impact resistance, scratching resistance, flexibility strength and resistance to temperature changes than glasses without chemical strengthening [8] and have a wide application in aircraft and high speed train windshields, bullet and blast resistant glasses, photocopier glasses, watch covers, and thin display glasses in electronic devices [7-9]. In 1964, Nordberg et al. [15] compared the strengths of four commercial glasses and two experimental glasses after identical ion exchange treatments and found that alkali aluminosilicate glasses were the best candidates for producing chemically strengthened glasses by ion exchange.

It is well known that the presence of water in glasses can affect their properties. Water in glass exists in two forms, as hydroxyl (OH) bonded to glass network formers and as molecular water dispersed in the interstices of the glass network [16]. Hydroxyl groups in oxide glasses are practically immobile while molecular water is mobile. Water molecules can be incorporated into glasses from surrounding, moisture-containing gas atmospheres by the reaction

$$H_2O\,(gas) \rightleftharpoons H_2O\,(glass). \tag{5.1}$$

Hydroxyl groups form when a water molecule diffusing within the glass encounters an energetically favorable oxygen bridge site through a reaction as that described in Eq. (5.2) [17].

$$R\text{–}O\text{–}R' + H_2O\,(glass) \rightleftharpoons R\text{–}O\text{–}H + H\text{–}O\text{–}R' \tag{5.2}$$

In Eq. (5.2) R and R' denote parts of the glass network. This reaction may cause in oxide glasses a water-assisted structural relaxation and sometimes, associated with this, glass property changes, especially changes of some structure-sensitive properties like the glass transition temperature, T_g, the viscosity, the density, the refractive index, the dielectric constant of glasses [16] and the diffusivity of sodium in silicate glasses [18].

The work described in this article has two main goals. One goal is to determine experimentally the temperature dependence of tracer diffusion coefficients for the diffusion of sodium in the considered sodium aluminosilicate glass. The second goal is to examine whether sodium aluminosilicate glass of interest in this study takes up water in a directly measurable amount upon annealing in moist air at elevated temperatures and also whether the uptake of water during diffusion-annealing in wet air influences the diffusivity of radioactive sodium in such a glass.

5.3 Experiments

The following sections provide details of the glass samples used in this study, how some information related to their composition was obtained, how their original water content was determined, how the uptake of water by such glasses was investigated and how the sodium tracer diffusion experiments were performed.

5.3.1 Glass Samples

As received, the sodium aluminosilicate glass specimens (Corning Code 2317, obtained from Corning Inc.) were in the form of square plates with dimensions of 25×25×0.9 mm with both large sides well polished. Each specimen was usually cut into nine squares to have a sufficiently large number of samples available for experiments. To avoid any contamination by alkali and alkaline-earth compounds introduced by fingerprints, all glass samples were washed ultrasonically in de-ionized water, acetone and ethanol and tweezers were used thereafter to handle the glass samples for tracer diffusion and water content measurements.

5.3.2 Glass Composition

Some information related to the chemical composition of the sodium aluminosilicate glass was obtained by X-ray photoelectron spectroscopy (XPS) and using a Surface Science Instruments (SSI) spectrometer Model SSX-100 which utilizes monochromated aluminum K-alpha X-rays with an energy of 1487 eV. The compositions of the original large surface and of a new cross-section surface created by breaking a glass sample in the middle were both determined in order to avoid any influence of contaminants possibly introduced during polishing.

5.3.3 Water Uptake Measurements

According to the literature, when the concentration of water is relatively small, almost all water in silicate glasses is accommodated in the form of OH groups [16]. A Bruker Optics Equinox 55 Fourier Transform Infrared (FTIR) Spectrometer was used in this study to determine the water content of glass samples by measuring the IR absorbance related to the presence of hydroxyl groups at wavelengths between 3500 and 3700 cm^{-1}. To minimize the adsorption of water on glass surfaces, glass samples were ultrasonically washed with de-ionized water, ethanol, acetone, then dipped in HPLC grade acetone and after that dried in an oven at 130 °C for 10 minutes before determining data for the water content. 64 accumulated scans were performed over a wavelength range corresponding to

wavenumbers between 400 and 4000 cm^{-1} to measure infrared spectra by using a KBr beam splitter and a deuterated triglycine sulfate (DTGS) detector. The three spectra with the lowest noise levels were selected for each sample for further data analysis.

The average concentration of water in the area of a glass sample through which the IR beam travels can be obtained from IR absorption measurements and using the Beer-Lambert law for data evaluation, Eq. (5.3) was used for this purpose.

$$c_{H_2O} = \frac{1}{2} \cdot \frac{A_g}{\varepsilon_{OH} \cdot d_g} \cdot \frac{M_{H_2O}}{\rho_g} = \frac{A_g}{\varepsilon_{H_2O} \cdot d_g} \cdot \frac{M_{H_2O}}{\rho_g} \tag{5.3}$$

with

$$A_g = -\log_{10}\left(\frac{I}{I_0}\right), \tag{5.4}$$

where c_{H_2O} is the mass fraction of H_2O in the glass, A_g is the measured absorbance of the glass, M_{H_2O} is the molar mass of H_2O (= 18.02 g/mol), ε_{OH} is the molar absorption coefficient related to the overall concentration of R-OH groups present in the glass (in $L/(mol_{OH} \cdot cm)$), d_g (in cm) is the thickness of the glass sample, ρ_g is the density of the glass (in g/cm^3) and I/I_0 is the ratio between the integral intensities of the transmitted and the initial IR signals. The molar absorption coefficient of R-OH groups is equal to one half of the molar absorption coefficient of the overall water present in the glass, i.e., $2\ \varepsilon_{OH} \approx \varepsilon_{H_2O}$; both coefficients correspond to the stretching of R-OH groups.

Since the value of the molar absorption coefficient ε_{OH} for the considered sodium aluminosilicate glass is not available, Eq. (5.3) was reorganized to avoid the problem of not knowing this value, leading to Eq. (5.5).

$$c_{H_2O} \cdot \varepsilon_{OH} = \frac{1}{2} \cdot \frac{A_g}{d_g} \cdot \frac{M_{H_2O}}{\rho_g}. \tag{5.5}$$

If ε_{OH} does not change with the variation of water concentration in a given glass, the water concentration variation is proportional to that of the product $c_{H_2O} \cdot \varepsilon_{OH}$.

For measuring the uptake of water by the sodium aluminosilicate glass, a piece of a glass sample was held upright in an alumina sample holder and was annealed in a tube furnace in wet air at 300 °C. The wet air with P_{H_2O} = 474 mbar was generated by bubbling common air through deionized water at 80 °C and was pumped into the furnace at a rate of 20 L/h. Overall water contents were determined using FTIR after the samples were removed from the furnace, washed using HPLC grade acetone, and dried in an oven at 130 °C for ten minutes.

5.3.4 Sodium Tracer Diffusion Experiments

5.3.4.1 Diffusion Mathematics

The thin film solution of Fick's second law applies to the diffusion of a tracer applied in the form of a thin film to a sample surface and diffusing in a homogenous glass sample in which the tracer diffusion coefficient is constant. The concentration of a tracer i, $c_i(\xi,t)$, at a distance ξ from the surface after diffusion-annealing for the time, t, is described by Eq. (5.6) [19].

$$c_i(\xi,t) = \frac{Q_i}{\sqrt{\pi \cdot D_i^* \cdot t}} \cdot \exp\left(- \frac{\xi^2}{4\, D_i^* \cdot t} \right) \tag{5.6}$$

where D_i^* is the tracer diffusion coefficient of the species i, i.e., in this study of the radioactive sodium tracer Na-22, and Q_i is the initial concentration of this tracer per unit area.

The absorption of the gamma-radiation from the decay of the radioactive isotope used in the sample is negligibly small and can be ignored for the data analysis due to the relatively small tracer penetration lengths considered and the small absorption coefficient of Na-22 in sodium silicate glasses. Therefore the normalized residual radioactivity, A(x,t)/A(x=0,t), as a function of the tracer diffusion coefficient of the species i, D_i^*, and the diffusion-annealing time, t, can be

described using Eq. (5.7) which was obtained by integration departing from Eq. (5.6).

$$\frac{A(x,t)}{A(x=0,t)} = \frac{\int_{x}^{\infty} c_i(\xi,t)\cdot d\,\xi}{\int_{0}^{\infty} c_i(\xi,t)\cdot d\,\xi} = 1 - \mathrm{erf}\left(\frac{x}{2\sqrt{D_i^*\cdot t}}\right). \tag{5.7}$$

To analyze experimental data, the inverse function of the error function, erfi, was used in order to achieve a higher precision by more emphasizing the influence of data points obtained for larger penetration depths on the final result. In order to determine values for the sodium tracer diffusion coefficients, Eq. (5.8) was fit to experimental data

$$\mathrm{erfi}\left(1 - \frac{A(x,t)}{A(x=0,t)}\right) = \frac{x}{2\sqrt{D_i^*\cdot t}} \tag{5.8}$$

When a = erf(b), then b = erfi(a).

5.3.4.2 Experimental Details

Tracer diffusion coefficients for the radioactive isotope Na-22 diffusing in sodium aluminosilicate glass samples, D^*_{Na}, were obtained by measuring residual radioactivities as a function of the distance from the surface where a thin film of tracer was initially applied. Na-22 tracer, in the form of an aqueous chloride solution, was applied by using a syringe to one of the two large surfaces of a glass sample pre-heated to 130 °C. After drying, the glass sample, with the radioactive tracer side facing up, was transferred to a tube furnace for diffusion-annealing at a preset temperature in dry air at 1 atm total pressure. After diffusion-annealing, to eliminate any influence of surface diffusion on the measured residual radioactivity profiles, about 1 mm of sample material was ground off from each edge perpendicular to the surface onto which the tracer had been applied. Thereafter, the sample was ultrasonically washed in water and dried before it was

glued onto a plane-parallel stainless steel sample holder in preparation for determining residual radioactivity profiles.

Residual radioactivities for two energies associated with the γ-radiation resulting from the decay of Na-22 (0.51 and 1.28 MeV [20]) were measured by using a high resolution, high-purity Ge detector (EG&G Ortec). Normalized residual radioactivities, A(x)/A(x=0), as a function of the distance from the surface, x, were obtained by recording the initial radioactivity of a sample, A(x=0), and the residual radioactivities of this sample, A(x), after removing material containing radioactive tracer with overall thicknesses of x parallel to the surface which originally contained all the tracer material.

5.4 Results

5.4.1 Glass Composition

The chemical compositions determined by using XPS for the original large surface of the sodium aluminosilicate glass of interest and for a new cross-section created by breaking a glass sample in the middle were almost the same. The concentrations found were 14.7 mol% Na_2O, 1.8 mol% K_2O, 7.3 mol% MgO, 9.5 mol% Al_2O_3 and 66.7 mol% SiO_2. The presence of any B_2O_3 and CaO was not indicated by the output generated by the instrument used for the analysis. The relative errors of concentrations determined by using XPS are typically on the order of 10 %.

5.4.2 Uptake of Water

To study the uptake of water by the sodium aluminosilicate glass, the increase in the water content determined for a sample after being annealed in wet air for different lengths of time, $\Delta c_{H_2O} \cdot \varepsilon_{OH}$ (in $(g_{H_2O}/kg_{glass}) \cdot (L/(mol_{OH} \cdot cm))$), was plotted against the square root of the annealing time, see Fig. 5.1. For determining the data shown for the water content, a density value for this sodium aluminosilicate glass of 2.44 g/cm^3, measured by using a glass pycnometer, was employed; this density value is in good agreement with those reported in the patents denoted in Ref. [21] for representative compositions of down-drawable chemically

strengthened glass for cover plate; the latter values vary between 2.453 and 2.463 g/cm^3.

5.4.3 Sodium Tracer Diffusion

A typical normalized residual radioactivity profile of Na-22 observed for a sample of sodium aluminosilicate glass after diffusion-annealing for about 21 h in dry air at 300 °C is shown in Fig. 5.2a. The curves displayed in this figure were obtained by fitting Eq. (5.7) to experimental data for A(x,t)/A(x=0,t). Values for the tracer diffusion coefficient of sodium, D^*_{Na}, were obtained by fitting the inverse function of the error function, erfi, see Eq. (5.8), to the same experimental data, as shown in Fig. 5.2b. Table 5.1 reports the values determined for tracer diffusion coefficients of sodium diffusing in as-received sodium aluminosilicate glass and in such glass after pre-annealing at the annealing temperature of 609 °C [1] for different lengths of time in dry air. This more recently reported value for the annealing temperature is only slightly different from that of 602 °C published in 2008 [22] for Corning Code 2317 glass. The annealing temperatures listed in the Corning patent for “down-drawable, chemically strenthened glass for cover plate” [21] vary to some larger extent around 600 °C for different examples for representative compositions provided in the patent. The tracer diffusion coefficients reported in this article are for diffusion annealing in dry air at different temperatures varying between 195 and 400 °C, which are far below the annealing temperature. The errors reported in Table 5.1 result from fitting Eq. (5.8) to the normalized residual radioactivities obtained from experiments. Additional errors related to the measurement of temperatures present in the annealing furnace, of diffusion-annealing times, of radioactivity net counts and of measuring lengths during profile determination make the actual errors of the tracer diffusion coefficient values significantly larger than those listed in Table 5.1. The actual errors are believed to be about ± 5 % based on estimates and past experiences. Measured tracer diffusion coefficients for the diffusion of sodium in the considered sodium aluminosilicate glass in dry air as a function of diffusion annealing temperature are shown in Fig. 5.3.

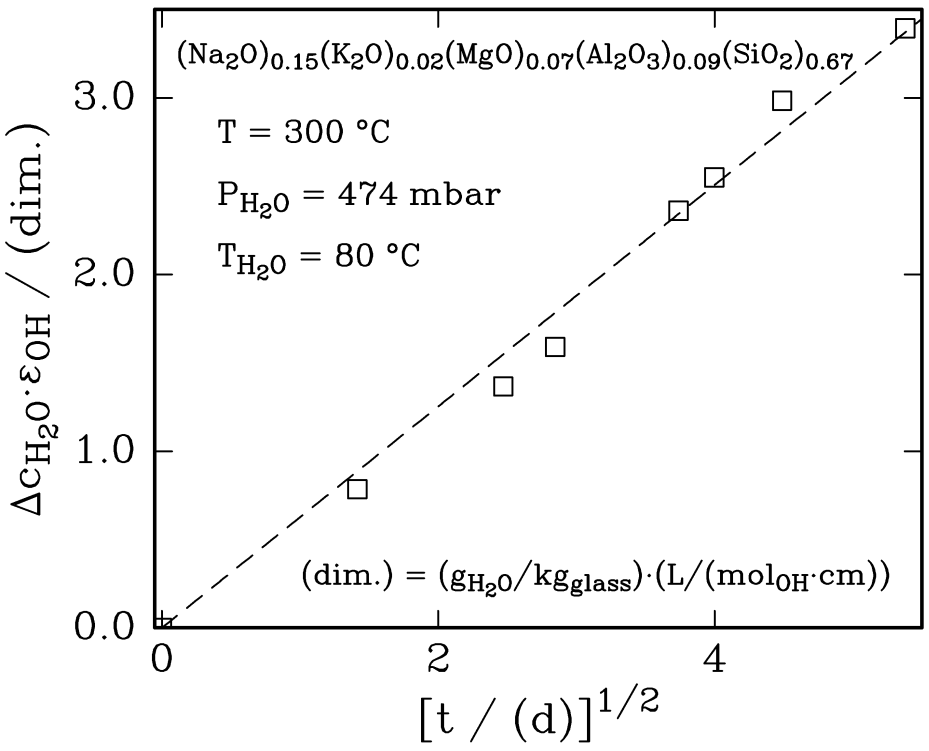

Fig. 5.1: Uptake of water by sodium aluminosilicate glass annealed at 300 °C in wet air with P_{H_2O} = 474 mbar. The straight line in the figure has been obtained by fitting Eq. (5.9) to experimental results for $\Delta c_{H_2O}\cdot\varepsilon_{OH}$. The results indicate that the kinetics of the uptake of water is controlled by diffusion in the glass.

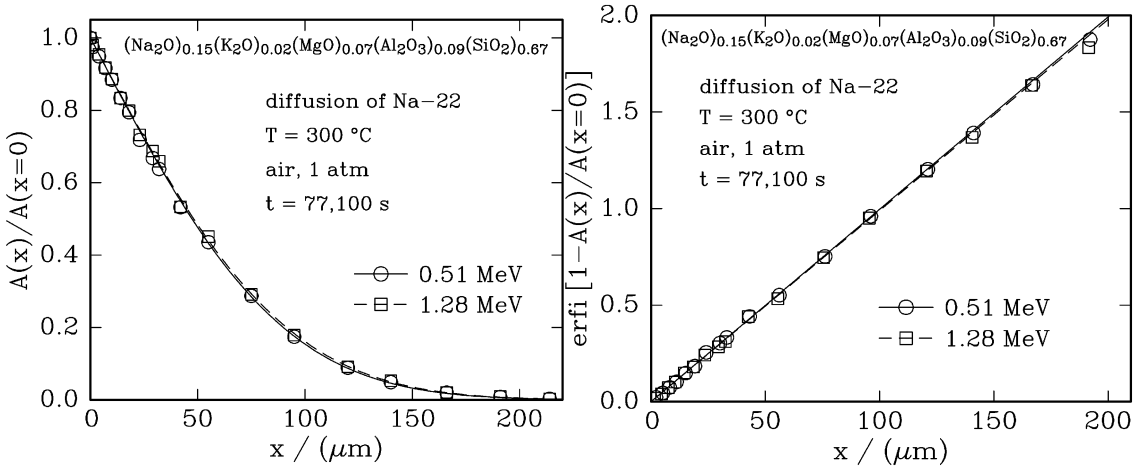

Fig. 5.2: Example for experimental data: (a) Normalized residual radioactivity profile of Na-22 observed in sodium aluminosilicate glass after diffusion-annealing for about 21 h in dry air at 300 °C. (b) Results of fitting Eq. (5.8) to the normalized residual radioactivity data shown in part (a) to determine values for sodium tracer diffusion coefficients. The lines shown in Figs. 5.2a and 5.2b were obtained by fitting Eq. (5.7) and Eq. (5.8), respectively, to the experimental data.

Table 5.1: Data for sodium tracer diffusion coefficients obtained at different temperatures for as-received and pre-annealed sodium aluminosilicate glass samples. Pre-annealing was done at the annealing temperature of 609 °C for different lengths of time. "– LD" stands for "– $\log_{10}$ (D^*_{Na}/(cm^2/s)). Data marked by * are weighted averages from two experiments. The errors reported in the table are from least squares fits of Eq. (5.8) to normalized residual radioactivity profiles. The overall errors in values obtained for D^*_{Na} are estimated to be of the order of ± 5 %, as stated in Section 3.3.

T (°C)	quantity	pre-annealing time (days)			
		0	1	5.5	10.3
195	– LD	11.012*		11.171	11.242
	error ±	0.015*		0.012	0.013
253	– LD	9.984	10.210	10.293	10.285
	error ±	0.076	0.027	0.012	0.027
300	– LD	9.484		9.694	9.689
	error ±	0.006		0.025	0.011
350	– LD	8.927*	9.037		
	error ±	0.003*	0.006		
400	– LD	8.547	8.616		
	error ±	0.010	0.004		

5.5 Discussion

5.5.1 Glass Composition

Information on the composition of the ion exchangeable sodium aluminosilicate glass (Corning Code 2317) provided by Corning and considered in this study is available from the patent issued to Corning Inc. [21]. In general, within the experimental uncertainties the composition information obtained by XPS is in agreement with the composition ranges reported in the patent. The data compare as follows (XPS result vs. composition range stated in patent): SiO_2: 66.7 mol% vs. 64-68 mol%, Na_2O: 14.7 mol% vs. 12-16 mol%, Al_2O_3: 9.5 mol% vs. 8-12 mol%, K_2O: 1.8 mol% vs. 2-5 mol%, and MgO: 7.3 mol% vs. 4-6 mol%. The XPS-derived concentration for MgO seems for unknown reasons to be too high. Efforts to find reasons were not made. Not finding any B_2O_3 and CaO in the XPS analysis is compatible with the concentration ranges for B_2O_3 of 0-3 mol% and for CaO of 0-5 mol% stated in the patent.

Although the compositions determined by XPS are not very accurate, some information can be derived from them. Sinton et al. [23] found that adding 5 to 6 mol% MgO in soda-lime-silicate glasses can increase the rate of the exchange of Na_2O by K_2O. Karlsson et al. [8] stated that concentrations of 10-18 wt% Na_2O and 5-15 wt% Al_2O_3 are beneficial for strengthening glasses containing Na_2O by exchanging Na_2O by K_2O. Converting the concentrations determined by using XPS from mol% to wt%, it was found that the concentration of Na_2O is close to 14 wt% and the concentration of Al_2O_3 15 wt%, i.e., close to the composition suggested in Ref. [8] to be beneficial for chemical strengthening by ion exchange. Using glasses initially already containing two types of alkali ions can increase the rate of exchange [11]; however, this can lead to a reduction of the degree of surface compression achieved. This may be the reason why a K_2O concentration of 1.8 mol% was found for the glass considered in this study. A small addition of K_2O may have been made to increase the rate of interdiffusion while maintaining a large compressive stress near the surface.

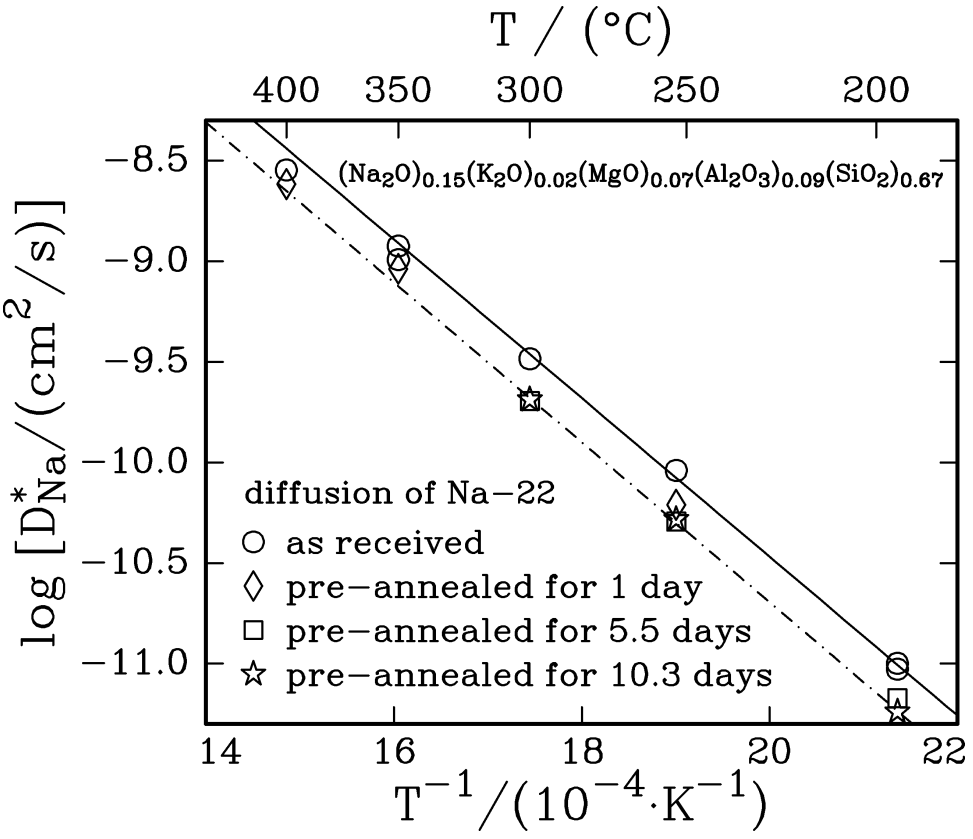

Fig. 5.3: Temperature dependence of sodium tracer diffusion coefficients determined for the sodium aluminosilicate glass of interest in this study. The lines were obtained by fitting Eq. (5.10) to the experimental data for as-received samples (upper line) and for samples pre-annealed for 10.3 days in dry air at 609 °C.

5.5.2 Uptake of Water

If the incorporation of water into the glass is diffusion-controlled, the increase of the water content with the annealing time t should follow a parabolic rate law, i.e., one should find

$$\Delta c_{H_2O} \cdot \varepsilon_{OH} \propto \sqrt{t}. \tag{5.9}$$

The difference between the water content after annealing in wet air with P_{H_2O} = 474 mbar at 300 °C for the time t and the original water content, both multiplied by ε_{OH}, $\Delta c_{H_2O} \cdot \varepsilon_{OH}$, of the glass of interest as a function of the square root of the annealing time t is shown in Fig. 5.1. The parabolic relationship denoted in Eq. (5.9) holds if a straight line can be fitted to the experimental data points. If such a fit is possible, this indicates that the uptake of water by the considered glass is diffusion-controlled. This is here the case.

Since the value of the molar absorption coefficient for OH in the considered sodium aluminosilicate glass is unknown, a typical value of it for borosilicate glasses, 40 L/(mol_{OH}·cm) [14], was used to estimate absolute values for the initial water content of the glass. The initial concentration of water in the sodium aluminosilicate glass was found to be 216 weight ppm. If the value of the molar absorption coefficient denoted above is used to estimate a value for Δc_{H_2O} per unit of the y-axis of Fig. 5.1 one finds that the water concentration change per unit of the y-axis is about 25 weight ppm.

5.5.3 Sodium Tracer Diffusion

5.5.3.1 Pre-annealing Time Dependence of the Sodium Tracer Diffusion Coefficient

As shown in Fig. 5.4, pre-annealing as-received glass samples at the annealing temperature of 609 °C leads to a decrease in the values of sodium tracer diffusion coefficients measured at temperatures between 195 and 400 °C by up to approximately 50 %. The degree of the reduction of D^*_{Na} changes with the pre-annealing time. The observed decrease of the sodium diffusivity upon pre-

annealing must be attributed to structural changes occurring during pre-annealing. The changes observed after pre-annealing are most significant after 1 day of pre-annealing. After that the structural relaxation slows down and after pre-annealing for 5.5 days changes of sodium tracer diffusion coefficients become relatively small.

5.5.3.2 Temperature Dependence of the Sodium Tracer Diffusion Coefficient

To analyze the temperature dependence of the sodium tracer diffusion coefficients obtained at temperatures far below the glass annealing temperature, an Arrhenius-type equation, see Eq. (5.10), was used.

$$D_{Na}^{*} = D_{Na}^{o} \cdot \exp\left(- \frac{\Delta E_a}{R \cdot T} \right) \tag{5.10}$$

Fig. 5.3 shows fits of Eq. (5.10) to sodium tracer diffusion coefficients for temperatures up to 400 °C for as-received glass samples and for samples pre-annealed for 10.3 days at 609 °C. It was found that the activation enthalpy, ΔE_a, for the diffusion of sodium tracer in as-received glasses is 75.5 ± 1.2 kJ/mol and for the diffusion of sodium tracer in samples pre-annealed for 10.3 days 76.1 ± 1.5 kJ/mol, i.e., the activation enthalpy is only very little affected by the pre-annealing. The logarithm of the pre-exponential factor, i.e., $\log_{10}$ [D_{Na}°/(cm^2/s)], changed from −2.58 ± 0.13 to −2.74 ± 0.15 when as-received glass was pre-annealed for 10.3 days at 609 °C. For obtaining the values for ΔE_a and $\log_{10}$ [D_{Na}°/(cm^2/s)] denoted above an estimated error of ± 5 % was attributed to each of the reported tracer diffusion coefficients. While the values obtained for ΔE_a are practically the same and well within the error limits, the values found for $\log_{10}$ [D_{Na}°/(cm^2/s)] are at the border of the error limits for this quantity.

5.5.3.3 Influence of Moisture in the Environment During Diffusion-Annealing on the Sodium Tracer Diffusion

Several sodium tracer diffusion experiments have been performed by diffusion-annealing in wet air with P_{H_2O} = 474 mbar at 300 and 350 °C. The presence of water in the sample environment seems to have no significant influence on the

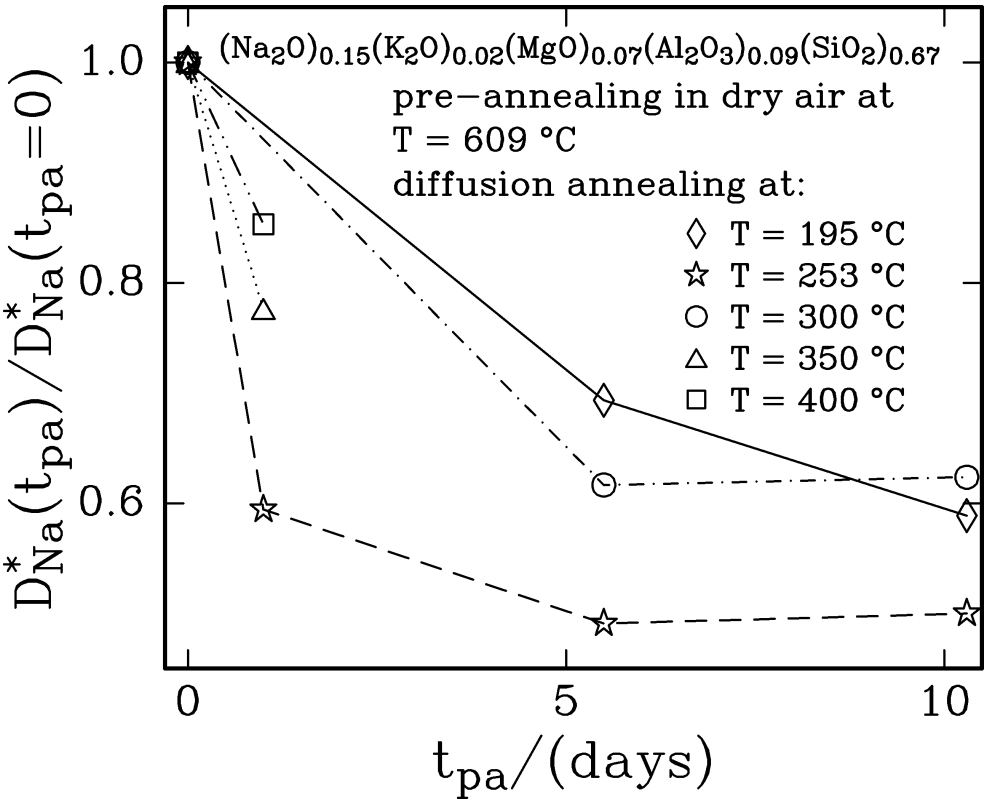

Fig. 5.4: Dependence of sodium tracer diffusion coefficients on the pre-annealing time, t_{pa}, determined for the sodium aluminosilicate glass investigated. The lines shown connect data points for constant temperatures to guide the eye.

residual radioactivity profiles obtained in comparison to those obtained after diffusion annealing in dry air. The reason for this could be that the total amount of water taken up by the glass sample within the relatively short diffusion annealing time (about 1 and 2 days for annealing at 350 and 300 °C, respectively) was not large enough to cause sufficiently significant structural changes, which could have led to changes in the sodium diffusivity in the glass near the surface. Further investigations are needed to clarify how large the local water concentrations within the glass become as a function of the annealing time and which concentrations of water are necessary to lead to significant changes in the sodium diffusivity in the glass considered.

5.6 Conclusions

Sodium tracer diffusion coefficients, D^{*}_{Na}, have been measured at different temperatures between 195 to 400 °C in a commercial, ion-exchangeable alkali aluminosilicate glass (Corning Code 2317) developed for being used to produce chemically strengthened glass by ion exchange. The composition of the sodium aluminosilicate glass was determined. In general agreement with patent information it was found that the major components of the glass are Na_2O, MgO, Al_2O_3 and SiO_2. At temperatures below the annealing temperature the temperature dependence of the measured tracer diffusion coefficients is of Arrhenius-type. The sodium tracer diffusion coefficients were found to decrease by up to about 50 % after pre-annealing as-received glass samples at the annealing temperature of 609 °C for 10 days.

5.7 Acknowledgments

This work was supported by the National Science Foundation under Award Number DMR-0710564. The work made use of the Cornell Center for Materials Research Facilities supported by the National Science Foundation under Award Number DMR-0520404. The authors thank CCMR shared facility staff, Jonathan B. Shu and John A. Hunt, for assistance related to a variety of topics. The authors thank Dr. A.J. Ellison from Corning Inc. for providing the glass samples used in this

study. Finally, the authors acknowledge all Cornell undergraduate students who helped in experimental work.

REFERENCES

[1] Corning® Gorilla® Glass, Product Information Sheet, Corning Incorporated, January [2011], http://www.CorningGorillaGlass.com.

[2] S.S. Kistler, Stresses in Glass Produced by Nonuniform Exchange of Monovalent Ions, Journal of the American Ceramic Society, **45** (2) [1962] 59-68.

[3] P. Acloque, J. Tochon, Measurement of the Mechanical Strength of Glass after Reinforcement, Compte Rendu Symposium sur la Résistance Mécanique du Verre et les Moyens de l'Améliorer, [1962] 687-704.

[4] R.F. Bartholomew, H.M. Garfinkel, Chemical Strengthening of Glass, Glass Science and Technology, Vol. 5 [1980] 217-267, Academic Press, New York.

[5] A.K. Varshneya, W.C. LaCourse, Technology of Ion Exchange Strengthening of Glass: A Review, Ceramic Transactions, **29** (Advances in Fusion and Processing of Glass) [1993] 365-376.

[6] A.K. Varshneya, Chemical Strengthening of Glass Products, Transactions of the Indian Ceramic Society, **60** (1) [2001] 1-6.

[7] R. Gy, Ion Exchange for Glass Strengthening, Materials Science & Engineering, B: Advanced Functional Solid-State Materials, **149** (2) [2008] 159-165.

[8] K. Karlsson, B. Jonson, C. Stalhandske, The Technology of Chemical Glass Strengthening - a Review, Glass Technology: European Journal of Glass Science and Technology Part A, **51** (2) [2010] 41-54.

[9] A.K. Varshneya, The Physics of Chemical Strengthening of Glass: Room for a New View, Journal of Non-Crystalline Solids, **356** (44-49) [2010] 2289-2294.

[10] C.R. Kurkjian, P.K. Gupta, R.K. Brow, The Strength of Silicate Glasses: What Do We Know, What Do We Need to Know?, International Journal of Applied Glass Science, **1** (1) [2010] 27-37.

[11] A.K. Varshneya, Chemical Strengthening of Glass: Lessons Learned and Yet to Be Learned, International Journal of Applied Glass Science, **1** (2) [2010] 131-142.

[12] R. Tandon, D.J. Green, The Effect of Crack Growth Stability Induced by Residual Compressive Stresses on Strength Variability, Journal of Materials Research, **7** (3) [1992] 765-771.

[13] D.J. Green, R. Tandon, V.M. Sglavo, Crack Arrest and Multiple Cracking in Glass Using Designed Residual Stress Profiles, Science, **283** (5406) [1999] 1295-1297.

[14] V.M. Sglavo, D.J. Green, Flaw Insensitive Ion-Exchanged Glass: II, Production and Mechanical Performance, Journal of the American Ceramic Society, **84** (8) [2001] 1832-1838.

[15] M.E. Nordberg, E.L. Mochel, H.M. Garfinkel, J.S. Olcott, Strengthening by Ion Exchange, Journal of the American Ceramic Society, **47** (5) [1964] 215-219.

[16] J.E. Shelby, Introduction to Glass Science and Technology, 2nd Ed. [2005] The Royal Society of Chemistry, Cambridge.

[17] R.H. Doremus, Diffusion of Water in Silica Glass, Journal of Materials Research, **10** (9) [1995] 2379-2389.

[18] R.H. Doremus, Glass Science, 2nd Ed. [1994] John Wiley, New York.

[19] J. Crank, The Mathematics of Diffusion, 2nd Ed. [1975] Clarendon Press, Oxford.

[20] B.J. Wilson, The Radiochemical Manual, 2nd ed. [1975] Clarendon Press, Oxford.

[21] Patents US20080286548A1, issued Nov. 20, 2008 and WO 2008143999A, published Nov 27, 2008.

[22] Corning® Gorilla™ Glass, Technical Materials, August 2008, PI 2317, Corning Incorporated, http://www.corning.com/docs/specialtymaterials/pisheets/PI2317.pdf

[23] C.W. Sinton, W.C. LaCourse, M.J. O'Connell, Variation in K^+-Na^+ Ion Exchange Depth in Commercial and Experimental Float Glass Compositions, Materials Research Bulletin, **34** (14/15) [1999] 2351-2359.

CHAPTER SIX

CONCLUSIONS

Sodium tracer diffusion coefficients, D^*_{Na}, have been measured as a function of composition in different oxide glasses containing more than one glass network former, including sodium borosilicate glasses, sodium boroaluminosilicate glasses and sodium aluminosilicate glasses.

At constant temperatures between 208 and 503 °C, for sodium borosilicate glasses of the type $(Na_2O)_{0.2}[(BO_{1.5})_x(SiO_2)_{1-x}]_{0.8}$, the tracer diffusion coefficient of sodium shows a shallow minimum at the composition parameter $x \approx 0.7$ as a function of the glass composition. For sodium borosilicate glasses following another composition cut in the Na_2O-B_2O_3-SiO_2 composition triangle, $(Na_2O)_{0.2}(B_2O_3)_y(SiO_2)_{0.8-y}$, at constant temperatures from 208 to 346 °C, the tracer diffusion coefficient of sodium decreases with an increasing value of the composition parameter y. At temperatures below about 2/3 of the glass transition temperature, the temperature dependencies of the measured tracer diffusion coefficients are of Arrhenius-type; at higher temperatures an increase in the temperature dependence with increasing temperature was observed.

Based on density data and information on the volume of different ions, the free volume of the $(Na_2O)_{0.2}[(BO_{1.5})_x(SiO_2)_{1-x}]_{0.8}$ glasses investigated was found to decrease with x and the free volume of the $(Na_2O)_{0.2}(B_2O_3)_y(SiO_2)_{0.8-y}$ glasses obtained shows a minimum around y = 0.18. Values of the Haven-ratio, H_R, were derived by comparing tracer diffusion and electrical conductivity data for the $(Na_2O)_{0.2}[(BO_{1.5})_x(SiO_2)_{1-x}]_{0.8}$ glasses. The values found for H_R are all smaller than one and show a shallow minimum at around x = 0.7 as a function of x. By combining the compositional variation of the Haven-ratio with that of the free volume, the effective mean jump frequency of sodium ions was found to vary by a factor of about 3 as a function of x at 300 °C, suggesting that about 60 % of the compositional variation of the sodium tracer diffusion coefficient in $(Na_2O)_{0.2}[(BO_{1.5})_x(SiO_2)_{1-x}]_{0.8}$ glasses is related to the change of the effective mean

jump frequency with the composition. Values of Haven-ratio of two glasses with y = 0.3 and 0.55 in the $(Na_2O)_{0.2}(B_2O_3)_y(SiO_2)_{0.8-y}$ glass system were calculated by using ionic conductivity data from literature; the values calculated were also smaller than one. When combining all the values for Haven-ratios discussed above, and including a value for H_R for sodium silicate glass, i.e., the type of glass denoted above with y = 0, it is found that the value of the Haven-ratio goes through a minimum at around y = 0.3 when y increases from 0 to 0.55 for the type of glasses denoted above.

The concentration of boron in tetrahedral coordination relative to the total concentration of boron atoms, N_4, obtained by analyzing ^{11}B magic-angle-spinning (MAS) nuclear magnetic resonance (NMR) spectra of sodium borosilicate glasses of the type $(Na_2O)_{0.2}[(BO_{1.5})_x(SiO_2)_{1-x}]_{0.8}$ decreases almost linearly with an increase of x. Sodium ions in sodium borosilicate glasses can be charge compensators either for non-bridging oxygen (NBO) or for tetrahedral BO_4 units. The concentration of sodium ions acting as charge compensators for tetrahedral BO_4 units increases when x increases. Since the interaction between sodium ions and BO_4 units is weaker than that between sodium ions and NBOs, this effect, competing with a decrease of the free volume, can be part of the reason for the shallow minima of sodium tracer diffusion coefficients observed around x = 0.75 when x increases from 0 to 1.

For $(Na_2O)_{0.2}(B_2O_3)_y(SiO_2)_{0.8-y}$ glasses, the value of N_4, based on literature data, was found to decrease with an increase of y. In glass samples with y = 0.32, 0.45 and 0.6, almost all of the sodium ions charge compensate for tetrahedral BO_4 units. Due to a lack of suitable $(Na_2O)_{0.2}(B_2O_3)_y(SiO_2)_{0.8-y}$ glass samples, NMR measurements were not performed for this type of glasses. However, glass samples of a similar type, $(Na_2O)_{0.17}(B_2O_3)_z(SiO_2)_{0.83-z}$, were made and ^{11}B MAS NMR spectra of these glass samples were collected. Values of N_4 were found to decrease from 0.83 to 0.37 when the composition parameter z increases from 0.15 to 0.6. The concentration of sodium ions acting as charge compensators for tetrahedral BO_4 units increases from z = 0.15 to 0.3 and becomes almost constant

at larger values of z, i.e., almost all of the sodium ions charge compensate for BO_4 units, which is in agreement with that what was predicted using data from the literature. Although all sodium ions in glasses with y or z larger than 0.3 charge compensate for BO_4 units, the different environments of the BO_4 units, like some BO_4 being isolated units and some being surrounded by other Si-containing or B-containing units, can also influence the strength of bonding between sodium ions and BO_4 units.

The initial water content in the $(Na_2O)_{0.2}[(BO_{1.5})_x(SiO_2)_{1-x}]_{0.8}$ glasses considered in this thesis varies from about 13 weight ppm to about 170 weight ppm when x increases from 0 to 1. For $(Na_2O)_{0.2}(B_2O_3)_y(SiO_2)_{0.8-y}$ glasses, when y increases from 0 to 0.6, initial water concentration increases from 13 weight ppm to 1000 weight ppm. The observed significant increase of the initial water concentration in boron-rich $(Na_2O)_{0.2}(B_2O_3)_y(SiO_2)_{0.8-y}$ glasses was suspected to be one reason for an observed decrease of the sodium diffusivity with an increase of y. To further investigate the influence of the water content on the sodium diffusivity, another type of sodium borosilicate glasses, $(Na_2O)_{0.17}(B_2O_3)_z(SiO_2)_{0.83-z}$, with initial water concentrations increasing from about 33 weight ppm to about 380 weight ppm, when z increases from 0 to 0.6, were made and used for measuring sodium tracer diffusion coefficients at different temperatures. Although some values of the diffusion coefficients of sodium tracer diffusing in $(Na_2O)_{0.17}(B_2O_3)_z(SiO_2)_{0.83-z}$ glasses are slightly smaller than those for sodium diffusing in $(Na_2O)_{0.2}(B_2O_3)_y(SiO_2)_{0.8-y}$ glasses (comparing samples with y = z) at the same temperature due to the lower sodium content, the trend and range of the decrease of the tracer diffusion coefficient with the composition parameter z or y is almost the same. Therefore, the relatively high water content in the studied boron-rich $(Na_2O)_{0.2}(B_2O_3)_y(SiO_2)_{0.8-y}$ glasses may not be large enough to lead to sufficiently significant structural changes, which could have caused pronounced changes in the sodium diffusivity in the glass samples studied.

Sodium tracer diffusion coefficients, D^*_{Na}, were measured in sodium boroaluminosilicate (NBAS) glasses, with and without about 1 mol% iron, and

containing aluminum, which can perform either as glass network modifier or as glass network former, at different temperatures between 198 and 350 °C. Since all as-received glass samples were in a metastable state, before tracer diffusion-annealing, 5-hour pre-annealing at the glass transition temperature was performed for all glass samples. The sodium tracer diffusion coefficients were found to decrease with a decrease of the alumina concentration for both iron-free and iron-containing glasses. Based on ^{27}Al and ^{11}B MAS NMR spectra of the NBAS glasses studied, in all glass samples almost all aluminum was found to be fourfold coordinated, acting as a glass network former, and N_4 decreases as the alumina content increases. The concentration of Na_2O acting as charge compensator for NBO increases with a decrease of the alumina content. Since the interaction between sodium ions and NBOs is stronger than that between sodium ions and tetrahedral BO_4 or AlO_4 units, this can be to some extent the reason for the decrease of the sodium tracer diffusion coefficient with a decrease of the alumina concentration. The NBAS glasses investigated were found to take up water at 300 °C in wet air with P_{H_2O} = 474 mbar. However, the effective chemical diffusion coefficient of water at this temperature was found to be much smaller than the sodium tracer diffusion coefficient and no significant influence from water taken up by glasses during diffusion-annealing on the sodium tracer diffusivity was observed.

A commercial, ion-exchangeable alkali aluminosilicate glass (Corning Code 2317), developed for producing chemically strengthened glass by ion exchange, was also studied to determine the sodium tracer diffusion coefficient of sodium diffusing in this glass at different temperatures between 195 and 400 °C. The composition of this sodium aluminosilicate glass includes Na_2O, K_2O, MgO, Al_2O_3 and SiO_2, which is more complicated than that of the other glass samples considered in this study. An Arrhenius-type temperature dependence was observed for the measured tracer diffusion coefficients at temperatures below the annealing temperature. As received, the glass samples were in a metastable state. After pre-annealing the as-received glass samples at the annealing temperature

of 609 °C for 10 days, the sodium tracer diffusion coefficients decreased by up to about 50 %. This alkali aluminosilicate glass sample also takes up water following a parabolic rate law but the amount of water taken up was too small to cause any structural changes, which can lead to modifications of the sodium diffusivity in the glass.

Currently, it is not yet possible to rationalize the experimental observations of how the sodium tracer diffusivities change with the glass composition in mixed glass network former oxide glasses due to a lack of sufficiently detailed information on the structure of the glasses investigated and of details about the strength of the bonding of sodium ions to different constituents present within the glasses and the nature of these constituents. The mixed glass network former effects observed in the different types of glasses investigated and others are not universal and more complicated than initially expected.